# OURNAL OF APPLIED

# PHYSICS

JOURNAL OF APPLIED

# PHYSICS

(Formerly PHYSICS)

JANUARY, 1938 Vol. 9, No. 1

## *In This Issue*

*Page*

**Use of Microfilm in Documentation** WATSON DAVIS 1

**Physical Interpretation of the Weather** EDGAR WOOLARD 5

**Acoustic Vibrations and Internal Combustion Engine Performance. I. Standing Waves in the Intake Pipe System**
PHILIP M. MORSE, R. H. BODEN AND HARRY SCHECTER 16

**Daniel Guggenheim Airship Institute** TH. TROLLER 24

**True Stress Strain Curves for Polycrystalline Material**
R. K. HASKELL 30

*Contributed Original Research*

**Hydrodynamic Analogy for Shearing Stress Distribution in Bending** M. A. BIOT 39

**Compressibility and Velocity of Pressure Waves in Petroleum Oils** ROBERT MATTESON 44

**Working Stresses for the Rational Design of Concrete Structures** JOSEPH MARIN 49

**On Convection Currents in High Pressure Mercury Arcs**
CARL KENTY 53

*In Every Issue*

**Here and There** 34

**Contributors to this Issue** 36

**Among the New Books** 37

**Current Literature of Physics** vi

**Advertising Index** xx

**BOARD OF EDITORS**

ELMER HUTCHISSON,
*Editor*

*Associate Editors*

R. M. BOZORTH
D. W. BRONK
W. P. DAVEY
O. S. DUFFENDACK
SAUL DUSHMAN
A. STUART HUNTER
C. H. KUNSMAN
J. T. LITTLETON
L. L. NETTLETON
W. B. NOTTINGHAM
A. R. OLPIN
JOHN T. TATE

**Publication of the American Institute of Physics**

**ADMINISTRATIVE STAFF**

HENRY A. BARTON,
*Director*

MADELINE M. MITCHELL,
*Publications Manager*

WILLIAM C. COPP,
*Advertising Manager*

**GOVERNING BOARD**

JOHN T. TATE, *Chairman*
KARL T. COMPTON
E. C. CRITTENDEN
WHEELER P. DAVEY
HOMER L. DODGE
HARVEY FLETCHER
PAUL E. KLOPSTEG
VERN O. KNUDSEN
MELVIN MOONEY
FREDERIC PALMER, JR.
R. L. PEEK, JR.
GEORGE B. PEGRAM
W. B. RAYTON
F. K. RICHTMYER
WALLACE WATERFALL

THE JOURNAL OF APPLIED PHYSICS, published monthly at Prince and Lemon Sts., Lancaster, Pa., is devoted to physics in its role as the science basic to other natural sciences and to the arts and industries. Previous to 1937 this publication was known as PHYSICS. It aims to be of service not only in physical laboratories, but also in the laboratories of industrial, chemical, geological, geophysical, meteorological, radio, and similar concerns. THE JOURNAL OF APPLIED PHYSICS publishes editorials, news of physicists and reviews, as well as technical papers of applied physics.

SUBSCRIPTION PRICE

| | U. S., POSS. AND CANADA | FOREIGN |
|---|---|---|
| To members of scientific societies | $5.00 | $5.70 |
| To all others | 7.00 | 7.70 |

**Manuscripts** should be submitted to Elmer Hutchisson, Editor, University of Pittsburgh, Pittsburgh, Pennsylvania.

**Changes of address,** proofs, and complaints of failure to receive the JOURNAL OF APPLIED PHYSICS should be addressed to the Publications Manager. New copies can be sent free only if notice of nondelivery is received within three months of date of issue.

**Subscriptions** and orders for back numbers should be addressed to Prince and Lemon Streets, Lancaster, Pa. or to the American Institute of Physics, 175 Fifth Avenue, New York, N. Y.

**Advertising rates** supplied on request. Orders, advertising copy and cuts should be sent to the American Institute of Physics.

Entered as second class matter at the Post Office at Lancaster, Pennsylvania, under the Act of March 3, 1897. Accepted for mailing at the special rate of postage provided for in the Act of February 28, 1925, authorized May 2, 1932.

Copyright 1938, by the American Institute of Physics.

Journal of Applied Physics

Volume 9 January, 1938 Number 1

# The Uses of Microfilm in Documentation

BY WATSON DAVIS

*President, American Documentation Institute*

*Director, Science Service, Washington, D. C.*

MICROFILMING promises to solve some of the most troublesome and difficult situations that face our intellectual and scholarly institutions and libraries.

The microfilm will substitute for the loan of a book from a library and can potentially bring the library resources of the world to the desk of the individual scholar. It will copy vast files of documents for preservation, protection and economy of space. The prodigious daily flood of newspapers of the world can be compressed photographically into little rolls of microfilm. It will allow scholars to read into the vital record of organized knowledge complete and detailed accounts, replete with illustrations, of their researches, and these publications will remain perpetually "in print." Microfilming offers the first real chance of marshalling the widely scattered bibliography of world literature, as for instance, in science and building up a centralized information file from which can be provided to researchers to-order bibliographies of any subject. The vast and necessary statistical compilations of government and business, such as censuses, birth and death records, financial files, business correspondence, can through microfilm be duplicated at a cost that can be afforded.

*Watson Davis*

Microfilm is perhaps the newest and most promising tool of documentation. Compact, to an extraordinary degree, promising to outlast our omnipresent paper, and capable of reproducing anything that the eye can see, even in natural colors, microfilms promise to hurdle some of the present barriers to easy and effective interchange of intelligence in many fields.

In many aspects the expert today is besieged just as effectively as Paris was in 1870 when the French photographer, Dagron, made the first microfilm and saw it flown out by carrier pigeon. The expert is ringed by high printing costs, by the scarcity of many publications published in small editions and not widely dis-

tributed, by inability to locate what has been published. Microfilm may very well lift this siege. It promises to give the specialist or research worker in science, both in its physical and more human aspects, in economics, literature, history and all other intellectual fields a new freedom in both publishing his own accomplishments and knowing what others have done.

Providing the instrumentation for microfilm, that is, the cameras, reading machines, projection printers, developing and other apparatus that are necessary, is still in its relatively early stages. Much progress has been made, but more must be accomplished. The period of gestation of an idea is long and arduous. The design, construction and merchandising of a machine also takes much longer than the eager customers wishfully expect. Nevertheless, progress is being made. There are three cameras of varying degrees of portability and adapted to different uses produced commercially in the United States and several more under construction and due for commercial appearance in the next year. There are several microfilm reading machines available, ranging from a monocular viewer for inspection and brief reading purposes selling for $1.50, to a newspaper microfilm reading machine that sells for about $200. Other apparatus is largely undeveloped or built to order. There is real need and hope for a satisfactory reading machine that will cost about as much as a portable typewriter and I hope that out of the development work of Science Service's Documentation Division there will come commercial production of such a reader by a commercial concern in a matter of months.

There is real opportunity of cooperative organization and conduct of documentation activities through the use of this new tool, the microfilm, as a unifying agency. As I said in an address before the World Congress of Universal Documetation, Paris, August 1937:

"Obviously documentation is truly universal, even in the literally astronomical sense since photographs taken through great telescopes now record the great stellar galaxies that dwarf our own Milky Way! Obviously also with such a field it is necessary to confine our aspirations and attention to the more immediate and practical aspects wherein there is some chance of effective international cooperation.

"Despite the seemingly chronic disturbed state of the world, it is a hopeful fact that exchanges of intellectual intelligence are almost uniformly continuous and effective. Scientists of one country conduct joint researches with fellow specialists of another nation, even though the political and military leaders of those two nations may be glaring at each other. Librarians work with foreign libraries almost as though they were under the same flag. Such exchanges in the intellectual world make for optimism for the world's future."

When such a technique as microfilming is young and not yet widely applied, there is larger opportunity of using it to bring about unified effort in the interests of efficiency, resulting in less duplication of effort within both intellectual and geographical areas. There is hope therefore that microfilms can catalyze cooperation in many efforts and projects that without it might have developed along isolated and specialized lines.

There are three operating functions that can be served by microfilm and it is difficult to see how they can be accomplished except with the advantages inherent to microphotographic duplication.

Most immediate and practical to put into operation is the microfilming of material in libraries upon demand. It will become fashionable and economical to send a potential book borrower a little strip of microfilm for his permanent possession instead of the book and then badgering him to return it before he has had a chance to use it effectively. I believe that reading machines for microfilm will become as common as typewriters in studies and laboratories. If the principal libraries and information centers of the world will cooperate in such "bibliofilm services," as they are called, if they exchange orders and have essentially uniform methods, forms for ordering, standard microfilm format and production methods and comparable if not uniform prices, the resources of any library will be placed at the disposal of any scholar or scientist anywhere in the world. All the libraries cooperating will merge into one world library without loss of identity or individuality. The world's documentation will become available to even the most isolated and individualistic scholar.

The practical nature of this project is indicated by three years of successful operation of Biblio-

film Service in the Library of the U. S. Department of Agriculture. This fall this service will be extended to the Library of Congress, the national library of the United States, and the Army Medical Library, America's largest medical collection. America is ready to do its share in the establishment of a world net of bibliofilm services. Perhaps this can be best organized on a national basis, with one library or agency in each country undertaking to handle and route orders from other countries in the interest of expediting and making effective such interchanges.

Supplementary to the problem of making available existing literature is the securing of publication for all the material that should be recorded and made available to the intellectual workers of the world. In this microfilm can play an important role, giving publication with economy and effectiveness.

The microfilm can be used to secure what can be called "auxiliary publication." It will supplement other forms of publication and make accessible material of all sorts that cannot now be printed because of economic factors. It will make available valuable research data that now go unrecorded. It will make available out-of-print and rare books. It is adapted to the publication of photographs and other illustrations. Auxiliary publication service (which might be named Docufilm Service) should be auxiliary to established channels of scholarly publication and it should aid and not hinder journals. Editors of journals and institutions should act as intermediaries between the authors of papers and the "Docufilm Service."

This idea has been given an experimental demonstration in America in connection principally with scientific papers. There a journal editor can publish as much or as little of a technical paper as he wishes. In the case of a very specialized paper it may be only an abstract or summary. He appends to the notice or article a note saying that the full article with diagrams, pictures, etc., can be obtained by remitting a certain price and specifying the document number under which this full article has been deposited at the central agency operating the auxiliary publication service. Orders are sent by readers directly to this central agency, which is the American Documentation Institute at Washington, D. C. Microfilms of the document are made only if and when ordered. In this way the document is perpetually "in print" but no extensive, space-consuming stocks need be stored, only the document itself and the microfilm negative from which positives are made for distribution. The operation of the plan is simple and uncomplicated and editors may use it when, how and if they find it helpful. No financial participation or guarantees on the part of the editor or author are required.

It is believed that this or analogous techniques can be adopted in other countries, preferably with central agencies serving those countries. If this is done there can be effective exchange of negatives between "Docufilm centers."

While the plan of auxiliary publication suggested could be used with other methods of duplication, microfilm is the least expensive and most universal in that it will handle text and illustration of any sort.

Bibliofilm and Docufilm are capable of immediate utilization. They can begin small and be allowed to grow as needed.

Another documentation project of importance to the world is much more formidable and cannot be accomplished without much planning, development and international cooperation. This is the possibility of a world bibliography, beginning in the field of science but eventually extending to all fields.

The economy and compactness of microfilm gives new hope that a world science bibliography may be accomplished without ambitious hopes and promising plans being drowned in a sea of cards and smothered in a maze of details. It is possible to visualize the creation in some world center of a card file with a card for every article, paper, book or document published in science that is important to the written record of science. Each card could be given multiple classifications. Now if for each of these classifications the card were microfilmed with a pattern representing that classification and if selection from microfilm is developed so that a roll of microfilm is run through a selector which prints only microfilm bearing a predetermined classification pattern, we shall have the mechanism whereby a great world file of bibliography can be made to produce special bibliographies in any subject to order.

And this should be done at a cost that would allow its use by every scientific research worker.

When it is considered that most of the scientific literature of the world has been listed by title or abstract bibliography somewhere in abstract journals, in special bibliographies or such large card compilations as exist in the Science Museum Library at London, the task while gigantic does not seem impossible. The last and essential link in the possibility is the use of microfilm for multiplying the cards under various classifications and in copying for distribution. I repeat that this is a large project needing international thought and probably years of gestation. Classification, the technique of bibliography and a dozen other factors in documentation to which many have unselfishly given their lives will find fruition in such a project.

The American Documentation Institute was founded this year (1937) on behalf of over 60 scholarly and scientific agencies, in various intellectual fields, which nominate its members and thus control it. It arose out of the need for a broad, energetic and intellectually motivated development of all phases of documentation, particularly microphotographic duplication and its ramifications, in the fields of physical, natural, social and historical sciences and the general sphere of libraries and information services.

It took over the functions of Science Service's Documentation Division on July 1, 1937. It operates Bibliofilm Service and the Auxiliary Publication Service which were operated by Science Service. The design and development of microphotographic apparatus carried on by Science Service with the cooperation of the Chemical Foundation, U. S. Navy, Bureau of the Census, Works Progress Administration, etc., is now being left in commercial hands. The American Documentation Institute will not engage in the sale and manufacture of apparatus, but will cooperate with all manufacturers and commercial concerns so far as practicable.

The American Documentation Institute will be able to serve as an informational clearing house on microfilming activities.

Activities not involving microfilm are planned. Auxiliary publication in cooperation with journals, societies and institutions is contemplated, not only through the use of microfilm, but through the use of other methods of duplication. An investigation is being made into the needs of a document preservation center applying the technique of cellulose sheet lamination, etc., developed by the National Bureau of Standards for the National Archives.

---

*With the passing away of Lord Rutherford, the life of one of the greatest men who ever worked in science has come to an end. For us to make comparisons would be far from Rutherford's spirit, but we may say of him, as has been said of Galileo, that he left science in quite a different state from that in which he found it.*

NIELS BOHR, *Nature*

# Physical Interpretation of the Weather

By EDGAR W. WOOLARD

*U. S. Weather Bureau*
*Washington, D. C.*

IN the days of ancient Greece, the word *meteorology*—or, rather, its Greek equivalent, *μετεωρολογία*—was introduced to designate a subject that, even then, was already old, *viz.*, knowledge and lore of the weather and other phenomena of the atmosphere. The word *meteor* was then used as a general term for any atmospheric phenomenon; this still is the preferred meaning given in modern dictionaries, but the more common usage now is for astronomical meteors which in ancient times were, like comets, thought to be entirely of atmospheric origin and were included under meteorology along with a number of other phenomena not now considered to come within its field. During the centuries since Aristotle wrote the earliest known formal treatise on meteorology, the scope of the subject has gradually been narrowed, until the modern tendency is to restrict it to only the phenomena that are directly involved in the weather, excluding even other atmospheric phenomena and drawing more or less of a distinction between meteorology and climatology.

It is not difficult to show that meteorology, in the preceding meaning, is a branch of physics (principally "classical" physics), and it is significant that many of the most notable contributions to meteorology in the past have been made by physicists: The state of the weather at a given time and place is specified by the values of six quantities known as the meteorological elements, *viz.*, air-temperature, barometric pressure, wind-velocity (direction and speed), humidity, clouds, and precipitation (rain, snow, hail, etc.). Now, these elements are completely determined by the temperature, pressure, density, and three velocity components of the air, and its total solid, liquid, and gaseous water-content; clearly, therefore, the weather is essentially a dynamic and thermodynamic phenomenon.

Unfortunately, formidable difficulties are encountered in attempting to base the systematic development and the practical applications of meteorology explicitly on principles of physics; even an empirical understanding of the storms and irregular weather changes of temperate regions was slow to develop: The standard method of representing the weather conditions over a given region at any particular time is by means of the familiar synoptic map which is prepared from observations taken simultaneously at a network of stations distributed over the region, and which shows the geographic distribution of the meteorological elements (Fig. 2). The synoptic map was introduced into meteorology early in the nineteenth century by Brandes and Redfield; and after the invention of the electric telegraph it came into daily use, for delineating and forecasting weather conditions, among the national meteorological services that were established in the principal countries of the world soon after daily telegraphic charts were first regularly issued in France in 1863. The daily synoptic map has been a powerful aid to meteorological investigation, while weather forecasting from these maps has rendered invaluable service ever since its inception; but even long after the development of theoretical meteorology on an exact physical basis had been initiated (largely through the work of William Ferrel in the United States about 1855, Fig. 3), progress was relatively slow in the attempt to interpret

FIG. 1(a). Tornado cloud, Oklahoma City, May 12, 1896.

the current weather phenomena shown on the synoptic charts in terms of the physical processes in operation.

Weather forecasts were based fundamentally on the fact of observation (demonstrated by Benjamin Franklin, Leverrier, Fitzroy and Buchan) that existing weather conditions travel over the globe in a fairly regular manner from day to day, altering more or less as they move (Figs. 2 and 9–10); and from a detailed study of the daily movements and transformations recorded on series of past synoptic charts, it is possible to estimate from a given current map the weather that will occur in the near future. For the most part, weather phenomena were empirically associated with the barometric pressure distribution, particularly with the cyclones or "lows" (regions of relatively low pressure), and anticyclones or "highs" (regions of relatively high pressure), which are continually moving over the temperate regions; and the emphasis was mainly on the weather conditions that had in the past been observed usually to accompany the particular movements and developments of these pressure formations that were to be expected on the basis of past experience, with little consideration of physical explanations and almost no attempt to make direct use of any physical principles.

The obstacles arise partly from the complexity of the phenomena, and partly from the difficulty of securing adequate observational data and effectively utilizing them. A complete investigation of the weather phenomena over a given region requires regular observations at fairly frequent intervals, both from the surface of the earth and aloft to moderately great heights in the free air, over a territory that extends far beyond the limits of the area under immediate consideration; a satisfactory understanding of the weather over the entire continental United States, e.g., would necessitate adequate data for at least the region from the mid-Pacific Ocean to Bermuda and from northern Alaska, Canada and Greenland to Mexico and the West Indies, and it would be desirable to extend this area over a still larger part of the northern hemisphere. This ideal is far from having yet been attained, and much remains to be learned as to how to interpret and apply even all the data that now are available; but during recent years, notable increases have

FIG. 1(b). Lightning flash in a thunderstorm cloud.

been effected in the number of reporting stations, including ships at sea and stations for upper air soundings, as well as in the extent of territory

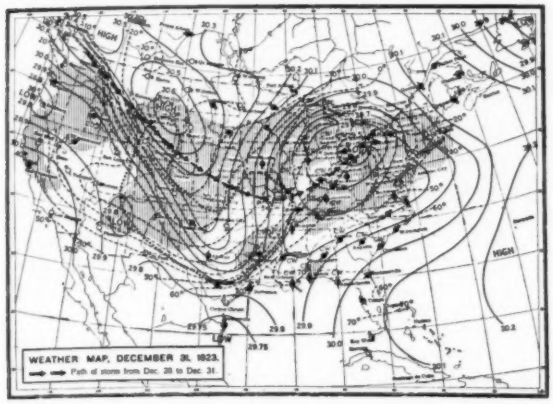


FIG. 2. Typical synoptic weather map, showing extra-tropical cyclone and anticyclone. The attendant wind circulations are shown by the arrows, which fly with the wind; isobars (solid lines) connect stations that have equal barometric pressures; isotherms (dotted lines) connect stations that have equal temperatures; shaded circles indicate clouded skies, *R*, rain, *S*, snow, and cross-hatched areas are regions over which precipitation has fallen during the preceding 24 hours. *CW* indicates cold wave warning; and the heavy dotted line encloses a region of marked temperature fall during the preceding 24 hours. (Compare with examples of analyzed maps, Figs. 5, 9, 10).

covered by the observing network, and in the completeness and frequency of the observations; while steady progress has been made in utilizing the data effectively, from both the empirical and the physical viewpoints.

The empirical association of weather conditions with pressure distribution, which prevailed from the earliest days of synoptic meteorology, was naturally suggested by the daily maps. It is, moreover, consistent with the fact of common experience that the *winds* are one of the principal immediate factors in daily weather; because it is the field of pressure which directly determines the flow of the air that constitutes the wind, while other weather phenomena are more or less directly produced by, or are incident to, the motions of the air. Great difficulty has been encountered in attempting to obtain from observations of the winds a satisfactory comprehensive knowledge of the atmospheric circulation over the globe, but for the purposes of the present discussion it is sufficient to recognize that the air motions which make up the circulation of the atmosphere as a whole constitute a complex and ever-varying system of innumerable different interacting currents by which great quantities of air are often transported from place to place over long distances; and during recent years, attention has been directed more and more to these air streams themselves—their motions, extent, and physical properties, and the relations of weather phenomena thereto—instead of being, as in the earlier days of synoptic meteorology, almost wholly concentrated on pressure formations as such.

It has been more or less vaguely realized for more than a century that on many occasions two atmospheric currents, markedly different in velocity and temperature, and sharply separated, may flow adjacent to each other and produce distinctive weather phenomena as one succeeds the other at a given place; this idea was clearly expressed as early as 1828 by H. W. Dove, who ascribed the storms of temperate latitudes to conflicts between polar currents and equatorial currents. Only very limited observation is needed to reveal striking instances in which all of the meteorological elements change simultaneously and abruptly in a pronounced manner (Fig. 4), as the boundary between two different currents sweeps over the observing station, the transition from one to the other amounting practically to an actual discontinuity. Such moving discontinui-

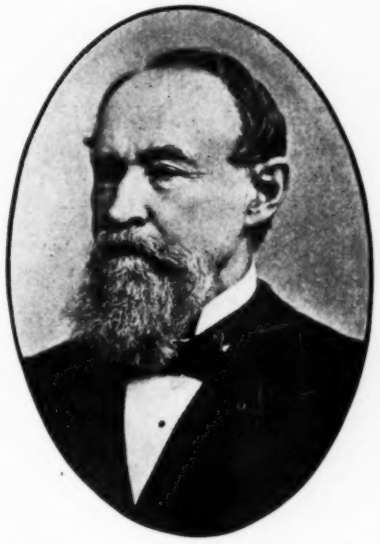

FIG. 3. William Ferrel, 1817–1891; American pioneer investigator of the dynamics of atmospheric phenomena.

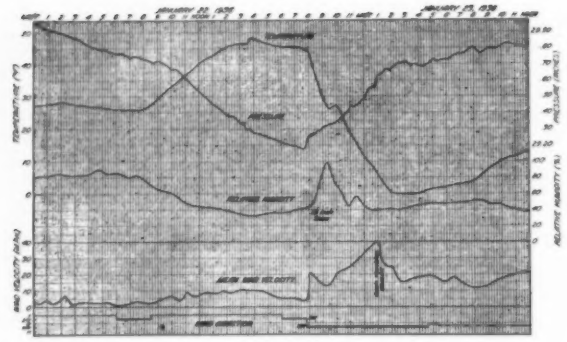

FIG. 4. Variations of the meteorological elements at Washington, D. C., January 22–23, 1936, recorded by self-registering instruments. Note the simultaneous abrupt changes in all the elements at about 8 P.M., January 22, 75 meridian time, as the boundary between a weak southerly current and a strong northwesterly current passed over the city; the total drop in temperature was nearly 50°F. Considerable property damage from wind occurred. See also Figs. 5 and 6.

ties, often hundreds of miles in length, between adjacent currents, frequently are quite conspicuous on synoptic charts (Fig. 5); they have long been recognized by the forecaster, and were the subject of extensive theoretical investigations by Helmholtz and Margules. It was not until during the World War, however, that an intensive effort was made to investigate the separate currents in detail, explicitly as a basis for the interpretation of the phenomena shown on the daily maps. The investigation was initiated in Norway, after the Scandinavian countries had ceased to receive meteorological data from other countries because of the war. On very detailed surface charts, prepared from unusually comprehensive observations at an exceedingly dense network of stations, it was found that a number of individual currents ordinarily could be identified and followed from day to day; they differed more or less from one another in direction of movement, speed, temperature, and other characteristics; and often ended abruptly against one another, with the clouds, precipitation, and other weather phenomena definitely related to these discontinuities.

It may be shown from dynamical theory that two atmospheric currents with different temperatures and velocities may, on the rotating earth, flow side by side in mutual dynamical equilibrium, provided the surface of discontinuity between them is inclined at an appropriate (in general, small) angle to the horizontal, with the colder current lying in wedge form under the warmer (Fig. 6). If the conditions necessary for this dynamical equilibrium are not fulfilled, however, a disturbance develops at the boundary between the two currents, and may result in the formation of a travelling cyclone: The warm current advances against, and flows up over, the cold current; while in the rear of the disturbance the cold air sweeps in under the warm current (Figs.

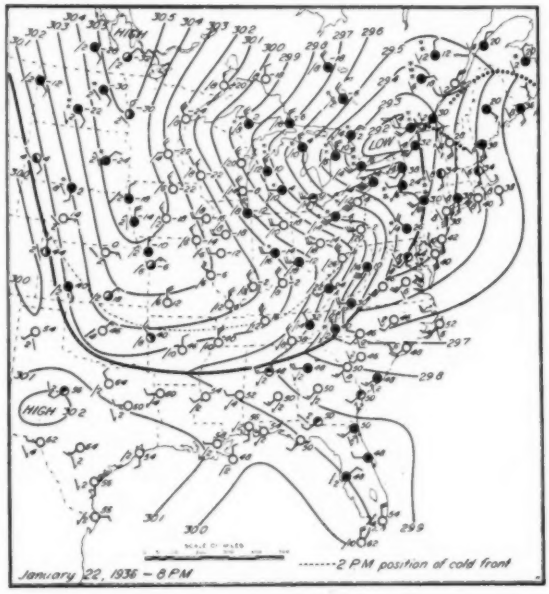


FIG. 5. Synoptic map of eastern United States at 8 P.M., 75 meridian time, January 22, 1936. The heavy solid line shows the boundary or "front" of advancing cold air, just before it reached Washington and produced the effects shown in Fig. 4: Arrows fly with the wind, and the number of barbs indicates the wind strength; the number to the right of each station is the Fahrenheit temperature; the number to the left or below is the net change in the barometer (in hundredths of an inch) during the preceding 3 hours, and the accompanying symbol shows the character of the barograph trace during that interval. Note the comparative uniformity in temperature over large areas ahead of the front, and the abrupt decrease at and behind the front; note also the abrupt change in the barometric tendencies at the front. See also Fig. 6.

7, 8). In the regions where warm air is forced to ascend, the adiabatic cooling may lead to condensation and precipitation of the admixed water vapor. This general conception of the cyclone is the outgrowth of ideas successively expressed and elaborated during the past hundred years by Dove, Helmholtz, Blasius, Margules,

Shaw, J. Bjerknes, Solberg, and others;[1] in an idealized schematic form, it is represented in Figs. 7 and 8, although of course actual cyclones usually depart more or less from the ideal. Much yet remains to be learned, however, about the detailed structure and the dynamical mechanism of the cyclone, concerning which several different theories exist.

Thus, it is not the cyclones and anticyclones as such that are important in determining the weather, but rather the interactions between the various moving air masses that are involved in the systems of winds that attend barometric pressure formations. The elaboration of a systematic technique for the delimitation of the individual currents on the daily maps, and the study of the weather phenomena produced by their interactions, have led to "air mass analysis," to which so much prominence has been given in recent years: Over large areas of the earth, especially in polar and in tropical regions, the meteorological conditions are so nearly uniform and steady, and the circulation so relatively weak or restricted for long periods that the atmosphere up to great heights above these areas takes on distinctive properties of temperature, moisture, and stability that are characteristic of the regions. For example, when air either stagnates, or else circulates for a long period, over the regions of the Gulf of Mexico and Caribbean Sea, it becomes warm, moisture-laden and unstable. Frequently an atmospheric current originates in one of these areas and transports large quantities of air to distant parts of the earth, as, for example, when a great body of intensely cold air pours out from the Arctic and flows down over the globe to lower latitudes, sometimes covering the larger part of the North American continent with its frigid winds (Figs. 2, 5). Moving masses of air from different localities tend as they travel to retain many of the initial physical properties characteristic of their respective source regions, especially at upper levels, although of course they gradually become more and more modified as time goes on by the conditions encountered during their progress. When air masses from widely separated places of origin, and with distinctly different properties, are brought into juxtaposition by the currents that are continually traversing the atmosphere, these bodies of air do not freely mix, but tend to retain their identity and to remain separated from one another throughout much of their history by more or less well-defined surfaces of discontinuity or sharp transition zones in temperature, humidity, and velocity; until eventually, after profound modification by the long continued action of external influences, they are subject to mixture, dissipation, and ultimate disappearance as separate bodies. It is at the interfaces where different air masses meet, or so-called "frontal surfaces," that the processes involved in weather phenomena are in general most active, although many important phenomena also frequently take place within the

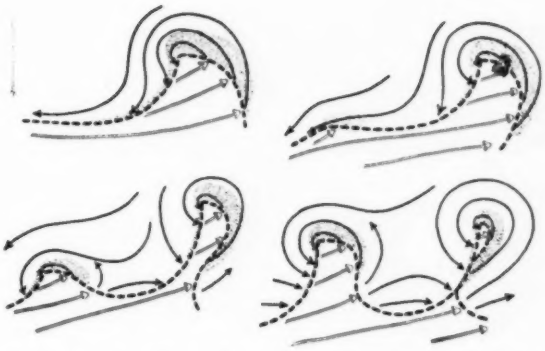

FIG. 7. Formation of an extratropical cyclone from a disturbance on the boundary between a cold and a warm current. See Fig. 8.

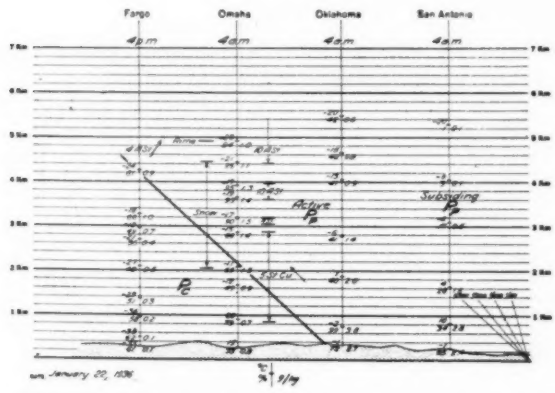


FIG. 6. Vertical (north-south) cross section through the cold front shown in Fig. 5, constructed from data obtained by airplane soundings in the early morning of January 22, 1936: The numbers show centigrade temperature, relative humidity, and moisture content in grams of water vapor per kilogram of air, at the points indicated, arranged as shown at the bottom of the diagram. Note how the cold (*Pc*) air lies in wedge form under the warmer air; *the vertical scale is greatly exaggerated——see scale of slopes in lower right corner.*

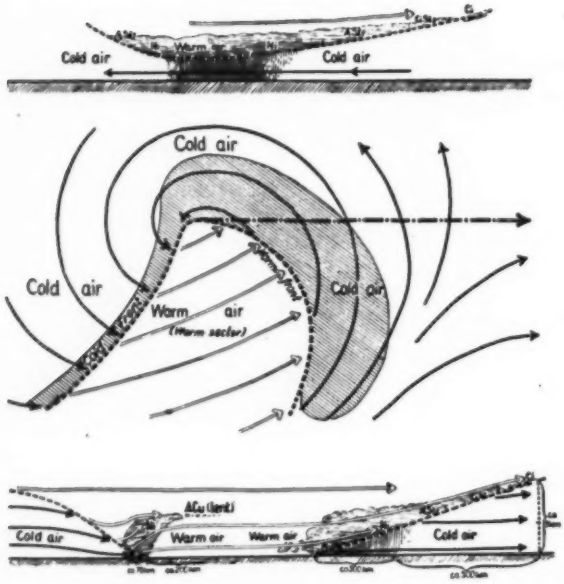


FIG. 8. Idealized extratropical cyclone formed by the process illustrated in Fig. 7, with vertical east-west cross sections through the northern part (above) and the southern part (below).

body of an air mass. In the analysis of synoptic maps, it is necessary to identify and delimit the separate air masses, assign them to their places in some recognized classification of air masses according to source region and characteristics, trace their movements and progressive modifications from day to day, and determine the associated physical processes and their relations to the attendant weather phenomena.

With respect to their physical characteristics, air masses may be classified[2] first into tropical and polar, and each of these types further subdivided into continental and maritime, according as the source region was over land or ocean; still further subdivision may be made on the basis of the geographical location of the source region. For example, in the United States, two types of tropical maritime air are important —tropical pacific (TP) and tropical atlantic (TA). When an air mass has become significantly modified from its original state, it is designated as a transitional mass and is distinguished by prefixing a capital N to its symbol—as, for example, NTA.

The development of air mass analysis has greatly stimulated efforts to obtain more adequate data and to devise effective means for their application to the physical analysis of day to day weather and the interpretation of synoptic maps. The daily location of the "fronts," or lines on the surface of the earth which bound the different air masses, presents a difficult problem in practice. The contrasts frequently are obscure and may not exist in all of the physical properties; broad and diffuse transition zones sometimes take the place of true fronts. Success in the analysis requires that appropriate and adequate data be available to a trained and experienced personnel. In particular, a network of aerological soundings to fairly great heights is indispensable, and until upper air data could be made quickly available by the introduction of airplane soundings, air mass analysis could not receive extensive application in daily work. The current characteristics of an air mass depend on both its source and the modifications it has undergone during its progress

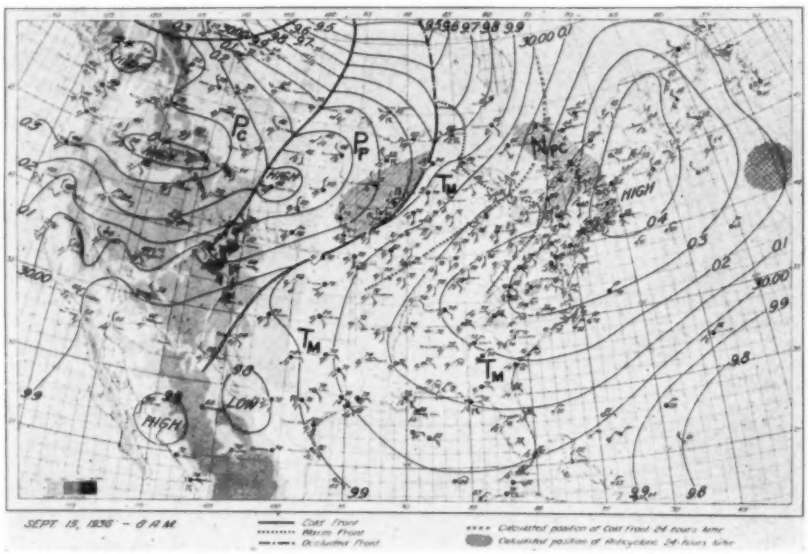


FIG. 9. Analyzed synoptic map, September 15, 1936, 8 A.M., 75th meridian time. See also Figs. 10 and 11.

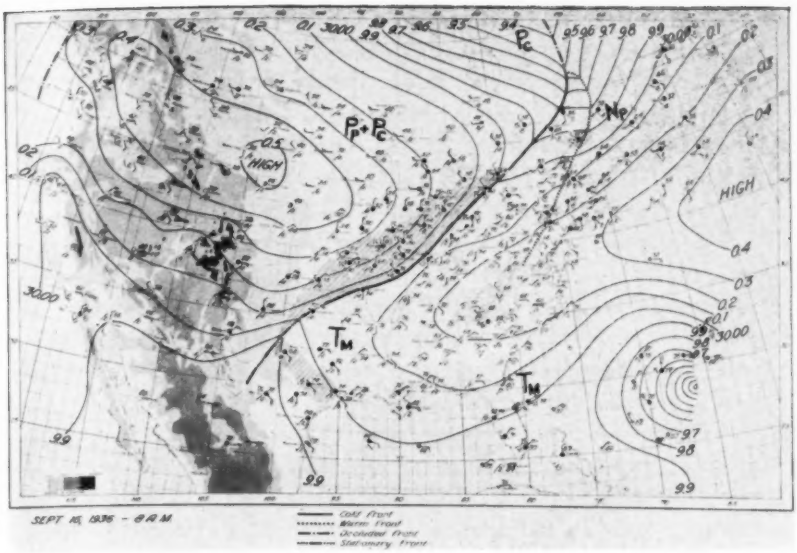


FIG. 10. Analyzed synoptic map, 24 hours later than Fig. 9. See also Fig. 11.

away from the source region; these modifications, which usually tend to weaken the distinctions, are in general much more rapid and extensive near the surface of the earth than aloft. Furthermore, surface observations alone frequently do not reveal conditions and physical processes aloft which on many occasions are the principal cause of important phenomena at the surface, and without a knowledge of which the latter cannot be explained or foreseen, nor the surface map interpreted. Methods are now being rapidly perfected for obtaining aerological observations under all conditions of weather, and from a denser network, by means of the radio meteorograph—a mechanism which is carried aloft by a small balloon, and by which pressure, temperature, and humidity are caused to actuate a short wave radio transmitting apparatus that conveys a record to radio receiving apparatus on the ground. Vertical cross sections through the atmosphere (Figs. 6, 11), so far as they can be constructed from data now available, are being used to supplement the surface map and the mere plots of upper air data against height.[3]

Examples of analyzed maps are shown in Figs. 9 and 10. When the movements of the currents are such that colder air is advancing over regions occupied by warmer air, the front between the two air masses is called a cold front; if warmer air is advancing into regions occupied by colder air, the discontinuity is called a warm front. Advancing warm air always tends to overrun colder heavier air; while advancing cold air tends to underrun warm air. The discontinuity formed when a cold front overtakes a warm front and displaces the warm air formerly between them to a higher level is known as an occluded front. Cold fronts often give rise to the well-known squall lines or wind-shift lines. Along the separating frontal surfaces, the overrunning of warm air over the slopes of cold air masses, or the lifting of warm air by underrunning cold air, leads to adiabatic cooling and eventually cloud and perhaps precipitation. The interaction of a cold and a warm air mass often leads to the development of a cyclone, with its center on the front. In the search for the fronts, important evidence is provided by temperatures, winds, dewpoints, pressure tendencies (that is, the pressure changes during the 3 hours preceding the observations), cloud forms and sequences, precipitation, and other auxiliary information.[4]

A number of special procedures have been devised for putting the data, especially those from the upper air, into a form that will facilitate their effective and convenient application in practice, both for the identification of air masses from place to place and time to time, and also for the purpose of analyzing the physical conditions and processes; investigations for this purpose have in recent years led to a particularly noteworthy development of the thermodynamics of atmospheric phenomena, and of practical means for applying it. Meteorological thermodynamics involves the investigation of the energy transformations and sequence of thermodynamic properties and states, during specified processes, in the atmosphere.[5] When, for example, humid air is forced to ascend in the atmosphere, it comes

under less and less pressure and expands and cools adiabatically; if this process continues, condensation and precipitation eventually take place. The resulting mixture of dry air and widely variable amounts of water distributed in continuously changing proportions between the gaseous, liquid, and solid phases, in the gravitational field of the earth, forms a highly complicated system; and the derivation of mathematical equations of state to show the condition of the system and the sequence of phenomena throughout the process is an intricate problem which involves relations far more complex than the familiar $PV=RT$ of elementary physics.

For purposes of air mass identification, conservative properties of the air are of especial importance. Some properties are more conservative than others during the modifications to which air masses are usually subject; in seeking an index which will remain as nearly as possible constant, two quantities known respectively as specific humidity and equivalent potential temperature have been found especially useful: The *specific humidity* is the mass of water vapor per unit mass of humid air; the *equivalent potential temperature* is the temperature to which air would come if subjected to a pseudoadiabatic lifting (that is, a lifting which is adiabatic except that all condensation products drop out immediately upon formation) until all moisture was precipitated, followed by an adiabatic return to a standard pressure.

In developing methods for representing the data from upper air soundings in a form that will show the meteorological import of the physical conditions and be adapted to practical needs, a number of special thermodynamic diagrams have been devised and have come into regular use.[6] In general, these diagrams consist of networks of lines, referred to appropriate coordinate systems, which show the thermodynamic states of atmospheric air over a wide range of conditions and by which the changes of state and the energy transformations during any prescribed process may be traced out; they correspond to the "indicator diagrams" of physics and engineering, but are much more complex. By plotting the data from a sounding on one of these diagrams, the conditions in the vertical with respect to stability, available energy, etc., at different levels in the atmosphere may be determined; and many of the phenomena to be anticipated under the existing meteorological circumstances may be inferred.[9] On the so-called tephigram, for example (Fig. 12), the sounding is plotted on a chart with absolute temperature as abscissa and entropy as ordinate, and with a background of lines that show pressures, water vapor contents, and irreversible adiabats, of saturated air; on the "Rossby diagram," which is particularly useful for bringing out significant properties of the air, the sounding is plotted with the so-called mixing ratio (mass of water vapor per unit mass of dry air) as abscissa and potential temperature of the dry air component of the atmosphere as ordinate, and with a background of lines that show equivalent potential temperatures, and pressure and temperature at the condensation level. Other widely used charts include the adiabatic chart, the emagram, and the Refsdal aerogram.

One of the methods most recently applied in daily practice as an aid in the representation and physical analysis of phenomena is the construction of charts that show the meteorological conditions on selected isentropic surfaces (surfaces of constant potential temperature) in the upper air, instead of on horizontal surfaces. These isentropic charts were suggested by Sir Napier Shaw some years ago, but their practical construction and use requires, of course, a network of daily aerological soundings. The charts show (among other things) the elevation contours of the selected isentropic surface, and the distribution of specific humidity and wind velocity over this surface. The motion of the upper air is in general so nearly adiabatic, as long as no condensation occurs, that the flow must everywhere be practically along an isentropic surface. The flow of individual dry and humid currents in each surface, and the gradual lateral mixing of these currents over the surface, can be followed from day to day by means of the specific humidity. The extent to which the motions of the currents are upward or downward along the slopes of the isentropic surface, together with the conditions of relative humidity, condensation levels, and motion of the surface itself, is intimately related to the occurrence of cloudiness and precipitation, and other meteorological

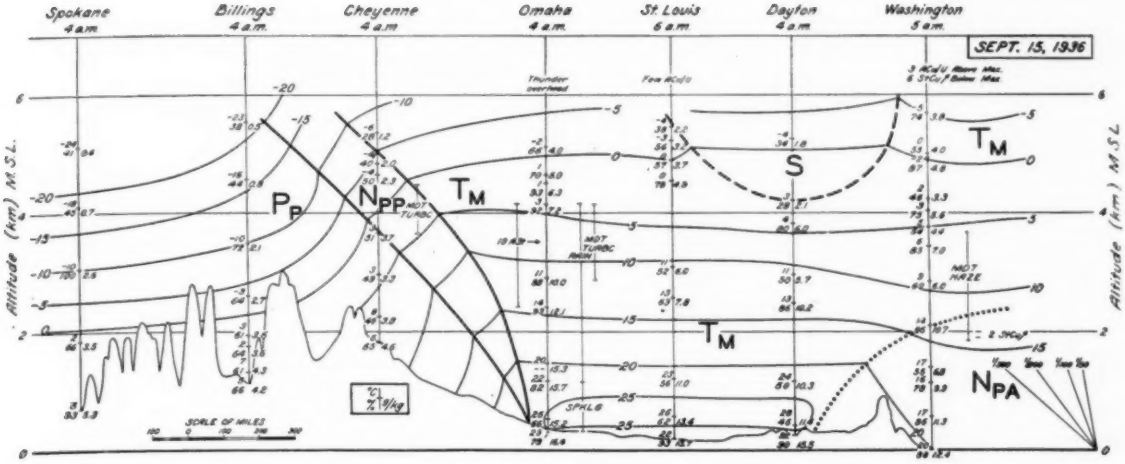


FIG. 11. East-west vertical cross section through the atmosphere, showing conditions aloft shortly before the time of the map in Fig. 9 (cf. explanations in legend to Fig. 6).

processes. Isentropic charts have shown considerable promise both for purposes of hydrodynamical investigations of atmospheric motions and for practical forecasting.

It must be emphasized that the physical *analysis* of maps and cross sections is quite distinct from the making of a *forecast;* the analysis must be followed by a determination of the expected displacements, transformations, and developments of the fronts, air masses and pressure formations, and an estimate of the weather conditions that will accompany them. Important progress has been made in developing methods for this purpose also on a quantitative physical basis; but the unusual demands of practical meteorological work, particularly the exceedingly limited time within which forecasts must be completed and issued, together with the extraordinary complexity of the phenomena involved, the great volume of data necessary and the wide areas from which they must be gathered, make it peculiarly difficult to adapt the results of theoretical investigations to meet the needs of applied meteorology. The majority of attempts to achieve anything that approaches an exact mathematical calculation of future weather on the basis of dynamical and physical theory have not been successful in practice, although some of them are of great theoretical importance.[7] Among the investigations with the greatest immediate practical promise, the most noteworthy, perhaps, are those by Sverre Petterssen of the Norwegian Meteorological Service, following earlier similar work by Gião and Angervo. On the basis of the ordinary kinematical theory of fluid motion, he has developed rigorous methods for a *kinematical* analysis of the synoptic chart in conjunction with the *frontal* and the *thermodynamic* analyses; and has derived procedures for detecting indications of important developments, and for calculating the movements and transformations of pressure systems and of fronts. His formulae,[8] when used with judgment by an experienced forecaster, are a valuable aid,[9] although they do not contribute to the dynamical interpretation of the kinematic phenomena. Fig. 9 shows some results of applying Petterssen's methods which may be compared with the actual occurrences shown in Fig. 10.

Under the influence of these and other modern developments, weather forecasting, at first exclusively empirical, is now progressing along sound physical lines; and it has become practicable during recent years to *supplement*, though not replace, the empirical methods of weather forecasting, as developed in the nineteenth century on the basis of experience alone, with practices based on an understanding and an explicit application of the physical laws to which the phenomena conform.[9] For a long time to come, however, weather forecasting must continue to be a *combination* of physical reasoning with methods based on accumulated practical experience with synoptic charts. We cannot yet,

and perhaps may never, safely do without the empirical judgment of the experienced forecaster.

Meanwhile, it may reasonably be expected that all investigations designed to elucidate the physical mechanism of weather phenomena will not only contribute toward a better understanding of these phenomena, but also lead, because of this increased understanding, to an eventual increase in the precision, and an improvement in the accuracy, of forecasts; and will moreover have the distinct advantage of making weather forecasting less of an esoteric art, irrespective of the extent to which they may effect actual improvements over the results already obtainable by empirical practices. The problems presented by weather phenomena and their prediction offer a fertile field of research for the application of the classical physics. In addition, the weather provides many examples of physical phenomena, on an impressive scale and often of a spectacular character (Fig. 1), which afford excellent illustrations of important physical principles; some of these illustrations are of peculiar interest and educational value, because the operation of familiar physical principles in the atmosphere frequently leads to results quite at variance with what is to be expected on the basis of ordinary experience, since, on the scale of

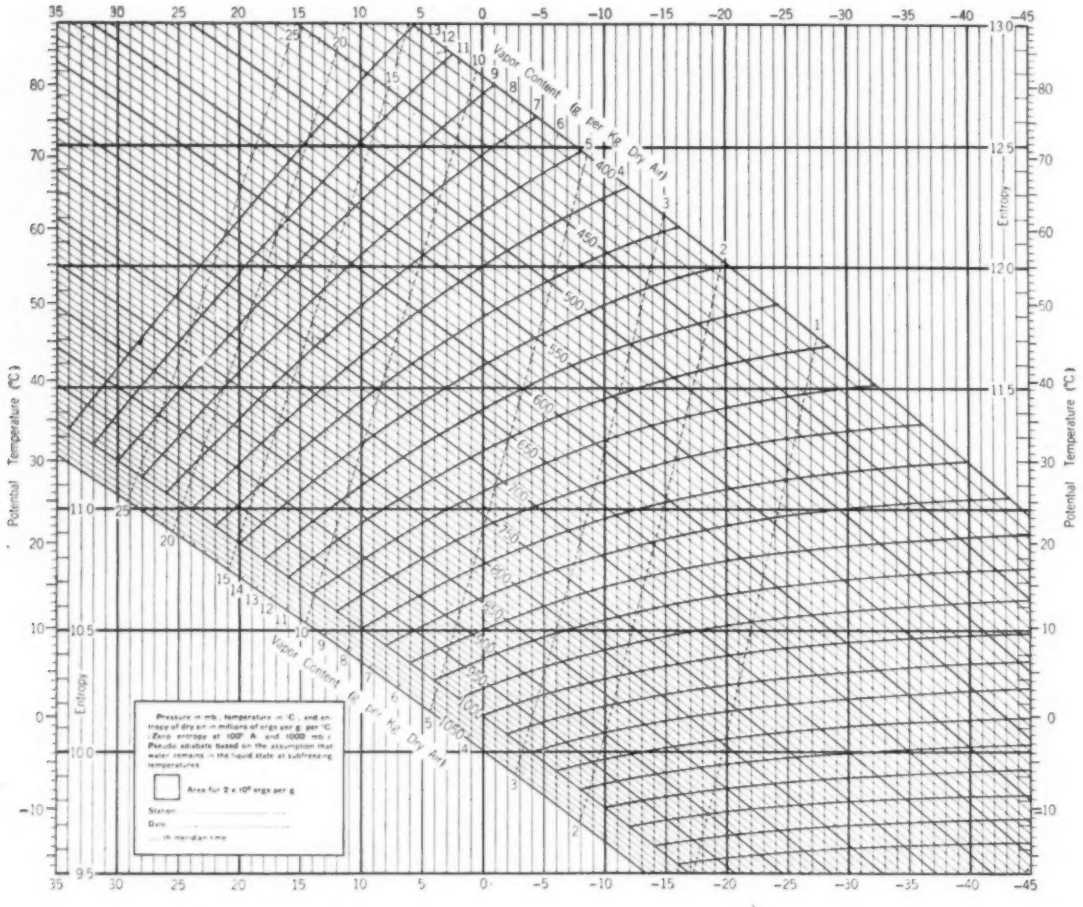


FIG. 12. Thermodynamic diagram for plotting the so-called tephigram of an upper air sounding. The observed temperature (centigrade) is plotted as abscissa, against entropy as ordinate (an equivalent logarithmic scale of potential temperature is added for convenience). The curved lines show the sequences of thermodynamic states followed by saturated air in pseudoadiabatic processes under different initial conditions, as specified by realized entropy of the air, temperature, pressure in millibars (shown by sloping solid straight lines) and water vapor content (sloping dashed straight lines). An area on this diagram represents energy. The relations of the graph of the sounding to the isentropic lines and pseudoadiabats indicate conditions of stability in the atmosphere, and the amount of energy available or required for the occurrence of meteorological processes.

atmospheric phenomena, many influences that are negligible in the laboratory become the dominating factors.[10] Weather phenomena are constantly in evidence, and vitally affect the daily life of everyone; the immeasurable pleasure to be derived from an ability to understand and appreciate this familiar element of our physical environment is ample reason for devoting attention to it in the general teaching of physics.

### *References*


1. J. Bjerknes, "On the Structure of Moving Cyclones," Geofysiske Publ. Vol. 1, No. 2 (1919). J. Bjerknes and H. Solberg, "Life Cycle of Cyclones and the Polar Front Theory of Atmospheric Circulation," Geofysiske Publ. Vol. 3, No. 1 (1922). Cf. Monthly Weather Rev. **47**, 90–100 (1919).
2. H. C. Willett, "American Air Mass Properties," Papers in Physical Oceanography and Meteorology, Mass. Inst. Tech. and Woods Hole Oceanographic Inst., Vol. II, No. 2 (1933); "Characteristic Properties of North American Air Masses," Bull. Am. Meteor. Soc. **17**, 213–238 (1936).
3. H. C. Willett, "Routine Daily Preparation and Use of Atmospheric Cross Sections," Monthly Weather Rev. **63**, 4–7 (1935); H. C. Willett, "Discussion and Illustration of Problems suggested by the Analysis of Atmospheric Cross Sections," Mass. Inst. Tech. and Woods Hole Oceanographic Inst., Papers in Physical Oceanography and Meteorology, Vol. IV, No. 2 (1935).
4. See J. Namias, "Introduction to Air Mass Analysis," Bull. Am. Meteor. Soc. **17**, 159–242 (1936); a selected bibliography is given on pp. 52–55. Horace R. Byers, *Synoptic and Aeronautical Meteorology*, (McGraw-Hill Co., New York, 1937).
5. See W. J. Humphreys, *Physics of the Air*, second edition (McGraw-Hill Co., New York, 1929), chaps. II, XV; D. Brunt, *Physical and Dynamical Meteorology* (Macmillan Co., New York, 1934), chaps. II–IV.
6. See Edgar W. Woolard, L. T. Samuels, and W. R. Stevens, "Graphical Thermodynamics of the Free Air," Monthly Weather Rev. **54**, 454–457 (1926); C. G. Rossby, "Thermodynamics Applied to Air Mass Analysis," Mass. Inst. Tech. Met'l Papers, Vol. I, No. 3 (1932); A. Refsdal, "Das Aerogramm," Met. Zeits. **52**, 1–5 (1935).
7. A brief account of a few of these is given by Edgar W. Woolard, "Recent Progress in the Physical Interpretation of Synoptic Weather Charts," Trans. Am. Geophys. Union for 1936, Part I, pp. 25–31.
8. Sverre Petterssen, "Kinematical and Dynamical Properties of the Field of Pressure with Application to Weather Forecasting," Geofysiske Publ. Vol. 10, No. 2 (1933); "Contribution to the Theory of Frontogenesis," ibid., Vol. 11, No. 6 (1936).
9. R. H. Weightman, "Forcasting from Synoptic Weather Charts," U. S. Dept. of Agric. Misc. Pub. 236, Washington (1936); "Advances and Developments in Weather Forecasting," J. Frank. Inst. **222**, 527–549 (1936).
10. See, for example, W. J. Humphreys, *Weather Proverbs and Paradoxes*, second edition (Williams & Wilkins, Baltimore, 1934).


---

*The splendour of Rutherford's contributions to science excites a wonder as to the means by which he could achieve so much. He made no claim to great mathematical ability, and many an experimenter has had fingers more clever than his. Yet he conceived and carried out a series of researches which have played a leading part in the marvelous advances of modern physics. To begin with, he brought to his work an intense interest, a tireless vitality, a singleness of purpose, a simplicity of conception and a bravery of attempt which carried him straight to the point.*

W. H. BRAGG, *Nature*, October 30, 1937

# Acoustic Vibrations

and

# Internal Combustion Engine Performance

## I. Standing Waves in the Intake Pipe System

By PHILIP M. MORSE, R. H. BODEN AND HARRY SCHECTER

*Massachusetts Institute of Technology*
*Cambridge, Massachusetts*

IT must be obvious that the behavior of a gasoline engine depends to a large extent on the motions of the fuel air and exhaust gas mixture through it. Ordinarily this motion is considered to be a steady flow; but since the flow is periodically interrupted by valves and accelerated by explosions, it is clear that each portion of the engine cycle is accompanied by acoustical vibrations of the gas concerned. These vibrations are sometimes of very large amplitude, and may hinder or aid the performance of the engine. It is the purpose of these papers to study the theory of these vibrations, and to indicate the possibilities of making them improve the engine performance as much as possible. The experimental work accompanying the study will be published elsewhere.

The present paper will concern itself with the vibrations in the intake system of a four-stroke, single cylinder gasoline engine.[1] Here the steady flow of the air[2] is interrupted for nearly three-quarters of the engine cycle, by the closing of the intake valve. This periodic interruption sets up standing waves in the intake pipe, waves which can build up an appreciable pressure amplitude just outside the valve port. Fig. 1 shows the periodic fluctuations in pressure outside the valve port of a single cylinder N.A.C.A. Universal test engine, for two different intake-pipe lengths, at one engine speed. We notice that the amplitude of one of these waves is about 5 lb./sq. in., or 1/3 atmosphere; and that waves for different lengths of pipe differ considerably. This is due to the possibility of resonance in the intake pipe. In other cases the amplitude is as large as 1/2 atmosphere.

When one of the harmonics of the engine frequency (=r.p.m./120) happens to equal one of the resonance frequencies of the intake pipe, then the pressure fluctuations at the valve will be large. If the portion of the cycle when the intake valve is just closing happens to coincide with the time when the pressure is less than average, then the waves will reduce the power output; but if the valve is just closing when the pressure is greater than atmospheric, then the waves will have a supercharging effect and will produce an increase in power.

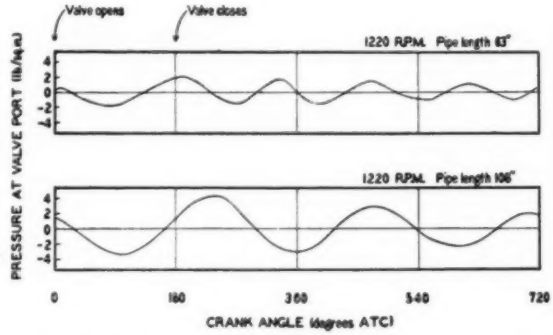


FIG. 1. Typical pressure records; constant engine speed, two different intake pipe lengths.

[1] The experimental work accompanying this paper was done by one of us (R. H. B.) in the Sloan Automotive Laboratory at the Massachusetts Institute of Technology, under the direction of Professor E. S. Taylor, and will be published by the National Advisory Committee for Aeronautics. We are grateful to Professor Taylor for considerable aid in the preparation of this paper. We are also indebted to the N.A.C.A. for permission to quote some of the material from the report submitted to them and for financial aid which made the experimental work possible.

[2] For convenience, we use the word "air" to denote the fuel-air mixture in the system.

Figure 2 shows the power output (measured as indicated mean effective pressure, i.m.e.p.) as a function of intake pipe length, for a given engine speed. The dependence on pipe length is given in terms of the frequency ratio, $q$, which is defined as the ratio of pipe frequency to engine frequency (pipe frequency being the fundamental frequency of the intake pipe when the valve is closed, and engine frequency being half the crankshaft frequency). The curve shows that when the pipe resonates to the third, fourth or fifth harmonic of the engine frequency (i.e., when $q=3$, 4 or 5) the power output increases considerably, sometimes by about 15 percent. In other cases, not shown here, the increase is as much as 25 percent.

Our purpose in this paper is to find reasons for the observed dependence of engine performance on intake pipe length, and to determine the possibilities of utilizing this effect to its fullest extent.

### *Analysis*

A simplified acoustical arrangement corresponding to the intake cylinder system is shown in Fig. 3. The intake pipe has a cross-sectional area $A_p$ and an effective length $l$; the valve port an effective cross-sectional area $A_v$ and volume $V_v$; and the cylinder an area $A_c$ and a volume which varies between $(1-\sigma)V_0$ at top dead center and $(1+\sigma)V_0$ at bottom dead center. This makes the piston stroke equal to $(2\sigma V_0/A_c)$ and the volume, when the piston is halfway up, equal to $V_0$. We shall let $\rho_0$ be the average

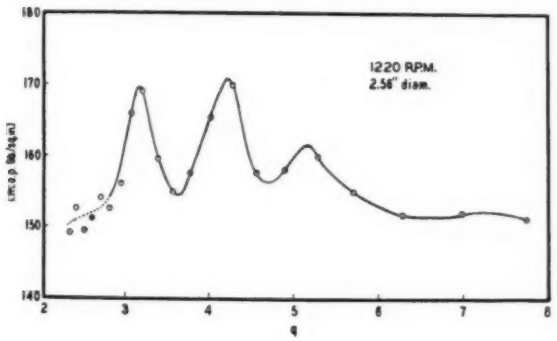


FIG. 2. Effect of intake pipe length on power output. (Power output measured as indicated mean effective pressure; frequency ratio $q$ defined as pipe frequency/valve frequency, i.e., $q \propto 1/\text{length}$, at constant engine speed.)

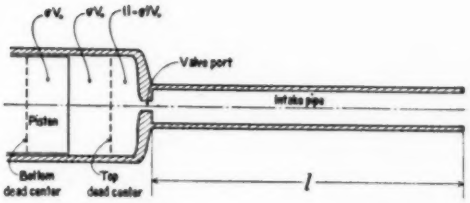


FIG. 3. Simplified representation of intake system.

density of the air, and $c$ the velocity of sound in it.

We first study the forced motion of the plug of air in the valve port. (The reaction of the air in the intake pipe on that in the valve will be considered separately.) The plug has an average mass $m=\rho_0 V_v$, an average resistance $R$, and an average stiffness constant $K=\rho_0 c^2 A_v^2/V_0$ due to the stiffness of the air in the cylinder.

If the valve were open during the whole cycle, the problem of the motion of air through the valve would be elementary. Its displacement would be sinusoidal, the reaction of the air in the pipe would therefore be easy to compute, and the amplitude of the motion could be easily obtained. However, the motion in the valve is stopped during three-quarters of the cycle, so that the motion is not sinusoidal. This affects the motion of the air in the intake pipe, which in turn may change the motion of the air in the valve when it can move. We must therefore study the motion of the air through the valve as a transient problem, coupled to the acoustic vibrations of the air in the pipe, which must be studied as a steady state problem.

We take the midpoint of the intake stroke as the origin of time. The force acting on the plug of air in the valve, while the valve is open, is $A_v[\sigma\rho_0 c^2(1+\sin 2\omega t)+p]$, where $p$ is the pressure at the valve port due to the waves in the intake pipe; the first term is the pressure due to the motion of the piston. The fundamental frequency, $\omega/2\pi$, is chosen to be the engine cycle frequency; if $N$ is the engine speed in r.p.m., $\omega=\pi N/60$.

The equation of motion of the plug is obtained by equating this force to the reaction forces of the plug,

$$m\ddot{x}+R\dot{x}+Kx=A_v[\sigma\rho_0 c^2(1+\sin 2\omega t)+p]; \quad (1)$$

where $x$ is the displacement of air through the

valve port into the cylinder (i.e., $x$ measured positive toward the left, Fig. 3).

The exact dependence of $p$ on $t$ can be known only when the dependence of $x$ on $t$ is known. An exact simultaneous solution for $x$ and $p$ can be obtained, but this solution is exceedingly complicated and impractical for general use. A little consideration of the magnitudes of the quantities involved, together with a knowledge of the experimental results, will show the possibility of an approximate solution which will be much more tractable than the exact solution, and which will be accurate enough for our purposes. We first note that for the values encountered in the experimental work, the mass and resistance of the plug may be neglected—i.e., the motion is essentially *stiffness-controlled*, and the equation of motion is (recalling $K=\rho_0 c^2 A_v^2/V_0$)

$$(\rho_0 c^2 A_v^2/V_0)x = A_v[\sigma\rho_0 c^2(1+\sin 2\omega t)+p]. \quad (2)$$

When there is no resonance in the intake pipe, the pressure $p$ is small compared to the first term on the right-hand side of Eq. (2), so it can be neglected. Consequently, while the valve is open, the motion of the air in the valve is given by

$$x=\frac{\sigma V_0}{A_v}(1+\sin 2\omega t), \quad \dot{x}=\frac{\sigma V_0 N\pi}{30A_v}\cos 2\omega t. \quad (3)$$

We shall assume, in the present paper, that the intake valve opens at top dead center and closes at bottom dead center. The velocity of the air in the valve is therefore

$$\dot{x}=\frac{\sigma V_0 N}{30A_v}\begin{cases}\pi\cos 2\omega t & -\pi/4<\omega t<\pi/4,\\ 0 & \pi/4<\omega t<7\pi/4.\end{cases}$$

This can be expanded into a Fourier series:

$$\dot{x}=\frac{\sigma V_0 N}{30A_v}\sum_n B_n\cos n\omega t, \quad (4)$$

where

$$B_0=\tfrac{1}{2}, \quad B_2=\pi/4,$$
$$B_n=-\frac{4}{n^2-4}\cos\frac{n\pi}{4} \quad (0\neq n\neq 2). \quad (5)$$

We must now turn our attention to the standing waves set up in the intake pipe. For a sinusoidal wave of frequency $n\omega/2\pi$ (i.e., the $n$th harmonic of the engine cycle frequency), the acoustic impedance at the valve is the complex quantity[3]

$$Z_n=-\frac{A_v}{A_p}\rho_0 c H_n e^{i\theta_n}, \quad (6)$$

where
$$H_n e^{i\theta_n}=\tanh\left(Fl+i\frac{n\omega l}{c}\right); \quad (7)$$

the constant $F$ is the frictional resistance term, due to the viscous drag of the air on the inside walls of the pipe. Measurements by Lehmann[4] indicate that for small amplitudes $F$ is about 0.0003/inch, but that for larger amplitudes (i.e., greater than about 0.4 lb./sq. in.), $F$ increases with amplitude. This increase is undoubtedly due to the turbulence and other irregularities which occur at large amplitudes, and is not at present susceptible to analytic investigation. Unfortunately Lehmann's measurements do not go beyond amplitudes of about 1 lb./sq. in. (where $F\simeq 0.0005$/inch); hence we have determined the value of $F$ empirically from our own measure-

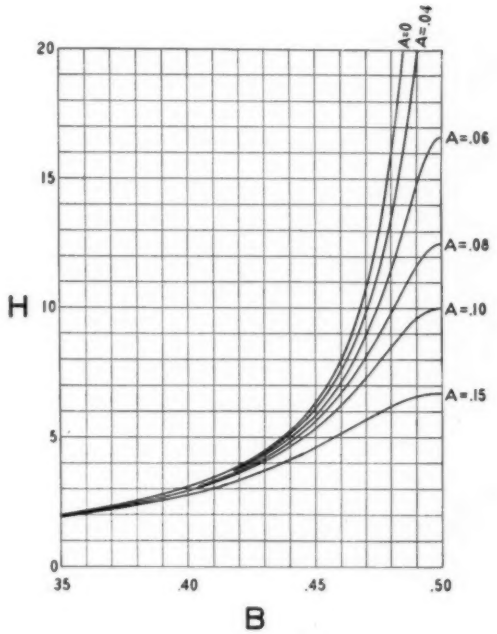


FIG. 4. Amplitude of tanh $(A+i\pi B)$ as function of $B$, for different values of $A$, from $A=0$ to $A=0.15$.

[3] Philip M. Morse, *Vibration and Sound* (McGraw-Hill, New York), page 214.
[4] K. O. Lehmann, Ann. d. Physik **21**, 533 (1934).

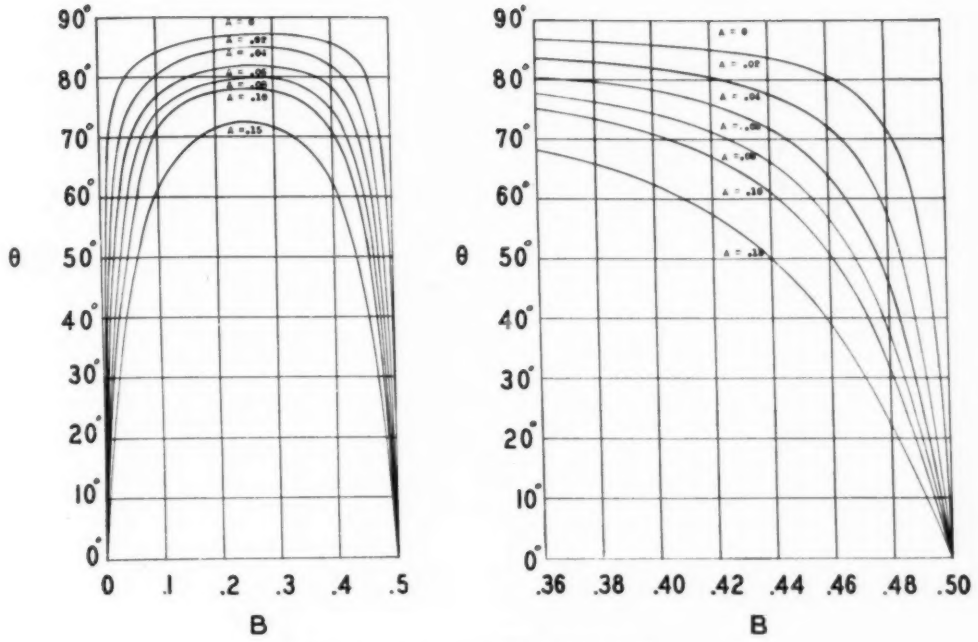


FIG. 5. Phase angle of tanh $(A+i\pi B)$.

ments and calculations: the value is about 0.001 per inch. (Note that all the foregoing values of $F$ are for pipes of about 2.6 inch diameter, and for frequencies of the order of 30 to 90 Hz.)

In terms of the frequency ratio $q=30c/Nl$ introduced above, Eq. (7) may be rewritten

$$H_n e^{i\theta_n} = \tanh (A+i\pi B) \qquad (8)$$

with $A \equiv 30cF/Nq$ and $B \equiv n/2q$. The magnitude $H_n$ is plotted in Fig. 4, and the phase angle $\theta_n$ in Fig. 5, both as functions of $A$ and $B$.

From Eqs. (6) and (4), the expression for the pressure just outside the valve port is

$$p = -\frac{\rho_0 c\sigma V_0 N}{30 A_p} \sum_n B_n H_n \cos (n\omega t + \theta_n). \qquad (9)$$

This is, of course, an approximate expression for $p$, and is valid only as long as $p$ is not large enough to alter the flow of air through the valve. Actually, we are interested in studying the cases where $p$ does influence the air flow, where Eq. (9) is not valid. However, a study of Eq. (9) is useful, for its general behavior will indicate to us where we should expect a supercharging effect of pressure, where we will need a more exact solution for $p$.

In the first place a study of the dependence of $H_n$ on $q$, the length factor for the pipe, shows that whenever $n/q=nNl/30c$ is an odd integer, resonance will occur, $H_n$ will become large, and the $n$th term in the series for $p$ will be large. When $q=1$, every odd value of $n$ satisfies this requirement, and $p$ has the dependence on time shown in Fig. 6a, corresponding to a negative-pressure pulse, caused by the suction through the valve, traveling down the pipe, reflecting once as a positive pulse, then returning as a negative pulse in time for the next valve opening. This case can give no supercharging effect, because the pressure is below normal during the whole time the valve is open. When $q=2$, $n=2$ and $n=6$ are exaggerated (but $n=6$ does not enter because $B_6=0$). The pressure wave has the form shown in Fig. 6b. Again there is no supercharging. In the cases $q=3$, 4 and 5, the $n=3$, 4 and 5 partial waves are exaggerated, as shown in Figs. 6c, d and e. In these cases, supercharging is to be expected, for the pressure rises above normal before the valve closes. In the case $q=6$, there is no resonance, for $B_6=0$. For the higher cases, $q=7$, 8, etc., the corresponding $B$'s are so small that resonance is not marked. Approximate formula (9), therefore,

predicts that the supercharging will occur when $q=3$, 4 or 5, and for no other values; that is, when the intake pipe, considered as a closed organ pipe, resonates to the third, fourth or fifth harmonic of the engine cycle frequency. This is just the result found experimentally, as shown in Fig. 2.

Thus our crude analysis for $p$, inaccurate as it is, at least indicates where supercharging occurs. To find out about the details of the air motion when these resonances occur, we must include, in our equations, the effect of $p$ on the air velocity through the valve port. This leads to analytic complications, but since we have limited our interest at present to resonance cases, we can simplify our expressions in other respects. We will assume that just the one large term in the expression for $p$ is present, when we study its effect on $\dot{x}$. Then we can work the problem through and find what value of $p$ makes the equations at least approximately self-consistent.

Suppose $q \backsimeq k$, where $k=3$, 4, or 5. We then assume that the pressure is of the form

$$p \backsimeq -P_k \cos(k\omega t - \phi_k) \tag{10}$$

and set this in Eq. (2), solving for $\dot{x}$ as before, to obtain

$$\dot{x} = \frac{\sigma V_0 N}{30 A_v} \begin{cases} \pi \cos 2\omega t & \\ \quad + \dfrac{k\pi P_k}{2\sigma\rho_0 c^2} \sin(k\omega t - \phi_k) & -\dfrac{\pi}{4} < \omega t < \dfrac{\pi}{4} \\ 0 & \dfrac{\pi}{4} < \omega t < \dfrac{7\pi}{4} \end{cases}$$

Next this expression is converted into a Fourier series. Making a small approximation in calculating the coefficients (neglecting all but the resonance term for $p$), this series becomes

$$\dot{x} = \frac{\sigma V_0 N}{30 A_v}\left[\sum_n B_n \cos n\omega t + \frac{P_k}{2\sigma\rho_0 c^2} D_k \sin(k\omega t - \phi_k)\right], \tag{11}$$

where the $B_n$ are the same as before (Eq. (5)) and to a small approximation

$$D_k = \frac{k\pi}{4}. \tag{12}$$

Near resonance, the $k$th term in the $\Sigma$ of Eq. (11) will predominate, so that, using Eq. (6), the pressure may be written

$$p \backsimeq -\frac{\rho_0 c V_0 N H_k}{60 A_p}\left[2\sigma B_k \cos(k\omega t + \theta_k) + \frac{P_k D_k}{\rho_0 c^2} \sin(k\omega t - \phi_k + \theta_k)\right] \tag{13}$$

Comparing this with Eq. (10), we have

$$\cos(k\omega t - \phi_k) = C_k \cos(k\omega t + \theta_k) + \delta_k \cos(k\omega t - \phi_k + \theta_k - \pi/2), \tag{14}$$

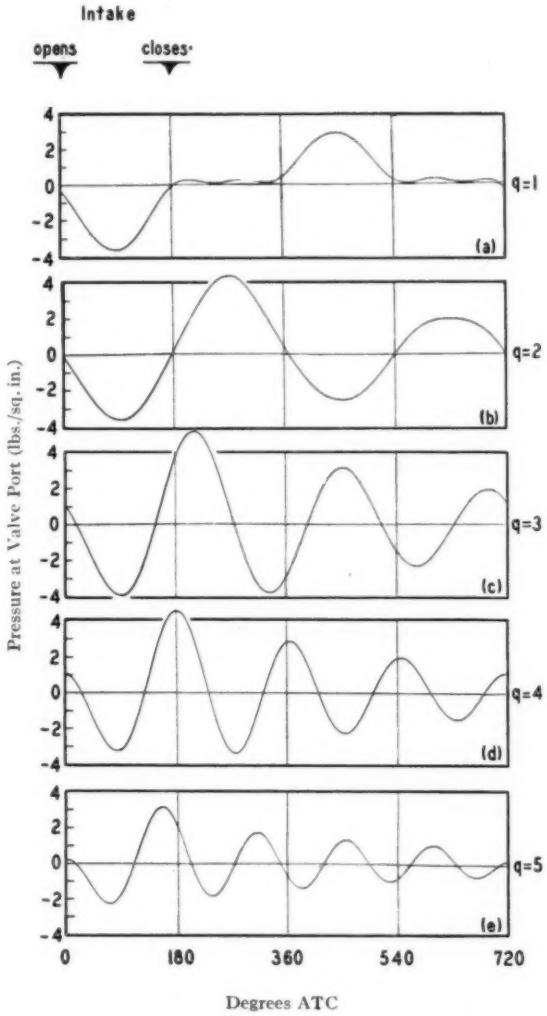


FIG. 6. Calculated pressure curves (first approximation, neglecting reactive effect of pressure waves in intake pipe). 1220 r.p.m., $A = 0.40/q$.

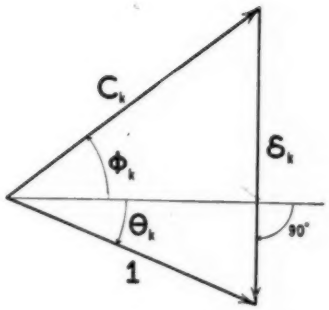


Fig. 7. Typical vector diagram for solution of Eq. (14).

where

$$C_k \equiv \frac{\rho_0 c\sigma V_0 N B_k H_k}{30 P_k A_p}, \quad \delta_k \equiv \frac{V_0 N D_k H_k}{60 c A_p}. \quad (15)$$

Since $\delta_k$ and $\theta_k$ are known in terms of the engine constants, Eq. (14) can be solved, by the use of a vector diagram such as shown in Fig. 7, for $C_k$ (hence $P_k$) and $\phi_k$. For instance, when there is exact resonance, $q=n$, then $\theta_k=0$, and

$$\tan \phi_k = V_0 N D_k H_k / 60 c A_p,$$

$$P_k = \rho_0 c\sigma V_0 N B_k H_k \cos \phi_k / 30 A_p.$$

This differs from the more approximate expression for $P_k$ given in Eq. (9), by the factor $\cos \phi_k$, and also by the presence of the phase angle $\phi_k$.

Therefore the interrelations between pressure and air movement in the valve, the fact that air *displacement* is proportional to pressure whereas pressure gradient is proportional to air *velocity*, produces a phase lag $\phi_k$ in the pressure wave. This phase lag is small when $H_k$ is small, i.e., when there is no resonance: then the pressure in the intake pipe plays an inconsiderable role in forcing the air into the cylinder. On the other hand, when the pipe has been tuned to resonance, and the diameter of the pipe has been made large to reduce viscous drag, then $H_k$ may become very large, and the phase lag of the pressure wave may be nearly ninety degrees.

### *Results and Discussion*

A corrected expression for the pressure at the valve port may now be obtained by using the term given in Eq. (10) in place of the $k$th term of the series in the uncorrected expression (Eq. 9), $k$ being the integer nearest to $q$. This corrected expression is (using Eq. (15))

$$p = -\frac{\rho_0 c\sigma V_0 N}{30 A_p}\left[\sum_{n\neq k} B_n H_n \cos(n\omega t + \theta_n) + \frac{B_k H_k}{C_k}\cos(k\omega t - \phi_k)\right]. \quad (16)$$

To find the volumetric efficiency, we note that at time $t$, the amount of air that has flowed into the cylinder since the beginning of the intake stroke is

$$Q = A_v x$$

$$\doteq \sigma V_0\left[1 + \sin 2\omega t - \frac{P_k}{\sigma \rho_0 c^2}\cos(k\omega t - \phi_k)\right]. \quad (17)$$

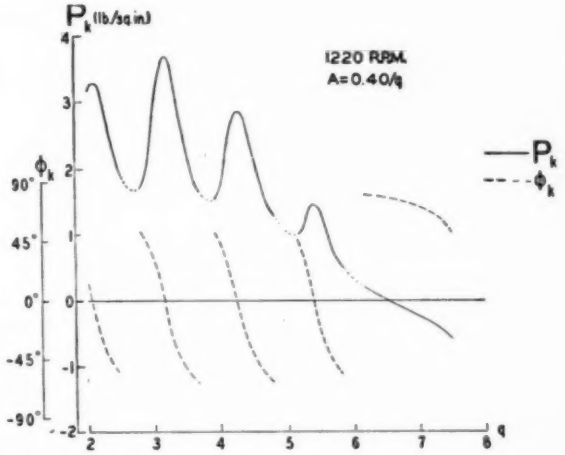


FIG. 8. Quantities $P_k$ and $\phi_k$ as functions of $q$.

The volumetric efficiency, defined as the ratio of air consumption per cycle to displacement volume, i.e., ($Q$ at time of intake valve closing)/($2\sigma V_0$), is thus given by

$$E \doteq 1 - (E_k/C_k)\cos(k\pi/4 - \phi_k), \quad (18)$$

where $E_k \equiv B_k \delta_k / D_k$. The volumetric efficiency can be taken as a measure of the supercharging effect of the intake pipe wave motion, and is presumably proportional to the power output of the engine.

From Eq. (18) it is apparent that the condition for maximum supercharging is not necessarily exactly $q=k$, for then $\theta_k$ is zero, and $\delta_k$ is a maximum, making $\phi_k$ large; perhaps too large. If $q$ be a little larger than $k$ (i.e., $l$ or $N$ a little

less than for exact resonance) then $\theta_k$ is larger than zero and there is a chance that $C_k$ decreases more than $E_k$ decreases. That this is borne out in practice will be shown later.

It is well to recapitulate here our assumptions and approximations. We have assumed that the intake valve port is large enough so that the friction here is small, and that the effective

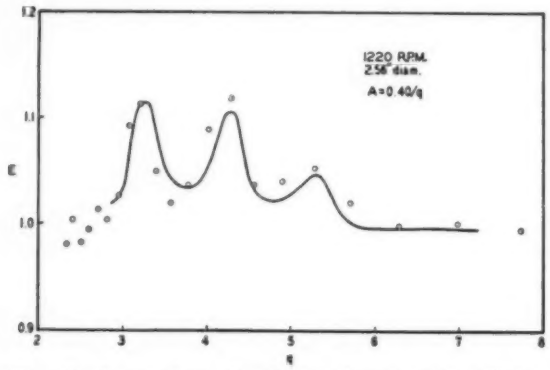


FIG. 9. Comparison of calculated volumetric efficiency and measured power output. The solid line shows the computed volumetric efficiency $E$ as a function of the frequency ratio $q$; for the experimental points the ordinates are measured i.m.e.p. (lb./sq. in.) divided by 152, and the abscissae are frequency ratio $q$ determined from $q=30c/Nl$ = 325/pipe length in inches.

length of the port is small enough so that it presents no appreciable inertial reaction to the forces. If this is true, then the displacement of the air will be proportional to the force. We have assumed that the diameter of the intake pipe is large enough so that the viscous drag on the air is not so large as to cut down the resonance. As a matter of fact, one should compromise on the choice of best pipe diameter: a large pipe decreases friction but its larger capacity is less responsive to the intermittent sucking action of the engine, as is evidenced by the factor $(1/A_p)$ in the expression for $E_k$. Presumably the pipe should be between 2 and 4 inches in diameter for 1200 r.p.m., though the lower limit might be reduced if the engine speed were made higher, since the length of intake pipe needed for resonance could thereby be reduced.

The equations also show a considerable increase in effectiveness of the standing waves as the engine speed increases, both directly through the factor $N$ in $E_k$, and indirectly through the reduction in length of resonating pipe and its possible decrease in diameter.

In this analysis we have made no mention of the effect on the results of a change of valve timing. It is clear that such a change may have a considerable effect on the results. The modifications necessary to include this effect are obvious, however, and need not be elaborated on here.

### *Numerical Computations; Check with Experiment*

Taking the velocity of sound as 1100 ft./sec., we have

$$q=396{,}000/Nl,$$
$$\delta_k=0.992\times10^{-6}kNV_0H_k/A_p,$$

where all dimensions are in inches. For the N.A.C.A. engine[1] used in this work, the constants were:

$$\sigma=2/3, \quad V_0=103.2 \text{ cu. in.}, \quad A_p=5.16 \text{ sq. in.},$$

so that $\delta_k=1.98\times10^{-5}kNH_k$. The value of $F$ has been chosen to be 0.00123/inch, making $A=488/Nq$.

The quantities $H_k$ and $\theta_k$ are found from Figs. 4 and 5; the quantities $C_k$ and $\phi_k$ are found by means of a vector diagram such as shown in Fig. 7. The quantity $E_k$ is found from $E_k=\delta_kB_k/D_k$, using the following values:

| $k$ | 2 | 3 | 4 | 5 | 6 | 7 | 8 |
|---|---|---|---|---|---|---|---|
| $B_k/D_k$ | 0.5000 | 0.2401 | 0.1061 | 0.03427 | 0.0000 | −0.01144 | −0.01061 |

Calculations have been made for an engine speed of 1220 r.p.m. The values of $\phi_k$ and $P_k$,

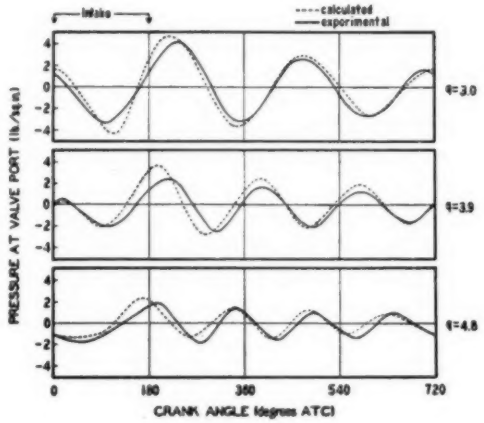


FIG. 10. Comparison of calculated pressure curves and measured pressure records. 1220 r.p.m., $A=0.40/q$.

as functions of $q$, are shown in Fig. 8, and the resulting values of the volumetric efficiency $E$, as a function of $q$, in Fig. 9 (solid line). The experimental measurements of power output are also shown in Fig. 9, for comparison. The pressure at the valve port, as a function of time, has been calculated (using Eq. (16)) for three intake pipe lengths; the resulting curves are shown in Fig. 10 (dotted lines), with the experimental curves (solid lines) superimposed for comparison. In view of the analytical intractability of the physical phenomena and the approximateness and relative simplicity of the analysis, the agreement between experiment and theory is considered quite satisfactory.

Thus we see that the acoustic vibrations in the intake system can have a marked effect on engine performance; and that calculations based on the usual acoustical theory check the experimental data sufficiently well. The work discussed here is for a single-cylinder engine; further work is in progress on multicylinder engines. Preliminary results indicate that simply using a single intake pipe as resonator for all the cylinders gives poor results; and that an acoustic filter network must be used to obtain optimum results.

---

*Students trained in physics can use their knowledge as a background in the essential job of keeping civilization going. The circuit work of a telephone company, for example, can only be done by a man thoroughly trained in physics. And there are countless examples in the automobile industry and elsewhere of the important work the physicist does for the everyday needs of mankind. The predicted exhaustion of natural resources for the use of mankind in his daily round and diminishing coal and oil resources for fuel purposes, make the physicist's work one of vital concern to every man, woman and child. It's the job of the physicist to find ways of conserving what we have and also of finding substitutes to use when the present supplies of oil and other fuels give out. A way is rapidly being found to use the ordinary heat energy of the sun and make it work for us. Up to now we have simply been wasting an available source of limitless energy.*

ROBERT A. MILLIKAN

# *The* Daniel Guggenheim Airship Institute

By TH. TROLLER

*Daniel Guggenheim Airship Institute*
*Akron, Ohio*

### *Introduction*

THE Daniel Guggenheim Airship Institute was founded in 1929 at the time when construction of the two large Navy airships, the Akron and the Macon, started. It was established as a cooperative project between the Daniel Guggenheim Fund for the Promotion of Aeronautics, the University of Akron and the California Institute of Technology.

The idea of a scientific institute entirely dedicated to the problems of this one branch of aeronautics was first conceived by Dr. George F. Zook, at that time president of the University of Akron, who first approached the Daniel Guggenheim Foundation for the Promotion of Aeronautics, for its assistance. The Guggenheim Foundation made possible the establishment of the Airship Institute by a substantial grant for the purchase of research equipment and for the operation of the Institute during the first years of its existence. The city of Akron, through the University of Akron, contributed the funds for the main part of the building to be situated near the airport, where the large airships were in construction. California Institute of Technology supervised the scientific work of the new laboratories for a period of five years, inasmuch as the University of Akron had no aeronautical department. California Institute of Technology appointed Dr. Th. von Kármán, director of research. Dr. von Kármán supervised the work of the Institute until October, 1934, at which time the University of Akron took over its full administrative direction, retaining Dr. von Kármán as scientific advisor.

The institute had to provide means of research required by the particular needs of airships. The plans called for aerodynamic, meteorological, structural and general physical research, with the emphasis on basic aerodynamic and aerological problems. The result of the specific requirements is a laboratory equipped with a number of unique test stands.

### *The Vertical Wind Tunnel*

The oldest part of the aerodynamic equipment is a vertical wind tunnel with a free jet of $6\frac{1}{2}$ feet in diameter, blowing upward with velocities up to 125 miles per hour. The wind tunnel (Fig. 2) is of the Göttingen type (Prandtl type), having a closed return and an open test section. The general layout follows the rather standardized pattern for such wind tunnels, being unusual only in that a vertical jet is used for testing rather than the more common horizontal one.

FIG. 1. View of Daniel Guggenheim Airship Institute at Akron airport.

The "vertical tunnel" was chosen because it gives a better accessibility of the model test set-up. Also it was considered important, at the time when the first plans for this tunnel were made, to be able to suspend an airship model hanging down by means of only one suspension wire, connected to the tail of the airship model; thus the interference of connections and their effect on the drag measurement was reduced to a negligible value. The layout of this wind tunnel was made upon suggestions of Dr. Arnstein and Dr. Klemperer of the Goodyear-Zeppelin Corporation, who helped with their advice on the early plans for the equipment of the institute.

### *The Whirling Arm*

A different type of aerodynamic test stand was built later. Whereas in the wind tunnel the model is stationary and an artificial wind blowing against it is created by means of a fan, the aircraft model on the whirling arm is moved around in a circle while observations are being made. The whirling arm was used in the early days of aeronautical research, for instance by Langley and Lilienthal, to investigate the characteristics of airfoil sections. Later the wind tunnel replaced these whirling arms as tools of aerodynamic research, except for special types of investigations such as the calibration of anemometers at very low speeds. The advantage of the wind tunnel lies in the fact that it duplicates straight movement, the most interesting flight condition, the stationary model making force measurements easy, whereas the models on the whirling arm, subjected to high centrifugal forces, require more complicated balance systems and are not accessible to direct observation. Also, due to the movement of the model on the whirling arm, a disturbing swirl is set up in the air which makes it difficult to obtain clear test conditions, while the wind tunnel delivers a relative wind with a high uniformity in time and space.

However, the whirling arm is again of considerable interest for aeronautical research, since the advancing aircraft development requires data on the effect of curved motion on the air forces on aircraft. The whirling arm of the Guggenheim Airship Institute is the only one available in this country for such tests on models of airplanes and airships. Also, it is larger and built more substantially—thereby permitting higher velocities —than the one of the National Physics Laboratory in England, which, to the knowledge of this writer, is the only other whirling arm used at present for aircraft model testing.

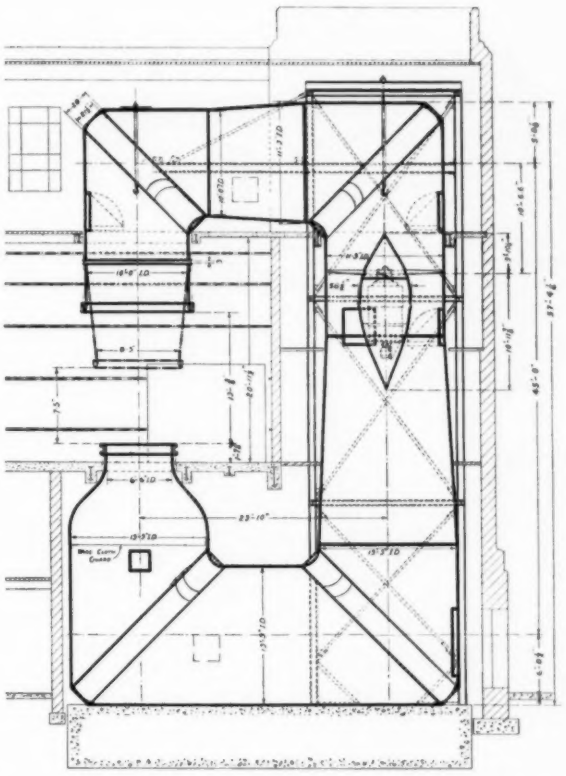

FIG. 2. Diagrammatic view of the vertical wind tunnel of the Daniel Guggenheim Airship Institute.

The Akron whirling arm is essentially a horizontal pipe, composed of four tapering sections, that turns about a vertical shaft (see Fig. 3). The horizontal arm has a radius of 32 feet to the center of the model under investigation and carries the model with velocities up to 175 miles per hour, the possible top speed depending mainly on the weight of the model. At 175 miles per hour model speed, equivalent to 75 r.p.m. of the arm, the model is acted upon by a centrifugal force 56 times its weight.

Circular walls eight feet outside and inside of the model path, with three wire screens across the round tunnel formed by these walls, floor and ceiling, reduce the swirl along the path of the

model to a tolerable amount. The inner circular wall has a slot just wide enough for the passage of the arm and eliminates the pumping effect of the turning parts. The wire screens have openings just wide enough to let the arm and model pass through with little influence on the potential air flow about the model, but offering a high resistance to the spreading frictional wake behind it. To make sure of the amount of the disturbance in the air, measurements of the air movement are made for models of high resistance by means of hot-wire anemometers, which record the momentary magnitude and direction of the swirl.

All types of records customary in aerodynamic investigations have been made on this whirling arm: investigations of the air flow about an aircraft model, pressure distribution measurements and force measurements.

Air flow pictures are obtained by painting the surface of wings with a lampblack kerosene mixture, which leaves traces in the flow direction on the surface after the kerosene has been blown off and evaporated. It is only necessary during the tests to make sure that the surfaces of the wing are essentially in a plane perpendicular to the resultant of centrifugal and gravity forces, so that there are no falsifying influences from the centrifugal forces on the lampblack particles. Flow investigations of another type are made by means of hot wire anemometers. This type of test and the force measurements undertaken so far will be discussed with the gust tunnel.

Pressure distribution measurements are made by means of a multiple manometer that turns with the arm. There are 60 glass tubes arranged around the vertical center shaft which can be connected through tubes inside the radial arm with pressure orifices distributed over the surface of an aircraft model. To record the pressure at these orifices, light sensitive paper is slipped behind the manometer tubes and some floodlights are turned on during the test run to expose the paper, marking the alcohol menisci of the tubes. The manometer tubes are interconnected and two or three of them serve as zero references, being open to atmospheric pressure. The true pressure at the location of one of the orifices is found by adding to the manometer reading the centrifugal force acting upon the air column between the manometer and the orifices. The distance of the manometer from the center of rotation being small, this correction is almost exactly equal to the velocity head $q=\rho r\omega^2/2$, with $\rho$, air density; $r$, radial distance of the orifice from center of rotation; $\omega$, turning speed.

The whirling arm seemed to offer an opportunity for the investigation of certain unsteady flight conditions which cannot easily be represented by wind tunnel tests: the approach of the ground during the landing or the passage through gusts. The possibility of such tests had already been under consideration when the first plans for the whirling arm were prepared and the balance system for use on airship models on the whirling arm was therefore designed so as to permit the recording of fast changing forces. This balance has been used in the meantime for tests regarding gust effects on airships. For the reproduction of such gust effects a special wind tunnel was built connected to the housing of the whirling arm.

### *The Gust Tunnel*

This tunnel, built in 1935, is also shown in Fig. 3. It is a vertical wind tunnel placed in the

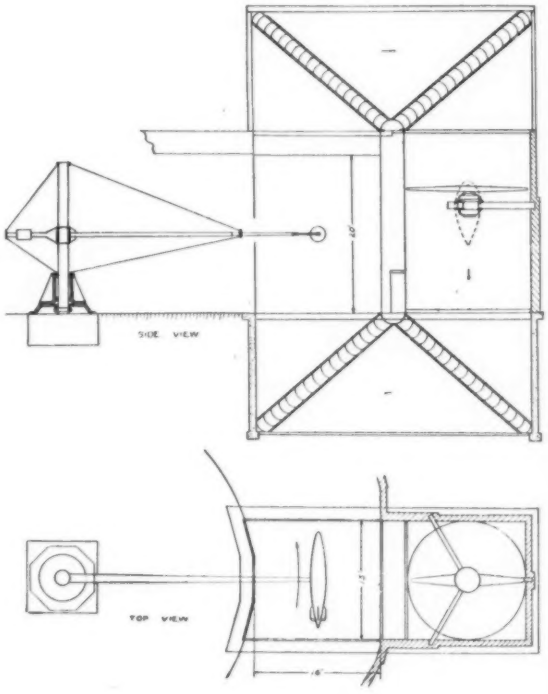


FIG. 3. Diagrammatic drawing of the whirling arm and gust tunnel of the Daniel Guggenheim Airship Institute.

path of the aircraft model on the whirling arm in such a way that the model, traveling horizontally, passes through a vertical updraft for a distance of 16 feet. The air forces acting upon the aircraft model are the same as those experienced by an aircraft when entering and passing through a gust before the flight path is changed by the gust influence.

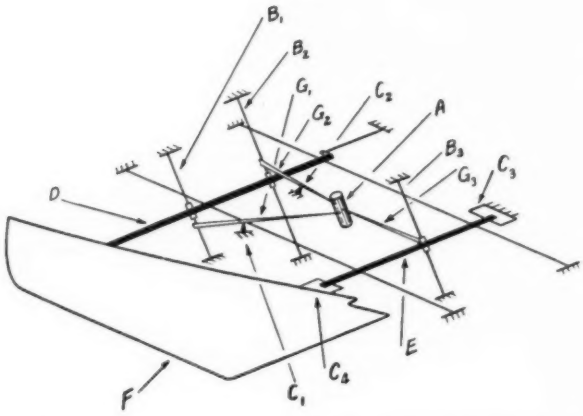


FIG. 4. Suspension of an airship fin against the hull for measurement of gust forces. $A$, Glass cylinder; $B_{1,2,3}$, lift wires; $C_{1,2,3}$, hinge points; $D$, front spar; $E$, rear spar; $F$, fin.

The vertical upward velocities inside the artificial gust are fairly uniform. At the two sides, where the jet of air forming the gust is passing the air at rest of the surrounding room, there is a transition zone, in which the vertical velocities fall from the full velocity value inside the gust to zero outside. The width of this transition zone—inversely proportional to the gust steepness—can be adjusted within certain limits. It can be narrowed by building up walls, from the edge of the gust tunnel jet entrance, which is eight feet below the model path. The width in one cross section of the transition zone is directly proportional to the distance of this cross section from the line at which the free jet starts. It can be widened by inserting guide vanes into the jet below the model path. The velocity distribution in these transition zones prepared for a particular test must be equivalent to that measured in a gust in the atmosphere. Measurements of such atmospheric gustiness also form a part of the institute's work and are discussed later. They indicate, for instance, that in the atmosphere a cross wind change of 8 m/sec. can occur over a horizontal distance of 37 meters. To have geometric similarity with such a gust on a 1/75 scale model of an airship, it is necessary to provide a transition zone width of about 0.5 meters.

Force records on models of aircraft passing through the gust are made at this institute by means of diamond points scratching on glass. This permits reading of forces with small displacement of the force carrying system. The general arrangement is that the model as a whole or a part thereof—if it is desired to measure the inner forces or stresses—is suspended by means of wires, which elongate under the action of air forces. The elongation of the wires is transferred through suitable lever systems to a diamond point which moves with slight pressure over a turning glass cylinder. The line traced by the diamond is then observed under the microscope with a linear enlargement of about 1 to 250. The suspension wires are chosen so that their elongation and the displacement of the model is about 0.1 mm. This small displacement, together with light models, reduces the inertia influence on the force records to a small value which can be corrected after some dynamic calibrations. The apparatus is illustrated here by one typical adaptation: the measurement of the air forces on an airship fin (Fig. 4). The whole suspension system supporting the fin is housed inside the tail of the airship hull. There are spars extending inside, from the fin itself, to which wires are fastened. Levers are clamped to one end of the wire, opposite to the end fastened to the hull, or the levers are connected to the spars. The diamonds at the free end of the levers move proportional to the wire extension in the direction of the axis of the glass cylinder. The glass cylinder is driven by a little synchronous motor.

It is a particular problem of the test technique of these whirling arm gust tests to build models light and at the same time strong enough to withstand the aerodynamic and centrifugal forces. In particular, models of airships with their large dimensions in the direction perpendicular to the radial arm, need careful design. One particular model of 12 feet in length was built by electroplating a copper shell of ten thousandths of an inch thickness. This shell, without inner sup-

porting structure was put under an inside pressure of about 0.4 atmos. over outside atmospheric pressure in order to have an initial tension in the whole shell. This insures strength against bending because compression stresses are avoided throughout the shell and there is no danger of buckling of the skin. The principle is the same as that of pressure type airships.

Investigations of the air flow about a model during its passage through the gust are made by means of hot wire anemometers. In addition to the well-known anemometer for the measurement of the magnitude of rapid fluctuations of air velocity an instrument for the recording of rapid direction changes, developed at the institute by F. D. Knoblock, is in use. The principle of such measurements is illustrated by Fig. 5. Two thin platinum wires, forming two legs of a Wheatstone bridge, are heated electrically. They are suspended between three prongs of a fork, so that they form an angle of about 100° at their apex, which points in the average flow direction. When the instrument is hit by an airstream inclined against its plane of symmetry, the wires are cooled unevenly, their resistance, changing with their temperature, unbalances the bridge and the current in the oscillograph across the bridge indicates the angle of flow. The instrument covers a range from zero to about 40° and has in this range the desirable characteristic that the indicated angle is very little affected by the magnitude of the velocity. This instrument, due to its small time lag has proved very helpful in finding out the general characteristics of the rapidly changing flow pattern in gusts.

### *The Water Tank*

It is of great interest for the aeronautical engineer to study in the laboratory the movement of aircraft in flight under the influence of atmospheric disturbances and willful operation of the steering surfaces. The prime requirement of such laboratory tests is dynamic similarity, so that the weights and moments of inertia of the model are reduced in the same ratio as the air forces and acting moments. It is considered impossible to build airship models in a size that can be handled in a laboratory and have the weight reduced proportional to the third power of the longitudinal scale. Such a reduction in size would mean, e.g., to build a 12-foot model of the Akron or Hindenburg weighing only about one pound and nevertheless strong enough to stand local air pressures of 20 pounds per square foot and bending moments of about 15 foot pounds at its center section without visible deformation. Because no means seemed available to construct such a model, Dr. A. M. Kuethe suggested tests in water to study airship movements experimentally. Accordingly, a water tank was built (Fig. 6) in which an airship model can be exposed to conditions similar to atmospheric gustiness. The tank consists of a rectangular circuit similar to a horizontal wind tunnel, except for the free surface of the water. The arms of the *C* forming the return ducts for the water and the free jet in the open gap of the *C* have a width of about eight feet and a depth of five feet three inches. The water also extends perpendicular to the axis of the jet, between the two end points of the *C*, forming a straight channel eight feet wide and five feet three inches deep. An airship model can be pulled along this straight section with a special carriage which permits it to turn freely about its

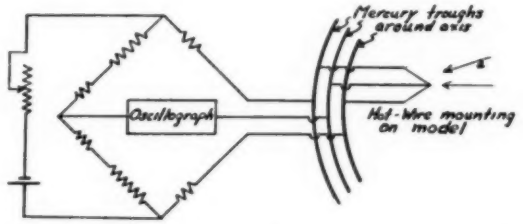


FIG. 5. Hot wire instrument for the measurement of flow direction about models on whirling arm.

center of buoyancy and to move sideways in the direction of the gust under the action of the "gust." The free movement is recorded and conclusions about acting forces and stresses created in a flying airship can be drawn.

### *Aerological Research*

The laboratory research about effects of atmospheric gustiness on aircraft can only be of value if the nature of this atmospheric turbulence is known and understood sufficiently to permit application of laboratory test results to free flight conditions. A part of the work of this institute is, therefore, dedicated to studies of features of the atmospheric gustiness about

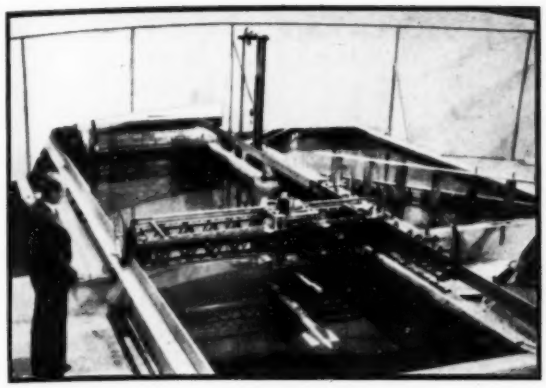

FIG. 6. Water tank for testing free movements of airships in flight.

which the knowledge available at present is unsatisfactory. The emphasis in these investigations is placed on atmospheric turbulence of such wave-length—or with air parts of such magnitude in discernible motion against the surrounding air—that appreciable forces on aircraft may be caused by it: this means then investigation of air waves of a length of the same order of magnitude as that of the overall dimension of an aircraft or of its important air force creating parts.

The investigations carried on at the institute are made by means of instruments mounted on towers. Magnitude and horizontal and vertical direction of the wind fluctuations are recorded together with the temperature lapse rate (vertical temperature gradient) which is measured by temperature difference recorders. A wind direction indicator of small inertia, but sturdy enough to serve as a field instrument, was designed for this investigation by Dr. R. P. Harrington. The temperature gradient is watched particularly, because during the early gust measurements at the institute, Dr. F. L. Wattendorf found that there was a marked influence of this temperature lapse rate on the gustiness of a wave-length of the order of magnitude of one airship length. The tests were first conducted with instruments on a 50′ meteorological tower on the roof of the institute and are at present proceeding with the cooperation and financial subsidy of the Navy Department at the airport of the Naval Air Station in Lakehurst, New Jersey. There are three towers available, one of them movable, permitting the synchronized reading of a number of instruments which show the momentary spatial extent of gusts.

### *Miscellaneous Research*

There is a small laboratory for general physical research and, in particular, for studies on metals used in aeronautical structures. It contains x-ray equipment for surface diffraction pattern photography, a surface microscope, strength testing machine, etc. Dr. R. H. Hobrock, who arranged the equipment of this laboratory, used it, in particular, for the study of welding properties of strong aluminum alloys.

At present a variety of industrial problems are handled by the Institute, ranging from standard strength tests to streamlining of trains or the wind pressure on open air structures.

---

*It is well known that Professor P. E. Tait measured the starting speed of a golf ball and thought he had proved mathematically that its range could not be more than about two-thirds of the distance that his son proceeded to drive it.*

SIR GILBERT WALKER, in *Nature*

# True Stress Strain Curves for Polycrystalline Material

R. K. HASKELL

*Captain, Ordnance Department, U. S. A.*
*Watertown Arsenal, Watertown, Massachusetts*

THE true stress strain curve has only within recent years been considered seriously as having any value. It has many interesting properties. Some of the most important are not yet well understood. In order that we shall all have the same concepts, a definition of a true stress strain curve is in order. The true stress strain curve is a plot of the actual plane stress on the least area of a specimen as ordinate and the corresponding values of elongation as abscissa. Various investigators have, from time to time, suggested plotting the true stress against change in diameter, or change in area or elongation based on change in area, etc. The method of plotting will be governed by the information desired.

Certain precautions in the obtaining of data for the curve must be observed. The testing machine used should be a straining type, as exemplified in the screw power machine. A loading type of testing machine, as exemplified in the hydraulic loading type, is unsatisfactory. The straining type of machine has the characteristics of rapidly relieving the applied load for small amounts of creep in the specimen. A specimen strained into the plastic region will undergo a small amount of crystal recovery accompanied by slight creep. Change in load with creep and crystal recovery stops when equilibrium conditions are established. Readings are taken after the machine is stopped, and equilibrium conditions established. The test specimen should have a slightly tapered cylindrical gauge section, bounded on each end by plane sections of approximately twice the gauge section diameter. The ratio of length to diameter of gauge section should preferably be the same as laid down for test specimens by the A.S.T.M. An extensometer, designed to measure between the parallel faces at the end of the gauge section, and a micrometer, for measuring the changes in diameter, are necessary.

The speed of pulling is most important. An autographic curve is not desirable. After a small straining of the specimen, the testing machine should be stopped and equilibrium conditions obtained before readings of load, elongation and diameter are made. The reasons for the waiting for equilibrium conditions will be discussed later. Values of stress are obtained by dividing the

*This paper formed part of the Round Table Discussion on the Physical Basis of Metallic Properties held in connection with the Metals Congress at Atlantic City, October 18, 1937. Approximately 200 people attended this meeting which was opened by Professor John T. Norton who is the permanent chairman of these Round Table Discussions. He introduced Professor L. W. McKeehan who acted as technical chairman for the session. Much of the success of the meeting was due to the informal discussions prompted by Dr. McKeehan. Other formal papers in the scheduled part of the program were "True Stress-Strain Curves for Single-Crystals" by Dr. S. L. Hoyt and "Internal Dissipation of Energy in Metals for Small Cyclic Strains" by Dr. R. L. Wegel. These papers will be published in the near future.*

load by the area calculated from the least diameter. Fig. 1 shows a true stress strain curve and Fig. 2 a load strain curve. Up to the yield point these curves are identical. Beyond the yield point the two curves differ. The load strain curve gives the maximum load which is roughly related to the initial material hardness; beyond that, it gives little information.

From the true stress curve considerable information can be obtained. The amount of tensile strain can be found which will be necessary to raise the yield point to a desired value. Fig. 3 is the true stress curve of a specimen taken from a bar of 18–8 stainless steel. The yield point of the original material was 32,000 psi. It was desired to increase the strength of the bar to a yield point of 100,000 psi. From the true stress curve it was found that the bar should be stretched 27 percent in order to obtain the desired strength. After the bar was stretched the indicated amount and stabilized to relieve residual stress, a second true stress specimen was taken. The curve is plotted in Fig. 3, starting

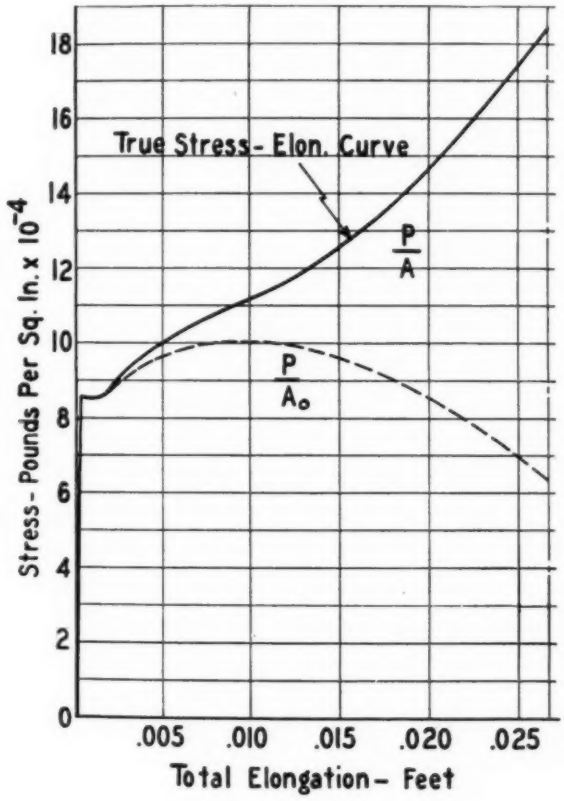


FIG. 1.

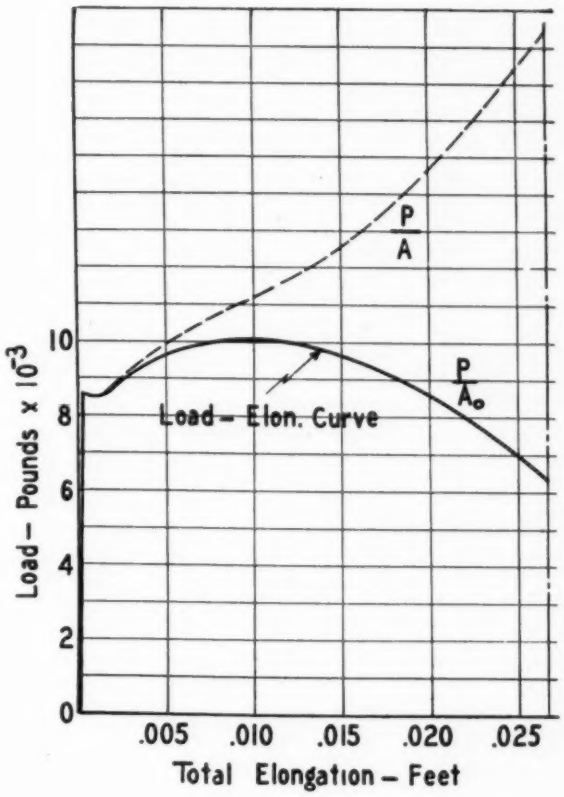


FIG. 2.

the origin from the 27 percent point of the original curve. The yield point occurs as pre-

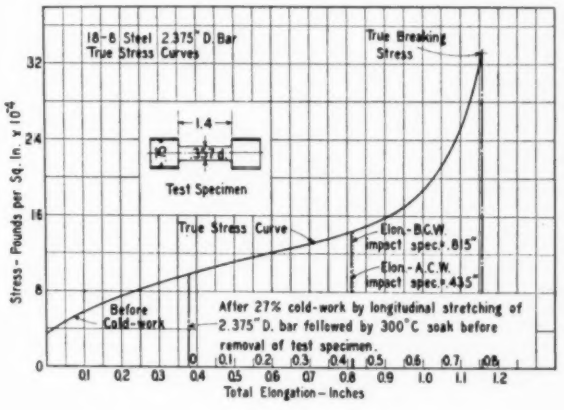


FIG. 3.

| | | |
|---|---|---|
| *Before cold work* | *Elon.* | *Red.* |
| Static tension | 1.155″ | 83.0% |
| Tension impact | .815 | 69.0% |
| Calculated ft. lbs. under static curve | | = 1225 |
| Calculated ft. lbs. under static curve at .815″ elon. | | = 666 |
| Actual ft. lbs. absorbed by tension impact | | = 664 |
| *After cold work* | *Elon.* | *Red.* |
| Static tension | 0.785″ | 78.0% |
| Tension impact | .435″ | 56.7% |
| Calculated ft. lbs. under static curve | | = 1006 |
| Calculated ft. lbs. under static curve at 0.435″ elon. | | = 443 |
| Actual ft. lbs. absorbed by tension impact | | = 444 |

dicted on the original curve and thereafter the second curve is superimposed on the first curve.

Figure 4 is a composite curve of a steel having an original heat treated yield point of 60,000 psi; it was reheat treated to a yield point of 82,000 psi, and then cold worked 6 percent in elongation to a yield point of 96,000 psi. True stress curves were taken for each condition.

From Figs. 3 and 4 it can be seen that the true stress curve is useful in predicting the yield point and elongation of a material after any given amount of cold work. Calculations for the amount of cold work to produce a definite increase in strength must be based on percentage strain, that is, a given percent strain of the test specimen will correspond to a similar percent strain in the structure being considered.

The true stress curve has another important use, the determination of the amount of energy a similar specimen will absorb in an impact machine. Mr. H. C. Mann, who obtained the data for the curves in Figs. 1 to 4, has presented papers before the A.S.T.M. announcing this

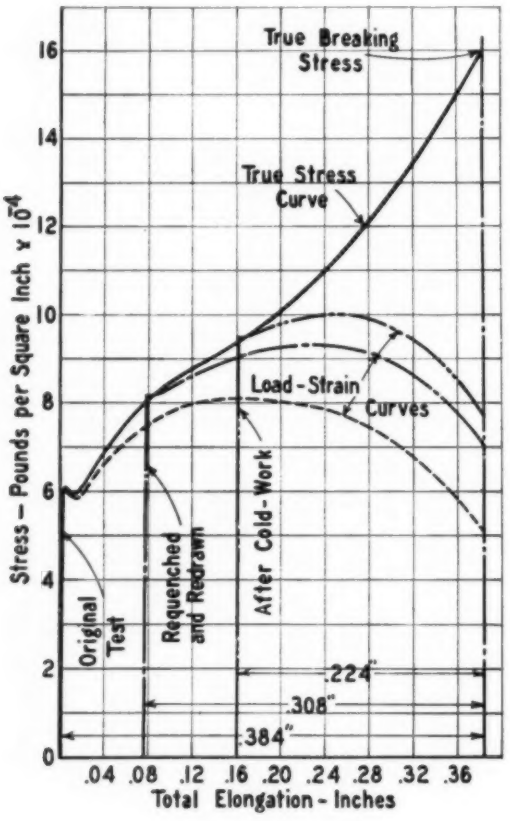


FIG. 4.

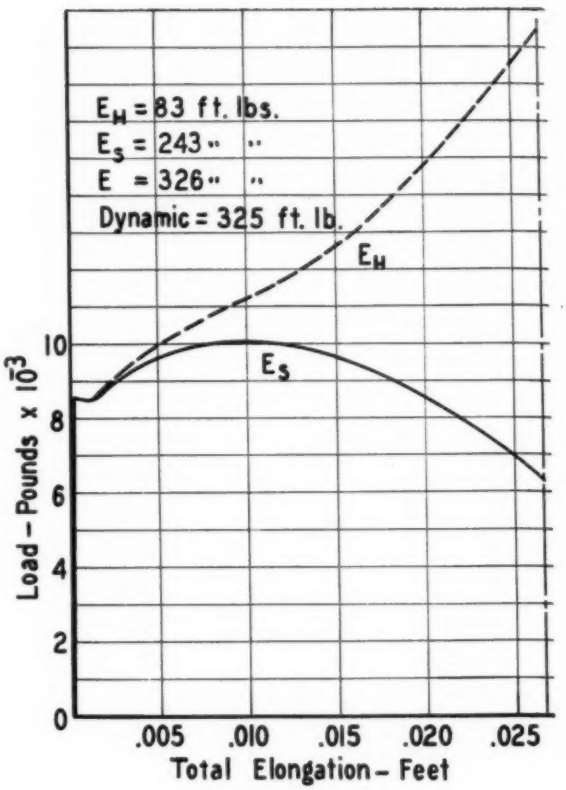


FIG. 5.

relationship. Many doubted and some still doubt this relationship. Several investigators endeavored to verify this relationship, and in every case where the essential precautions were observed, the relation was found to be true.

A storm of criticism was raised because the true stress curve has been considered as a load strain curve. It is certainly true that the true stress curve is not a force distance diagram. It is equally as true that the work under this curve, if it is considered as a force distance diagram, will equal the value of the energy obtained from an impact machine. The above is true when the test specimen is geometrically similar to the static specimen and the impact velocity does not exceed the transition velocity for the material.

The above two facts raise the question, "Why should an incorrect curve repeatedly give the correct answer with all kinds of material and condition?"

It is desired to present some facts not yet published and to present a theory which appears to be correct and which certainly should be subject to a lot of discussion.

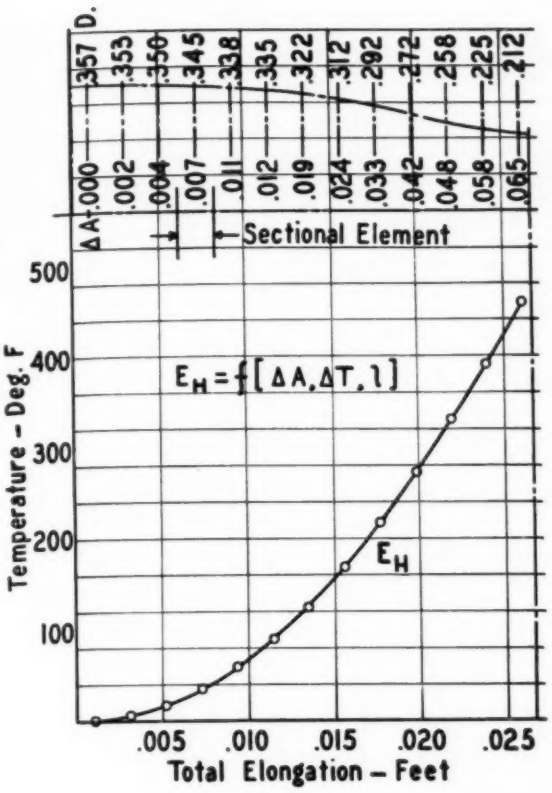


FIG. 6.

One known fact is that the rise in temperature at any section normal to the axis of the specimen is directly proportional to the change in area of that section. This fact was determined by spot welding fine wires of iron and constantan on opposite sides of a test specimen and at several sections along the specimen from the shoulders to the break. The specimens were broken in both impact and static machines and the temperatures determined from the thermocouple effect. From these tests the heat evolved was found to be the same for both the static and impact test.

The quantity of heat energy calculated from data obtained in the above manner, added to the work energy determined from the load strain curve, equalled the energy absorbed in the impact test. In Fig. 5 is plotted a true stress curve superimposed on a load strain curve. In Fig. 6 is a plot of the heat energy liberated on impact from a specimen similar to that used to obtain Fig. 5. The energy to fracture in an impact machine was 325 ft. lb. The energy given by the load strain curve was 243 ft. lb. The heat energy found from the temperature curve was 83 ft. lb. The energy given by the true stress curve was 326 ft. lb. The sum of the heat energy and the load strain energy was also equal to 326 ft. lb.

The above information is believed correct and reproducible. Based thereon, the following theory is advanced as an answer to the question, "Why does the area under the true stress curve represent the work of breaking the specimen in impact?"

First, the load elongation curve is considered to be isothermal and the true stress curve is considered to represent adiabatic conditions. The load strain curve is considered isothermal because the load and strain readings are only taken after the specimen has reached room temperature and the load and strain reach equilibrium conditions. It has been observed that when an increment of strain is suddenly applied to a specimen, a higher load is noted immediately after the machine is stopped than will be noted after equilibrium conditions are reached. The load strain curve, therefore, does not represent all the work done by the machine on the specimen.

The equilibrium load is supported by the elastic strength of the material. The elastic strength is a function of the strain energy distorting the lattice structure. If the load strain curve does not contain heat energy, then the energy represented by the curve is strain energy; in other words, the work absorbed by the specimen in lattice strain.

As previously stated, the heat energy is proportional to the change in area of the specimen. The true stress curve which is based on area changes is plotted from the load strain curve adding to the strain energy curve the integrated heat energy.

There is more that should be known about this relationship. Load strain curves taken on machines having load measuring and strain measuring mechanisms that are faithful to changes when pulling speeds vary from zero feet per second to impact velocities would be of great value. A machine which would measure both load and energy would furnish interesting information. We are yet to see the complete answer to this problem. It is of sufficient importance that work done in different laboratories should be coordinated by the technical societies.

# Here and There

### New Appointments and Promotions

Dr. Merit Scott has been promoted to an associate professorship of physics at the Pennsylvania State College.

★

George H. Carragan and Stanley B. Wiltse of the department of electrical engineering and physics have been promoted from associate professors to professors at the Rensselaer Polytechnic Institute at Troy, New York.

★

At Cornell University the title of professor emeritus has been conferred on Dr. Frederick Bedell, of the department of physics, on Dr. Wilder D. Bancroft, of the department of physical chemistry, and on Professor Edgar H. Wood, of the School of Engineering.

★

Mr. L. W. Wallace has been made director of a new division of engineering and research at the Crane Company in Chicago.

★

### Brown University Laboratory

A new chemical research laboratory is being built at Brown University. This laboratory was made possible by a $500,000 gift from the former United States Senator Jesse H. Metcalf. The laboratory will be especially fitted for research in photochemistry and electrochemistry.

★

### Westinghouse Research Fellowships

The Westinghouse Electric and Manufacturing Company announces the establishment of ten post-doctorate fellowships for research in physics, including chemical physics and physical metallurgy, to enable investigators to carry on their work at the Westinghouse Research Laboratories, one of the nation's leading industrial research laboratories. It is planned to appoint five Fellows for 1938–1939 and five more in each succeeding year.

The objects of the company in establishing the fellowships are, briefly, (1) To make a worth-while contribution to the development of the fundamental sciences on which modern industry is based. The company feels that all research leading to a better understanding of the nature of matter and energy will ultimately prove valuable to technology even though its immediate field of application is not apparent. (2) To enable a group of able investigators to become familiar with the scientific problems confronting the electrical industry. It is felt that this contact will be of great value whether the men turn to industrial research or to academic work after completion of their fellowship period.

Fellows will devote their entire time and energies to work on their research project at the Westinghouse Research Laboratories in East Pittsburgh. It is expected that they will also participate actively in the seminars and colloquia held at the laboratories in the neighboring institutions of higher education. Fellows are allowed the usual two weeks vacation at the end of each year, together with liberal time for attendance at scientific meetings and for visits to other laboratories. Fellows will be called on from time to time for progress reports and will be expected to present a final report in form suitable for publication toward the end of the fellowship period.

Appointments are made for a period of one year and Fellows are eligible for one reappointment for a like period. The salary will be paid semi-monthly at the rate of $2400 a year. The laboratories are organized into six divisions—mechanics, electromechanics, electrophysics, chemical and metallurgical, magnetic, and insulation. The work of the Fellows will be carried on in the appropriate division under the general supervision of Dr. E. U. Condon, associate director for the program of fundamental research. In conformity with company regulations, Fellows will be required to sign the usual Employment and Patent Agreement relating to the assignment of inventions, a copy of which agreement will be supplied upon request.

It is not necessary that the proposed research be one for the results of which a technological use is evident. In the interest of efficiency it is desired to confine the fields of work to those for which the laboratories are well equipped. Owing to the breadth of interests represented this is not a serious limitation. Problems in the fields of nuclear physics, electric conduction in gases, ferromagnetism, dielectrics, thermionics, semi-conductors, elastic and plastic properties of metals, crystal structure, are appropriate. Applications outside these general fields will also be given consideration, but preference will be given to projects broadly related to the electrical industry.

Application should be made on available forms and should be addressed to the office of the Manager, Technical Employment and Training Department, Union Bank Bldg., Pittsburgh, Pa. Applicants must be American citizens under the age of thirty-five, who have had scientific training equivalent to that represented by a doctor's degree from a recognized university. Applications will be received at any time up to March 1, 1938, and formal announcement of awards will be made early in April, 1938.

Tenure of the fellowship may begin at any time thereafter except that all Fellows are expected to begin their work not later than October 1, 1938.

★

### International Conference

An International Conference on Physics was organized on November 25 to November 27 to commemorate the centenary of the birth of Professor J. D. van der Waals. The sessions were held in the van der Waals laboratory in Amsterdam. The scheduled program was as follows:

F. LONDON, **La theorie des forces de van der Waals**
M. BORN, **Statistical Mechanics of Condensing Systems**
J. E. LENNARD JONES, **The Equation of State of Gases and Critical Phenomena**
R. H. FOWLER, **A Calculation of the Surface Tension of a Liquid Vapor Interface in Terms of van der Waals Forces**
W. H. KEESOM, **Thermodynamische und andere Eigenschaften des Heliums bei niedrigen Temperaturen**
F. SIMON, **On the Third Law of Thermodynamics**
K. CLUSIUS, **Ueber Umwandlungen des festen Mono- und Tetradeutero-methans. Die Enthropieverhaltnisse des Monodeutero-methans $CH_3D$ und des Deuteriumhydrids HD**
J. H. DE BOER, **Adsorption by van der Waals Forces and Surface Structure**
J. ERRERA, **Examen spectrographique infrarouge des liaisons intermoleculaires**
A. J. RUTGERS, **The Effect of Pressure on Some Slow Reactions in Solution**

★

### Chemical Engineering Award

The Monsanto Chemical Company, St. Louis, Missouri, has been given the 1937 award for Chemical Engineering Achievement, instituted by *Chemical and Metallurgical Engineering* to stimulate a broader participation of chemical engineers in the affairs of industry and to honor every two years the company which has contributed most to the advancement of the chemical industry and of the chemical engineering profession. Formal presentation of the 1937 award was made on December 10. The award was given in 1933 to the Carbide and Carbon Chemicals Corporation for the development of an organic chemical industry based on natural gas and petroleum, and in 1935 to E. I. du Pont de Nemours and Company, Inc., for the development of synthetic rubber and camphor compounds.

★

### Institute for Advanced Study

The School of Mathematics of the Institute for Advanced Study each year allocates a small number of stipends to gifted young mathematicians and mathematical physicists for the purpose of enabling them to broaden their scientific outlook and to work on their research programs at Princeton in contact with the members of the institute and university faculties. Only such candidates will be considered as have already given evidence of ability in independent research comparable at least with that expected for the degree of doctor of philosophy. Applications for the academic year 1938–1939 should be filed before February 1, 1938. Blanks for this purpose may be obtained from the School of Mathematics, the Institute for Advanced Study, Fine Hall, Princeton, N. J.

*Science*, November 19, 1937

Dr. Edward Elway Free, consulting physicist, is scheduled to give a lecture before the New York Academy of Medicine on March 24. The title of his lecture is to be "The Physicists' Contribution to Medicine."

★

### Westinghouse Research Grant

A grant of $50,000 to provide for a three-year program of research on disease has been made to the University of Pittsburgh School of Medicine by the Westinghouse Electric and Manufacturing Company. Under the grant a study will be made at the university of the value of artificial fever as a weapon against rheumatism, arthritis, venereal disease, the common cold, influenza, heart diseases, tuberculosis and brain disorders. The Westinghouse Company itself will not participate in the research, and has agreed to make the results available to all medical authorities as a contribution to public health. The research program will include attempts to find facts relating to humidity and temperature in their effects upon the body.

★

### a.c.-d.c. Relay

A new low cost compact relay adapted to electronic and radio fields has just been released by the G-M Laboratories, Inc. of Chicago. It is known as type *D* and is an electromagnetic relay for operation on either a.c. or d.c. Its dimensions are: $2\frac{5}{8} \times 1\frac{5}{16} \times 1\frac{1}{2}$ inches high. With a.c. coils it is furnished for use up to 60 volts without series resistors. Contact capacity is 10 amp. a.c. and 2 amp. d.c. Contact pressure and contact travel are adjustable. The frame and armature are made entirely of silicon steel which holds heat losses on a c. at a minimum.

★

### Intense Mercury Arc Sources

Very intense arcs have been laboratory realities for some time. The fact that general commercial use of very high power mercury arcs is one step nearer was announced by J. W. Marden of the Westinghouse Lamp Division. A logarithmic relationship is found to exist between the candlepower per unit volume and the watts per unit volume of the arc stream. In addition, it has been found that a constant ratio holds between watts per centimeter and lumens per centimeter. From measurements of the arc stream in lamps already in practical laboratory application, it is possible to determine the wattage required to operate mercury arc lamps of any desired brightness. Materials must be found to be used in a lamp capable of withstanding the abnormal pressure of 1100 pounds per square inch, three times that of the steam in a locomotive, and the extreme temperature of 14,000 degrees, hotter than the surface of the sun.

In recent studies, light intensities of various types of lamps were measured at right angles to the axis of the arc stream by means of a calibrated photronic cell which had approximately the sensitivity of the eye. The readings were taken in terms of lumens, candlepower per cm or per cu. cm of arc stream. The length and diameter of the arc streams

were in most cases determined by projecting the magnified image on a screen for direct measurement. The distribution of the intensity across the arc streams was determined by recording the energy passing through a narrow slit fastened on the face of the photronic cell.

The following table records readings made on various lamps. Some of the mercury lamps were operated within an outer glass housing, others had none. Cooling was with stagnant air, air-blast and with water.

| | Candle-power per cm |
|---|---|
| 100-w mercury lamp in double glass housing | 80 |
| Commercial 250-w high intensity glass lamp | 100 |
| Commercial 400-w high intensity glass lamp in outer housing | 100 |
| Large 2000-w quartz lamp, stagnant air | 400 |
| Quartz lamp 350 watts, air blast cooling | 900 |
| Commercial 85-w quartz | 1,900 |
| 750-w tungsten bi-plane filament | 2,400 |
| Quartz mercury arc with magnetic field to control arc stream | 8,400 |
| Quartz mercury arc, vertical burning, air cooling | 10,000 |
| Quartz mercury arc with air blast cooling | 16,000 |
| Water-cooled quartz mercury arc No. 1 | 20,000 |
| Water-cooled quartz mercury arc No. 2 | 21,000 |
| Carbon arc | 45,000 |
| Water-cooled quartz mercury arc lamp | 70,000 |
| Beck arc | 110,000 |
| Sun | 165,000 |
| Elenbaas super-pressure quartz mercury arc lamp (max.) | 180,000 |
| High pressure carbon arc | 280,000 |

★

### G-E Exposure Meter

A new photographic exposure meter has been developed by the General Electric Company which is designed for use over a wide range of light values. One of the outstanding features of the new meter is the use of a hood which cuts down the angle of the light entering the exposure meter to approximately that of a camera. The particular shape of the opening on the meter is advantageous because, when pointed at a normal scene, the full angular width of the camera is included in a horizontal direction, but in the vertical direction a much narrower angle is used. The hood is arranged to slide on the sides of the meter case, so that when the instrument is not in use, the face is protected by the hood. A direct-reading scale giving the *f* values is provided for taking "stills," and the exposure readings are calibrated for a film emulsion speed of 16 (Weston system), the speed of the several types of film most commonly used. Values for films of different speeds can be obtained either by interpolating mentally or by using the calculator provided on the hood. When the hood is removed, the exposure meter becomes a light meter having a range of from 0 to 75 footcandles.

★

## New Booklets Received

**Cenco News Chats** (15 pp.) Vol. III, No. 16, December, 1937. This issue contains articles on the American Institute of Physics, "New Glass Absorber for Heat," and "Nothing New Under the Sun?" and other laboratory equipment.

**Oscillographer** (4 pp.) Vol. 1, Nos. 8 and 9, October and November, 1937. "The Cathode-Ray Oscillograph Applied to Materials Testing," "Two New Cathode-Ray Tubes Especially Designed for Television" and "Memory Machine Aids Research" are the articles which make this issue.

## Contributors to this Issue

**Dr.** Maurice A. Biot graduated from the University of Louvain, Belgium, in mining engineering in 1929 and in electrical engineering in 1930. In 1932 he received his Ph.D. from California Institute of Technology. He was an instructor in mechanics at Harvard University in 1934–1935. From 1935–1937 he was a professor at Louvain University. Recently he was appointed assistant professor at Columbia University.

**Mr.** Robert Matteson was born in Los Angeles, California, on May 2, 1906. He received his B.S. in mechanical engineering from the University of California in 1929; and since that time has been connected with the Research and Development Department of the Standard Oil Company of California.

**Dr.** Joseph Marin received degrees of B.A.Sc. in 1928 from the University of British Columbia; M.S. in C. E. in 1930 from University of Illinois, and a Ph.D. in 1936 in engineering mechanics from the University of Michigan. He has served as topographic surveyor for the Geological Survey of Canada, as research assistant in civil engineering at the University of Illinois, as structural designer for the Byllesby Engineering and Management Corporation of Chicago, as an instructor in civil engineering at Rutgers University, and since 1934 he has been assistant professor of engineering materials at Rutgers University.

**Dr.** Carl Kenty was born at Elmsdale, Novia Scotia, in 1902. He received the degree of B.Sc. from Dalhousie in 1923, and of M.Sc. in 1925. In 1929 he received his Ph.D. in physics from Princeton. He then joined the General Electric Vapor Lamp Company, Hoboken, N. J. His chief research has been in the field of gaseous discharges.

# Among the New Books

**Electricity and Magnetism.** S. LEROY BROWN. Pp. 310+v, Figs. 126, 15×22 cm. Henry Holt and Company, New York, 1937.

Brevity and clarity in exposition, emphasis on physical principles rather than on mathematical developments, an abundance of problems, both with and without answers, and a series of review assignments so printed that they can be detached and handed in, are some of the features which make this book a welcome addition to the list of available second-year texts. A section entitled *Laboratory Experiments* is also included, with the explicit statement that it is not intended to take the place of a regular laboratory manual. Certainly this section will be of little use to the student who regards laboratory work merely as a necessary evil to be carried out with as little thinking as possible. However, the intelligent student, who uses the laboratory as a place for *learning*, will find these outlines of sixteen typical exercises very suggestive and helpful.

The conventional historical order of treatment has been abandoned. The first chapter starts with current electricity and the next ten treat direct currents, magnetism, and magnetic circuits. The discussion of electrostatics in Chapter XII is followed by a chapter on alternating currents; then a chapter on thermionics and vacuum tubes and another on electromagnetic radiation conclude the book.

Energy and power relations are stressed throughout. In fact, the units for current, resistance and e.m.f. are so defined that Ohm's law is *deduced* as a necessary consequence of the power relationships. Since no familiarity with calculus notation or methods seems to be assumed before page 93, it is a little surprising to have the solution of a group of six simultaneous equations by determinants introduced in the chapter on Kirchhoff's laws on page 52, admirable though this may be from the viewpoint of convenience and mathematical elegance. As intimated above, most mathematical developments are greatly abbreviated. For example, the equation for the circuit containing resistance and inductance is stated and then its solution is given without proof, thus putting the emphasis on the physical interpretation of $i=(E/R)(1-e^{-Rt/L})$ rather than on the mathematics by which it is obtained from $E=Ri+L(di/dt)$. The theory of alternating current circuits containing resistance, inductance, and capacitance in parallel is treated before that of series circuits. In both cases the equations for the steady state are deduced directly from the rotating vector diagrams, and transient effects are not mentioned.

In so brief a text it is inevitable that only selected topics can be treated, and the choice of what to include is often a matter of personal preference. To this reviewer it seems unfortunate that the concept of potential has been omitted completely and that no distinction has been made between potential difference and electromotive force. Also to him the treatment of magnets, magnetic fields, and magnetic units seems the least satisfactory characteristic of the book.

The text is surprisingly free from typographical errors and the diagrams are clear and adequate. Professor Brown has done a real service in preparing this book.

W. W. STIFLER
*Amherst College*

**Fundamentals of Physical Optics.** FRANCIS A. JENKINS AND HARVEY E. WHITE. Pp. 453+xiv. Figs. 278, 16×23½ cm. McGraw-Hill Book Company, Inc., New York, 1937. Price $5.00.

One of the difficulties attending collaboration in writing a text is that the authors may so differ in point of view and in style of composition that the effect is "patchy." This criticism cannot be made of *Fundamentals of Physical Optics*, for either by a felicitous distribution of labor or by a natural aptitude for collaboration the authors have produced a book which shows a high degree of unity in style.

Unity is also enhanced by a deliberate limitation of the scope of the book. In the present era of rapid development of physical ideas it is an effort for most workers in physics to maintain perspective or to seek such unity as may be possessed by apparently conflicting theories. Consequently an intermingling of what we have up to this time called "classical" and "quantum" theories often tends to destroy unity. The authors have chosen to avoid this difficulty by presenting their subject only from the standpoint of the classical wave picture of light, and have referred the reader to other books at large for the adequate treatment of those optical phenomena which require the quantum theory. Within the scope indicated, their book is a quite complete compendium of the details of classical physical optics.

The principles of simple harmonic motion and wave motion are adequately discussed in the first two chapters. These are followed by two on interference, respectively devoted to the phenomena obtained with double and multiple beams. The four chapters following, on diffraction, constitute the largest subdivision of the book, and should justify its use as a reference on that subject. An admirable choice of emphasis is the devotion of a whole chapter to the double slit, which is important in optics not only from a historical standpoint but because it is the simplest case in which diffraction and interference are both present. The concept of visibility is omitted. The amount of space given to the next chapter, which progresses from Römer's deter-

mination of the velocity of light to a brief statement of the principle of relativity, is small, as it should be in an intermediate text. The rest of the book contains an excellent chapter on electromagnetic theory, four which treat quite completely the polarization of light, and chapters on sources of light and their spectra, absorption and scattering, dispersion, reflection of light, and electro- and magneto-optics.

The book is profusely illustrated, reflecting a desire to leave few details to be worked out from the verbal exposition. A few illustrations are so complicated as to be rather difficult to interpret, no single idea standing out in bold relief. Most of the photographs are original, and those which illustrate interference are particularly good. A pleasing feature of the book is the inclusion of a brief footnote reference to the name of each person historically famous for research in optics, giving his life period and his principal contributions. There are problems at the end of each chapter. The publishers have done an excellent job in the make-up of the book, although some of the line drawings are reduced to too small a size.

The reviewer has experienced pleasure at finding a familiar theme well discussed in this book. It is a valuable contribution to the literature of physical optics, which has been all too scanty in recent years, and should be useful both for text and reference purposes.

GEORGE S. MONK
*University of Chicago*

**Catalysis from the Standpoint of Chemical Kinetics.** GEORG-MARIA SCHWAB. Translated by Hugh S. Taylor and R. Spence. Pp. 357+xii. Figs. 39, 15½×23½ cm. D. Van Nostrand Company, Inc., New York, 1937. Price $4.25.

Authors on catalysis have never agreed upon the true scope of their subject, but the tendency has been very strong to claim more territory than there are reasonable prospects of utilizing. Colonists on our Atlantic seaboard had similar maps a few hundred years ago, and very comical they look now. The present treatise is governed by the view that a catalyst is any substance which alters the velocity of a chemical reaction without appearing in the end products in a fixed stoichiometric proportion. There are of course both positive and negative catalysts. In addition, when two or more catalysts are present together, the action may be more than additive (promotion) or one may cancel the effect of the other (poisoning).

These barren categories may well have retarded the study of catalysis. In spite of all efforts to weld them together, the subjects of homogeneous and contact catalysis remain disunited, and homogeneous catalysis itself divides sharply into the study of ionizing and of nonionizing fluids. In the latter case it is of questionable value to separate catalysis from other reactions, since the goal in this field is a mechanism composed of uncatalyzed elementary reactions. Representative examples of such mechanisms are briefly presented in somewhat limited space. It seems unfortunate that the disproven catalysis of the hydrogen-chlorine reaction by water vapor was not more completely eliminated. The scheme adopted here and in several other instances is to repeat the errors of the 1931 German text, and append a final paragraph of denial. Dr. Schwab's original preface stated, ". . . many things described in the text as doubtful, are more certainly known today." It is perhaps helpful that a few anachronisms remain to remind the reader that the converse of this proposition also holds good.

As might be expected from its authorship, the book is most interesting and most authoritative when dealing with contact catalysis. The discussion of activated adsorption is particularly good. Opportunity is found here for fuller treatment of many controversial points than could be given in the original literature.

LOUIS S. KASSEL
*Universal Oil Products Company*

**A Catalogue of the Epstean Collecting on the History and Science of Photography and Its Applications Especially to the Graphic Arts.** Columbia University Library, edited by H. Lehmann-Haupt. Pp. 110, illustrated, 16×24½ cm. Columbia University Press, 1937. Price $1.50.

Although this little book is primarily a catalogue of Mr. Edward Epstean's working library, now placed by him in the custody of the Columbia University Library for the use of the public, "it may very well serve as a key to the accumulated wealth of photographic literature," in the words of the editor. And fourteen hundred items ranging from Daguerre's own description of his process, written in 1839, to the current *American Annual* is no impotent key.

This collection is an excellent nucleus for a more extensive one on the development of photography since it contains works not readily available elsewhere, especially some in foreign languages. But its deficiencies are also noteworthy. For example, Hay and von Rohr's *Handbuch* is missing, although it is but fair to add that Eder's is present. Then, too, Sheppard and Mees' *Investigations into the Theory of the Photographic Process*, which is a landmark in the history of the science and is still of interest although thirty years old and out of print, is represented only by the German translation. Of recent textbooks, all too few are included. The periodicals are spotty, and the abstract journals are not up to date. On the other hand, there are included numerous reprints of scientific papers that one would not be likely to seek there; one would be more likely to refer to an abstract journal.

All this is not to disparage the collection or to belittle Mr. Epstean's generosity in making it widely available. The catalogue will indeed serve as a key to the literature, but one should be warned against considering it to be a critical bibliography of the most significant works.

Typographically, the book is a treat to the eye. It is done in the olden style and is amusingly illustrated with reproductions of old wood cuts. Judging from some of these, aerial photography is old stuff, nor is it a novel experience to dodge a barrage of candid (5″×7″, *sic*) cameras concealed behind every tree and bush!

FRED H. PERRIN
*Eastman Kodak Company*

# Contributed Original Research

## A Hydrodynamic Analogy for Shearing Stress Distribution in Bending*

M. A. Biot
*Columbia University, New York, N. Y.*

It is shown here that the shearing stress distribution in the combined shear and bending is represented with practical accuracy by the distribution of velocity in the flow of a perfect fluid over the area of the cross section. This flow is produced by a linear distribution of sources above the neutral axis and of sinks below the neutral axis, the intensity of these sources and sinks being proportional to the distance to the neutral axis. For hollow beams the additional condition must be added that the circulation of the velocities is zero around each hole of the cross section. The analogy which is rigorous for a material of zero Poisson ratio holds within a small correction for the general case.

IT was established by Saint-Venant from the mathematical theory of elasticity that the combination of bending and shear in a uniform beam of arbitrary cross section yields a very simple distribution of the bending stresses, which coincides with the one derived from elementary strength of materials. The shearing stresses, however, do not obey such a simple law and the usual mathematical treatment does not yield easily a fairly approximate idea of their distribution.

Our purpose is to show that the shearing stress distribution can be visualized by means of a rather simple physical analogy and furthermore that the fundamental equations at the base of this analogy may be reached directly by a short-cut method.

### I. The General Case of Combined Bending Shear and Torsion

We consider a uniform beam (Fig. 1) referred to a system of rectangular coordinates $x$, $y$, $z$. The $z$ axis is parallel with the beam, the $x$ axis passes through the center of gravity $G$ of the cross section and coincides with one of the principal axes of inertia of this cross section. The location of the origin along the $x$ axis is left arbitrary. As will be shown hereafter a system of stress components $\sigma_z \tau_x \tau_y$ (Fig. 1) is compatible with the theory of elasticity and may be selected in such a manner as to result in the combination of a bending moment $M$ and a total shear $S$ perpendicular to $x$.

We impose upon the stresses the further restrictions:

(1) That $\sigma_z$ has a linear distribution along $z$ and $y$ by putting

$$\sigma_z = (S/I)yz. \tag{1}$$

$I$ is the moment of inertia of the cross section with respect to the $x$ axis.

(2) That the shearing stress $(\tau_x, \tau_y)$ acting on the cross section be independent of the location of this cross section, i.e. independent of $z$.

The above stress system, in order to be compatible with the theory of elasticity, must verify the following set of equations:

(1) The generalized Hooke's law

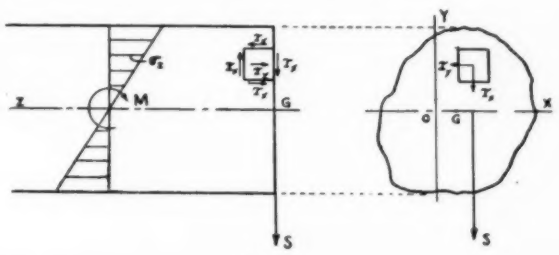


Fig. 1.

* Publication assisted by the Ernest Kempton Adams Fund for Physical Research of Columbia University.

$$\partial u/\partial x = -(\mu/EI)Syz, \quad (2)$$

$$\partial v/\partial y = -(\mu/EI)Syz, \quad (3)$$

$$\partial w/\partial z = (S/EI)yz, \quad (4)$$

$$\partial u/\partial y + \partial v/\partial x = 0, \quad (5)$$

$$\partial u/\partial z + \partial w/\partial x = \tau_y/G, \quad (6)$$

$$\partial v/\partial z + \partial w/\partial y = \tau_x/G. \quad (7)$$

(2) The condition of internal equilibrium

$$\partial\tau_x/\partial y + \partial\tau_y/\partial x = -\partial\sigma_z/\partial z = -(S/I)y. \quad (8)$$

In these equations $u$, $v$, $w$ are the coordinate increments; the original coordinates $x$, $y$, $z$ of a

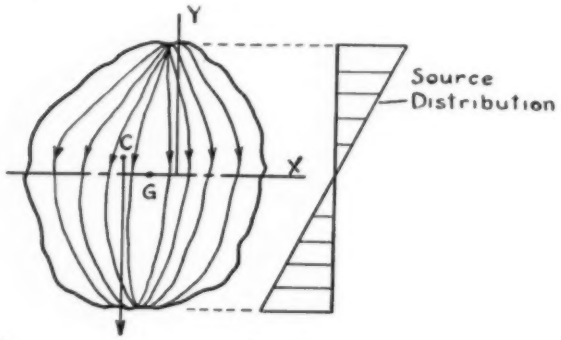


FIG. 2.

point attached to the material become $(x+u)$, $(y+u)$, $(z+w)$ after deformation.

$E$ is the elasticity modulus, $G$ the shear modulus and $\mu$ the Poisson ratio of the material.

It can be readily verified that Eqs. (2), (3), (5) become identities and that the other Eqs. (4), (6), (7) are compatible if we put

$$u = \partial f/\partial x, \quad v = -\partial f/\partial y, \quad (9)$$

$$f = ((S/6EI)yz^3) + ((\mu S/6EI)zy^3) - ((\mu S/2EI)x^2yz) + \omega xyz, \quad (10)$$

where $\omega$ is a constant to be determined later.[1]

Since we are primarily interested in the distribution of $\tau_x$ and $\tau_y$ we now proceed to eliminate $w$ between (6) and (7). Taking into account (9) and (10) we find

$$\partial\tau_y/\partial y - \partial\tau_x/\partial x = -(\mu/(1+\mu))(S/I)x + 2G\omega. \quad (11)$$

This last equation with the condition of equilibrium (8) solves our problem. It is convenient to introduce the two stress functions $\varphi$ and $\psi$ in the following way.

$$\tau_y = -\partial\varphi/\partial x - \partial\psi/\partial y,$$
$$\tau_x = -\partial\varphi/\partial y + \partial\psi/\partial x. \quad (12)$$

From (8) and (11) we deduce that these two stress functions verify the following equations,

$$(\partial^2/\partial x^2 + \partial^2/\partial y^2)\varphi = (S/I)y, \quad (13)$$

$$(\partial^2/\partial x^2 + \partial/\partial y^2)\psi = (\mu/(1+\mu))(S/I)x - 2G\omega. \quad (14)$$

We also have as boundary condition that the shearing stress is tangent to the contour of the cross section

$$\tau_y dy - \tau_x dx = 0$$

or $$(\partial\varphi/\partial x)dy - (\partial\varphi/\partial y)dx - d\psi = 0.$$

We may split this condition into the following two:

$$(\partial\varphi/\partial x)dy - (\partial\varphi/\partial y)dx = 0, \quad (15)$$

$$\psi = \text{const.} \quad (16)$$

From Eqs. (13) and (14) it appears that the shearing stress distribution is made of the superposition of the following systems of stress (a) and (b) one being represented by a hydrodynamic analogy and the other by a membrane analogy.

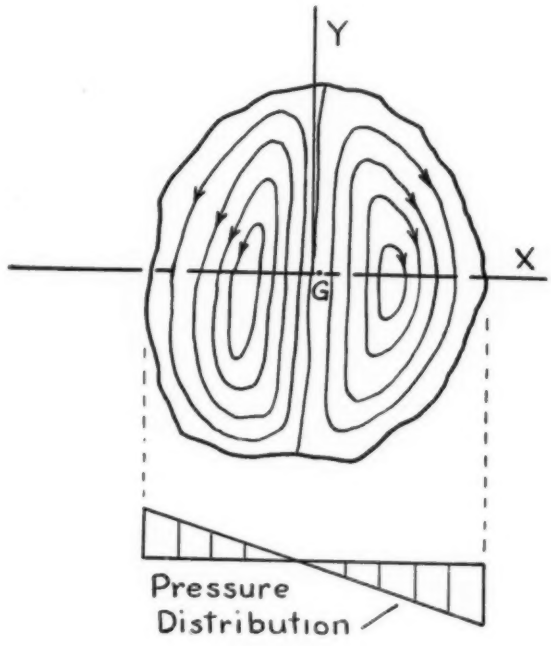


FIG. 3.

[1] Form (10) of $f$ is not the most general that can be found. However, it only differs from this general form by terms which correspond to a displacement of the whole beam as a solid body.

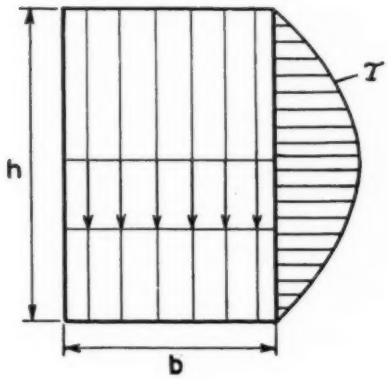


FIG. 4.

(a) One is the gradient of the function $\varphi(x, y)$. Eqs. (13) and (15) show that it may be represented by the velocity distribution in the two-dimensional flow of a perfect fluid with sources of intensity $(S/I)y$ per unit area. The function $\varphi(x, y)$ is the hydrodynamic potential of this flow. Above the $x$ axis we have positive sources of intensity proportional to their distance to this axis, and below the $x$ axis we have negative sources of intensity also proportional to their distance to this axis. Since we have assumed the $x$ axis to pass through the center of gravity of the section, the total flow out of the sources equals the total flow disappearing in the sinks.

(b) The other part of the stress defined by the stress function $\psi(x, y)$ depends on the Poisson ratio. It may be represented by the membrane analogy. The membrane is stretched so as to rest on a horizontal plane boundary the contour of which is the same as that of the beam section. The membrane is submitted on one side to a pressure $p$ distributed linearly in a direction parallel with the neutral axis according to the law $p=-(\mu/(1+\mu))(S/I)x+2G\omega$. The stress is equal to the slope of this membrane and tangent to the contour lines of equal height. The local rotation of the section is $-(1/2G)(\mu/(1+\mu))\times(S/I)x+\omega$. Both this rotation and the stresses (b) represented by the membrane depend on the choice of the constant $\omega$ and the location of the origin on the $x$ axis.

It can be proved as in the theory of the membrane analogy for pure torsion that the (b) stresses result in a torque of value equal to twice the volume under the membrane.

## II. The Case of Pure Shear and Bending

*Let us first assume that the Poisson ratio $\mu=0$.* In that case by choosing $\omega=0$ the stress system (b) disappears and there is no rotation of the cross section. This is a case of pure shear and bending. The shear stresses are rigorously determined by the hydrodynamic analogy, and they result into a total shear $S$ applied along a definite line of action perpendicular to the $x$ axis. We could also find in the same way the line of action of a pure shear acting in a direction parallel with the $x$ axis. The point of intersection of these two lines of action defines the *center of shear C* (Fig. 2).

*If the Poisson ratio is not zero* a force acting through the center of shear produces not only the above stress system (a), but also a certain stress system (b). For instance if the total shear acts through the center of shear $C$, the corresponding system (b) will be found by choosing

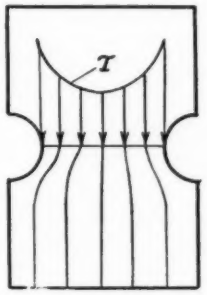


FIG. 5.

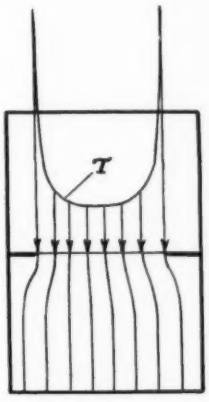


FIG. 6

the constant $\omega$ so that the system will be composed of two equal and opposite torques. In terms of the membrane analogy this means that we must choose the zero pressure line so as to make the amount of positive volume under the membrane equal to the amount of negative volume. This additional system (b) appears as a correction to (a) when the effect of lateral contraction is taken into account. It originates from the fact that the lateral contraction due to the existence of the normal bending stresses on the cross section varies from one section to the other, thus changing the shape of these sections

relative to one another and introducing additional shears and rotations (Fig. 3).[2]

This effect will in general be very small and it is justified to *neglect the influence of the lateral contraction in the applications* and to take only into account the stresses given by the hydrodynamic analogy. We note that when $\mu$ is not zero there is no such thing as really pure shear since there will always be a rotation whatever the location of the resultant shear $S$.

## III. Examples for Solid Beams

(1) *Rectangular cross section* (Fig. 4). The flow lines are vertical and the velocity is calculated from the value of the total flow. The stress $\tau$ being at a distance $y$ from the neutral axis we have

$$b\tau = \int_y^{h/2} (Sy/I)bdy,$$
$$\tau = (S/2I)[(h/2)^2 - y^2]. \tag{17}$$

It is the well-known parabolic distribution. From the theory above it appears that this is rigorously correct when $\mu = 0$ and when $\mu \neq 0$ the correction is generally very small, so that it can be considered as a very good approximation in the latter case.

(2) *Section with a fillet.* It is known that the effect of a semi-circular fillet on potential flow is to double the velocity of the fluid at the fillet. Such a fillet will be expected to introduce a stress concentration factor of about two (Fig. 5). For a section with a sharp slit the total shear will be infinite at the slit. In practice this will produce local plastic flow (Fig. 6).

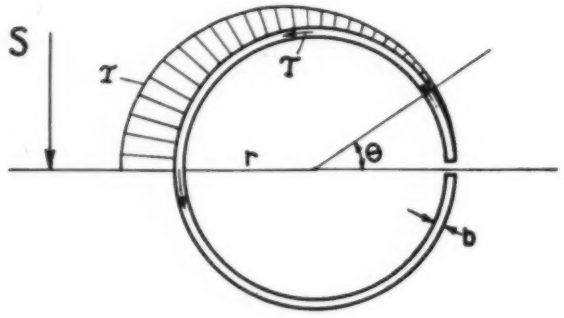


Fig. 7.

(3) *Open thin section.* For a circular thin tube (Fig. 7) of thickness $b$ cut open along its length the flow at an angle $\theta$ is

$$b\tau = \int_0^\theta (Sr \sin\theta/I)brd\theta,$$
$$\tau = (Sr^2/I)(1-\cos\theta). \tag{18}$$

## IV. Hollow Beams

In a hollow beam the cross section contains one or more holes. The hydrodynamic potential $\varphi$ is not necessarily single-valued since an arbitrary circulation may be added around each hole. Moreover the value of the function $\psi$ is not given along the boundary. It has only been derived in the general theory that $\psi$ must be a constant along one boundary contour, but this constant may be different for each different contour.

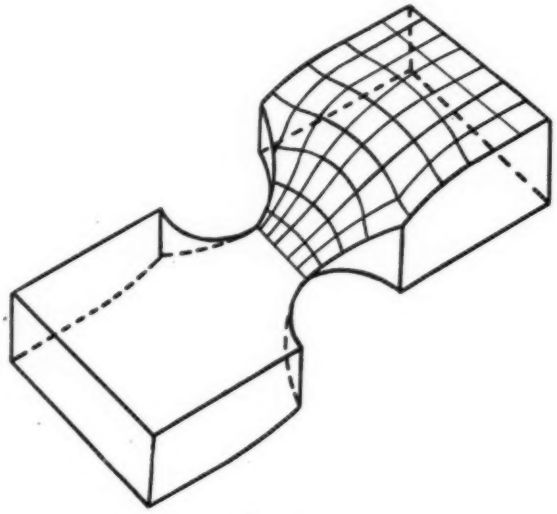

Fig. 8.

In order to determine the problem we must introduce the extra condition that the displacement $w$ will be single-valued. We have

$$dw = (\partial w/\partial x)dx + (\partial w/\partial y)dy.$$

Using relations (6), (7), (9), (10), this becomes

$$dw = (1/G)(\tau_y dx + \tau_x dy) - ((\partial^2 f/\partial x \partial z)dx) + ((\partial^2 f/\partial y \partial z)dy).$$

The function $w(x, y)$ will be single-valued if

[2] The separation of the shearing stresses in these two systems has also been considered by C. Weber, "Biegung und Schub in geraden Balken," Zeits. f. angew. Math. u. Mech. 334–348 (1924).

$$\oint_C \tau_y dx + \tau_x dy = \oint_C G\left(\frac{\partial^2 f}{\partial x \partial z} dx - \frac{\partial^2 f}{\partial y \partial z} dy\right), \quad (20)$$

where these integrals are taken on a closed contour $C$ around each hole. The right-hand side of this equation may be expressed as a double integral extended to the area $D$ inside the contour $C$ and we may write condition (20) as

$$\oint_C \tau_y dx + \tau_x dy = \int\int_D (1\mu/(1+\mu))(S/I)x - 2G\omega) dx dy.$$

Considering now relation (12) this last condition may be replaced by the following two

$$\oint_C (\partial\varphi/\partial x) dx + (\partial\varphi/\partial y) dy = 0, \quad (21)$$

$$\oint_C (\partial\psi/\partial y) dx - (\partial\psi/\partial x) dy = \int\int_D ((-\mu/(1+\mu))(S/I)x + 2G\omega) dx dy. \quad (22)$$

This amounts to stating that the stress system (a) given by the hydrodynamic analogy and the stress system (b) due to the lateral contraction considered separately both yield a single-valued displacement $w$.

Condition (21) expresses that the hydrodynamic potential must be single-valued, i.e., the circulation around each hole must be zero. Here again it is legitimate to assume that in most cases the stress due to the lateral contraction is negligible and to consider as a *good approximation the system of stresses represented by the hydrodynamic analogy with the condition that the circulation is zero.*

## V. Remarks Regarding the Elastica and the Distortion of the Section

From (9) and (10) we deduce for the vertical displacement of the points originally on the $z$ axis

$$v = -(S/6EI)z^3.$$

This coincides with the shape of the elastica found by elementary strength of materials.

It must be added that *in practice* this is not the only deformation that occurs since we must also take into account the local effect of the distribution of stress at the boundaries and around the points of application of the load. A small additional deflection depending only on this local effect will have to be added, and it is to be expected that this additional value is roughly proportional to the total shear.

It is quite obvious that a cross section does not remain plane after the deformation of the beam. The amount of distortion and the shape of the distorted section may easily be deduced from the hydrodynamic analogy if we neglect the effect of the lateral contraction.

Assuming $\mu = 0$, $\omega = 0$ in (10) and the consequence $\psi = 0$ we obtain from (6) and (7)

$$\partial w/\partial x = -(1/G)(\partial\varphi/\partial x),$$
$$-(S/2EI)z^2 + \partial w/\partial y = -(1/G)(\partial\varphi/\partial y).$$

We conclude

$$w = -(1/G)\varphi + (S/2EI)z^2 y.$$

The second term represents the rotation of the section as a plane perpendicular to the elastica, hence the first represents the distortion. *Hence the distortion is represented by the hydrodynamic potential.*

By use of this result the distortion of a rectangular section with circular fillet is represented in Fig. 8.

# Compressibility and Velocity of Pressure Waves in Petroleum Oils

ROBERT MATTESON
*Standard Oil Company of California, Richmond, California*

Curves are presented from which it is possible to obtain the adiabatic compressibility of a petroleum oil in the range of 40°–200°F and up to 5000 pounds per square inch when only the specific gravity at 60°F and the kinematic viscosity at 100°F are known. A chart is given for obtaining the velocity of a pressure wave in an oil in which both the viscous drag and expansion of the containing tube are neglected. A table showing compressibilities and wave velocities for a number of Diesel fuel oils at 120°F and 1750 pounds per square inch pressure is given. The effects of viscosity and tube wall expansion on wave velocity are discussed and a chart is presented to aid in determining the wave velocity in steel tubes. The paper is concluded with a discussion of the effect of wave velocity on the point of injection of the fuel in the Diesel cycle.

## I. INTRODUCTION

THE tremendously increased industrial activity directed in recent years toward the construction and use of high speed Diesel engines has magnified problems which heretofore have been of little or no significance to the industrial world. One problem of major importance is the accurate control of the fuel injected into the cylinder of a small Diesel engine operating at high speed. With reference to the jerk pump system of fuel measurement the satisfactory operation of the engine is dependent upon proper control of the pressure during the period of injection. The extremely short interval of time allowed for this phase of the engine cycle demands a most careful consideration of the related variables. The fuel is in general regarded as an incompressible medium. Such an assumption is not valid in the light of the pressures encountered in the Diesel injection system. The pressure during injection may vary widely for any given system and is dependent upon the geometry of the fuel system and the properties of the fuel used.

Theoretical analyses of fuel systems have indicated the influence of the different characteristics of the fuel, particularly the adiabatic compressibility. Although considerable information on this property is available in the literature its relation to the physical characteristics of the fuel and the dimensions of the line are incomplete. Much of the published information has been collected and correlated here, and it is hoped presented in a form which will be useful to the designer of equipment in which this property of the fuel manifests itself.

## II. COMPRESSIBILITY

Physical properties of petroleum products which influence design problems must be obtainable by simple standardized laboratory tests to be of use to the industry. The equipment and time necessary to obtain, for example, the adiabatic compressibility of a petroleum oil prevents the investigation of this property to be added to the already extensive list of routine inspections. From the point of view of the designer who requires a knowledge of this property it is desirable, if possible, to correlate it with the present accepted standard inspections.

Results of experiments conducted at the

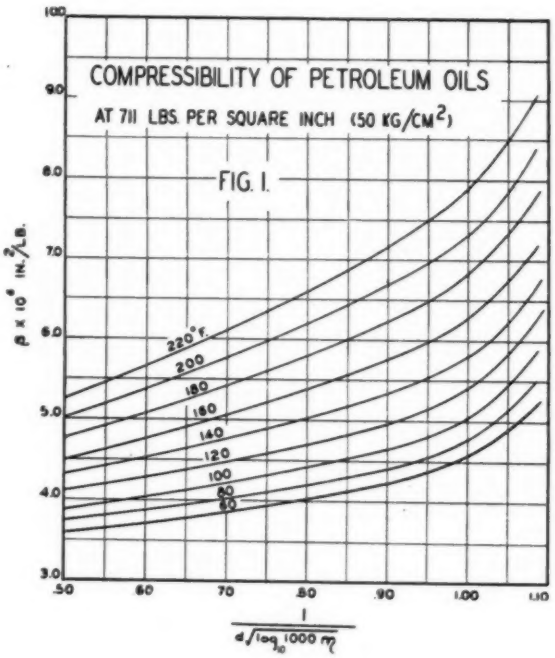

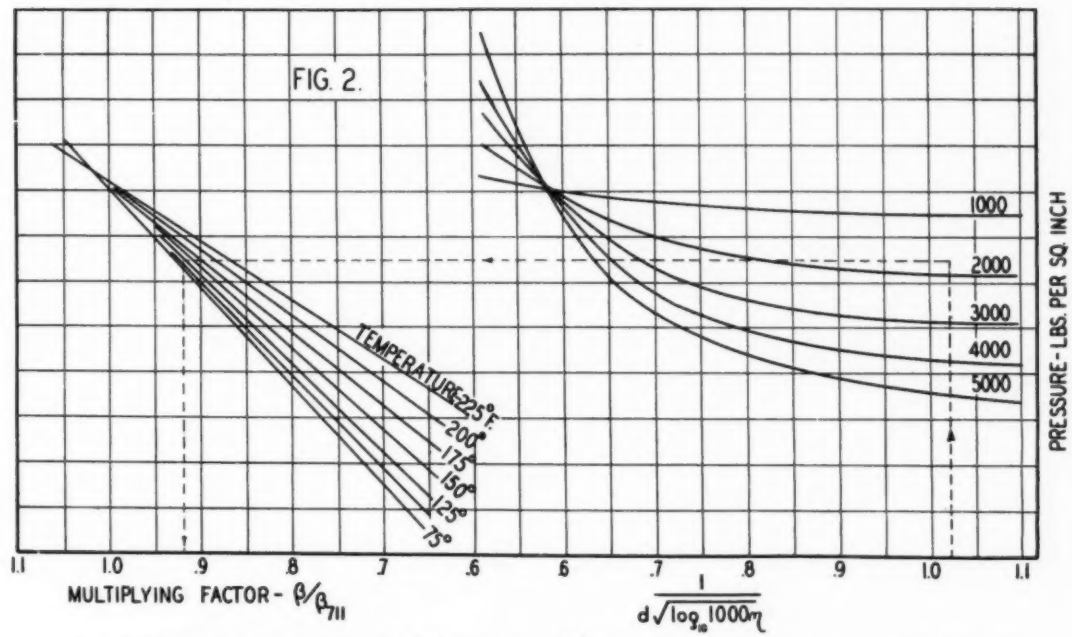


FIG. 2. Multiplying factor for obtaining compressibility at various temperatures and pressures.

National Bureau of Standards by R. S. Jessup[1] have indicated that compressibility of petroleum oils is a function of the specific gravity and the kinematic viscosity of the oil under consideration. The "mean" compressibility of petroleum oils ranging from lubricating stocks through light gas oils has been shown to be related to the specific gravity and kinematic viscosity when plotted as a function of Cragoe's modulus.[1]

$$C = 1/d(\log_{10} 1000\eta)^{\frac{1}{2}}, \qquad (1)$$

where $d$ = specific gravity at 60°F and atmospheric pressure, and $\eta$ = kinematic viscosity in stokes at 100°F. The correlation of this modulus with the *adiabatic* compressibility is shown in Fig. 1 for tests[1–3] carried out on nineteen different petroleum oil samples. The temperature range chosen covers normal engine operating conditions. The pressure of 711 pounds per square inch (50 kg/cm²) is the maximum pressure to which the greatest number of the oils were subjected.[1]

The curves in Fig. 1 were obtained from the pressure-volume relation, at constant temperature, from the available data.[1–3] From these plots the tangent, $dv/dp$, of the curve and the volume $V$ were obtained at the point corresponding to a pressure of 711 pounds per square inch. The values gave all of the data necessary for computing the adiabatic compressibility from the relation

$$\beta = (1/V)(dv/dp) \text{ square inches per pound.} \qquad (2)$$

In order to determine the value of compressibility up to 5000 pounds per square inch the data of several investigators[2–4] were used to compute multiplying factors to be used with Fig. 1. Compressibilities were calculated by the method described above and the multiplying factor was taken as the ratio

$$\frac{\beta}{\beta_{711}} = \frac{\text{Compressibility at a given pressure.}}{\text{Compressibility at 711 pounds per square inch}}.$$

These values have been plotted in Fig. 2.

[1] R. S. Jessup, "Compressibility and Thermal Expansion of Petroleum Oils in the Range 0° to 300°C," Nat. Bur. Stand. J. Research, **5**, 985–1039 (1930).
[2] R. B. Dow, "P. V. T. Relations for Six Oils," J. Wash. Acad. Sci. **24**, 516–526, (1934).
[3] A. C. Talbot, "Velocity of Waves in Oil Under Pressure," Phil. Mag. **19**, 1126–1141 (1935).
[4] J. H. Hyde, "Compressibility of Lubricating Oils," Report of the Lubrication Inquiry Committee Dept. Sci. Indust. Research Adv. Council, 1920.

For purposes of illustration assume that it is desired to find the compressibility of a 32.7°A.P.I. gas oil having a kinematic viscosity of 1.94 centistokes at 100°F and one atmosphere when subjected to a pressure of 1750 pounds per square inch and at a temperature of 120°F. The specific gravity at 60°F (from circular No. 410 of the National Bureau of Standards) of a 32.7°A.P.I. oil is 0.8618 which yields a value of 1.024 for the Cragoe modulus. Fig. 1 gives a value of $5.57\times10^{-6}$ square inches per pound for the compressibility at 120°F and 711 pounds per square inch. Fig. 2 gives a multiplying factor of $\beta/\beta_{711}=0.921$ for obtaining the compressibility at 1750 pounds per square inch. Hence

$$\beta=5.57\times10^{-6}\times0.921$$
$$=5.13\times10^{-6} \text{ square inches per pound.}$$

## III. Velocity of Pressure Waves in Oil

The velocity of a pressure wave in a liquid infinite in extent is given by the relation

$$v=(144g/\gamma\beta)^{\frac{1}{2}} \text{ ft./sec.} \qquad (3)$$

where $g$ = acceleration due to gravity, ft./sec.$^2$
$\gamma$ = weight per unit volume, lb./ft.$^3$
$\beta$ = adiabatic compressibility, in.$^2$/lb.

In order to use this equation it is necessary to determine the unit weight of the liquid as well as the compressibility. Hyde's and Talbot's data show how the density of oils varies with temperature and pressure. These data have been used as a basis for a chart from which it is possible to obtain a multiplying factor for determining unit weight at temperatures other than 60°F and atmospheric pressure. Fig. 3 is such a graph.

To determine the unit weight of an oil of given A.P.I. gravity it is necessary only to consult the National Bureau of Standards circular No. 410 to obtain the specific gravity at 60°F, multiply by 62.37 (the unit weight of water at 60°F), and finally multiply by the relative density factor given in Fig. 3.

Thus with the aid of Figs. 1, 2, and 3 it is possible to determine the velocity of a pressure wave in an oil, infinite in extent, at any temperature and pressure commonly encountered in pumping problems. The only physical data necessary are the A.P.I. gravity of the oil and the kinematic viscosity at 100°F. Fig. 4 is added to simplify the determination of "$v$" once the compressibility and unit weight have been obtained.

In order to demonstrate that a fairly wide range of wave velocities may be expected among different oils of nearly the same density and at a given temperature and pressure the velocities at 120°F and 1750 pounds per square inch have been computed for the Diesel fuels listed by Hetzel.[5] These are tabulated in Table I.

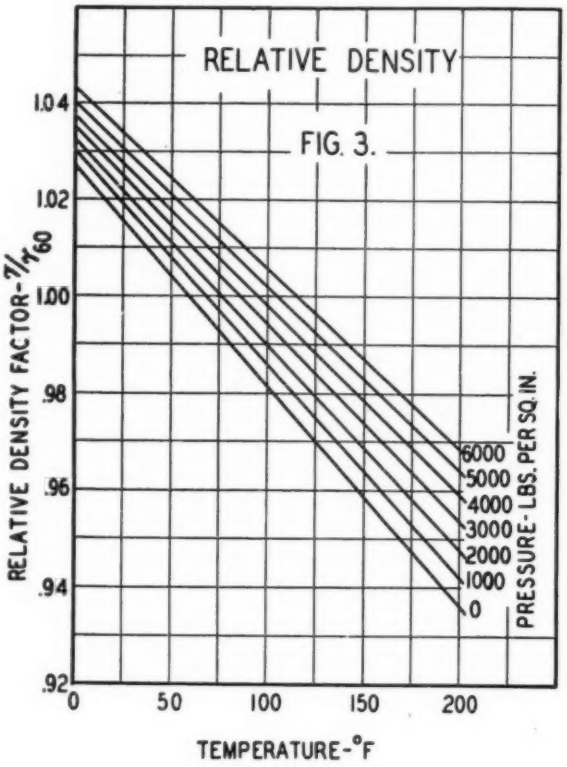


## IV. Effect of Viscosity on Pressure Wave Velocity

Up to this point the discussion has been concerned with the velocity of pressure waves in a medium in which the effect of containing walls could be neglected. In actual practice, however, this factor may become of such magnitude that it must be considered. Talbot[3] found that

[5] T. B. Hetzel, "The Development of Diesel Fuel Testing," Bull. 45, Penn State College Eng. Exp. Station Vol. XXX, No. 37, Sept. 12, 1936.

TABLE I.

| OIL NO. | °A.P.I. | $d_{60}$ | $\eta_{100}$ CENTISTOKES | $\frac{1}{d(\log_{10} 1000\eta)^{\frac{1}{2}}}$ | $\beta$ (in.²/lb.) AT 1750 LB. AND 120°F | $\gamma$ (lb./cu. ft.) AT 1750 LB. AND 120°F | VELOCITY (ft./sec.) AT 1750 LB. AND 120°F |
|---|---|---|---|---|---|---|---|
| B-1 | 32.7 | 0.860 | 1.94 | 1.024 | $5.13\times10^{-6}$ | 52.6 | 4145 |
| B-2 | 35.8 | .846 | 1.55 | 1.082 | 5.72 | 51.7 | 3957 |
| B-3 | 37.0 | .840 | 2.72 | .995 | 4.93 | 51.3 | 4282 |
| B-4 | 36.8 | .841 | 3.81 | .945 | 4.72 | 51.4 | 4372 |
| B-5 | 39.6 | .827 | 4.15 | .951 | 4.745 | 50.6 | 4397 |
| B-7 | 37.8 | .836 | 3.07 | .983 | 4.875 | 51.1 | 4315 |
| B-8 | 37.8 | .851 | 1.94 | 1.040 | 5.27 | 52.0 | 4115 |
| B-9 | 31.7 | .867 | 5.45 | .876 | 4.515 | 53.0 | 4405 |
| B-10 | 35.6 | .847 | 3.47 | .952 | 4.76 | 51.8 | 4339 |
| B-11 | 31.9 | .866 | 9.48 | .824 | 4.415 | 52.9 | 4460 |
| B-12 | 26.6 | .895 | 8.65 | .804 | 4.370 | 54.7 | 4405 |
| B-13 | 20.3 | .932 | 4.48 | .845 | 4.465 | 56.9 | 4274 |
| B-20 | 31.1 | .870 | 4.15 | .903 | 4.60 | 53.2 | 4354 |
| B-21 | 30.0 | .876 | 3.07 | .936 | 4.69 | 53.6 | 4295 |
| B-22 | 33.8 | .856 | 4.15 | .918 | 4.615 | 52.3 | 4387 |
| B-23 | 26.4 | .896 | 3.47 | .899 | 4.56 | 54.8 | 4309 |
| B-24 | 29.7 | .878 | 4.48 | .886 | 4.55 | 53.7 | 4359 |

decreases in wave velocity as high as 10 percent could be attributed to the viscous drag due to the walls of small diameter steel tubes he used. He points out that the following formula,[6] first obtained by Helmholtz, may be used to determine "$v$:"

$$v=(144/\beta\gamma)^{\frac{1}{2}}\cdot(1-(1/r)(\mu\cdot/2\gamma\omega)^{\frac{1}{2}}) \text{ ft./sec.} \quad (4)$$

where $g$ = acceleration due to gravity ft./sec.²
$\beta$ = adiabatic compressibility in.²/lb.
$\gamma$ = weight per unit volume lb./ft.³
$r$ = radius of tube ft.
$\omega=2\pi f$ —
$f$ = frequency c.p.s.
$\mu$ = absolute viscosity lb./sec. ft.

Since ordinarily $f=v/2L$, where $L$ is the length of the tube, it becomes evident immediately that for short tubes, say under three feet in length for example, the square root term involving viscosity and frequency can be neglected unless viscosities are high. In other words, for gas oils under moderate pressure and in short tubes the viscosity effect need not be considered. On the other hand, at very high pressures (6000 pounds per square inch) the viscosity of gas oil may be double its value at atmospheric pressure in which case the viscous drag might again reach a value too large to neglect.

[6] I. B. Crandall, *Theory of Vibrating Systems and Sound* (Van Nostrand, 1926), p. 238.

## V. EFFECT OF TUBE EXPANSION

A second factor causing decrease in wave velocity is the expansion of the containing tube.

Sass,[7] in applying Allievi's theory to the problem, has shown that the inner diameter and wall thickness as well as the Young's modulus of the tube material play important parts in governing the wave velocity. The equation for wave velocity (neglecting viscous drag) as given by Sass, p. 212, is equivalent to:

$$a=(144g/\gamma(\beta+(1/E)\cdot(d/s))) \text{ ft./sec.} \quad (5)$$

where $g$ = acceleration due to gravity ft./sec.²
$\gamma$ = weight per unit volume lb./ft.³
$\beta$ = adiabatic compressibility of oil in.²/lb.
$d$ = internal diameter of tube inches
$s$ = tube wall thickness inches
$E$ = Young's modulus lb./in.²

Some authors have mistakenly interpreted Sass' $d/s$ as $D/d$, the ratio of outer to inner diameter, and have concluded that the effect of tube expansion is in general negligible. This is not the case, however, for $d/s$ values above 2.[8]

Combining Eqs. (3) and (5) yields

[7] F. Sass, *Kompressorlose Dieselmaschinen* (J. Springer, Berlin, 1929).

[8] *Additional references:* A. M. Rothrock, "Hydraulics of Fuel Injection Pumps for Compression Ignition Engines," N.A.C.A. Technical Report No. **396.** E. Blaum, "Vorgänge in Einspritzsystemen schnellaufender Dieselmotoren" Forsch. IngWes. **7**, 93–103 (1936).

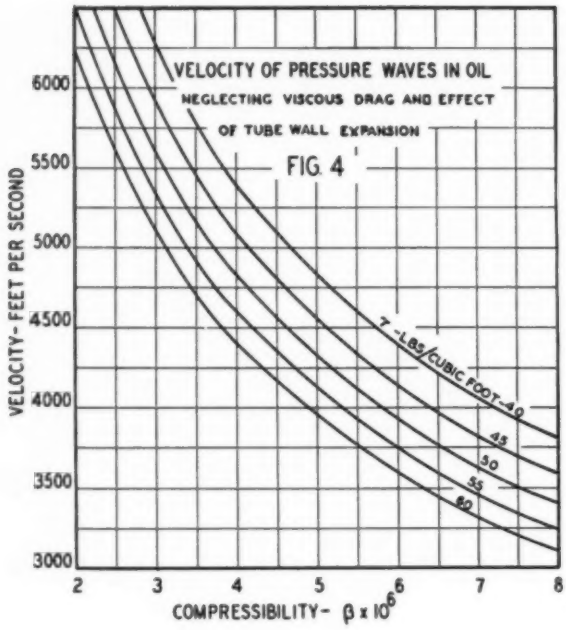


$$a = v(1/(1+1/\beta E \cdot d/s)) \qquad (6)$$

or
$$a = k \cdot v, \qquad (7)$$

where "$k$" is equal to the ratio of the velocity of a pressure wave in an oil confined within a tube to the velocity in an oil infinite in extent. In Fig. 5 are plotted the values of "$k$" as a function of $d/s$ for steel tubing.

## VI. Application to Diesel Injection Systems

A piece of equipment wherein pressure waves play a part of immense importance is the fuel injection system of a Diesel engine, and in particular, the modern high speed Diesel. An example will serve to illustrate the effect of differences in wave velocity on the point in the cycle at which injection takes place.

Assume an engine is operating at 2500 r.p.m., the injection pressure 1750 pounds per square inch, temperature of fuel in line 120°F, $d/s$ ratio of injection tube is 4, injection tube is 3 feet long, and viscous drag may be neglected. The effect of changing from fuel B-2 to B-11 in Table I is brought out in the following analysis:

The pressure wave velocity for B-2 is 3957 feet per second and for B-11 it is 4460 feet per second in an oil infinite in extent. The compressibilities for these two oils are $5.72\times10^{-6}$ and $4.415\times10^{-6}$ square inches per pound. From Fig. 5, $k=0.9890$ for B-2 and $k=0.9855$ for B-11. Hence, the wave velocities in the oils contained in the tube will be

$$3957\times0.9890=3910 \text{ feet per second}$$

and

$$4460\times0.9855=4400 \text{ feet per second, respectively.}$$

The time necessary for the wave to travel the length of the injection tube is

$$3/3910=0.000767 \text{ second}$$

and
$$3/4400=0.000681 \text{ second.}$$

The number of degrees of crank angle turned per second by the engine is

$$2500\times360/60=15{,}000 \text{ degrees per second.}$$

and the difference in the point of injection between the two oils may be a minimum of

$$15{,}000\times(0.000767-0.000681)=1.3 \text{ degrees.}$$

That the difference in point of injection may amount to much more than the above value can readily be appreciated by considering the effect of tube length or wider differences in density of the oil at given values of compressibility. Simply doubling the injection tube length in this

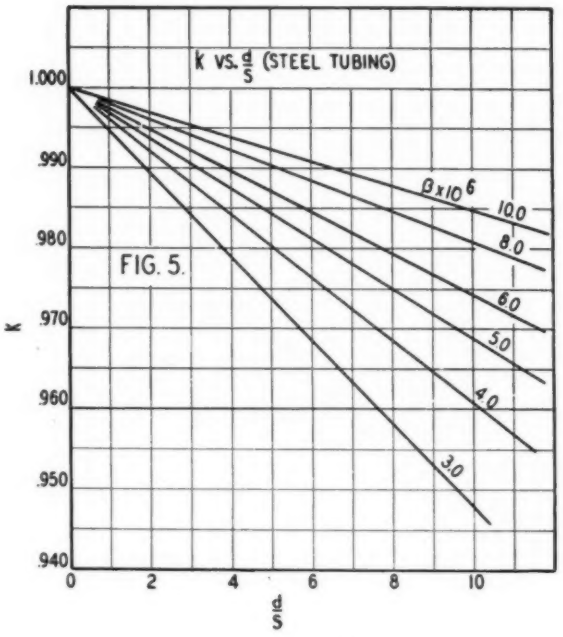

problem, for instance, would make the difference in the point of injection 2.6 degrees of crank angle.

### VII. Experimental Program

A program of research has been instituted at the mechanical engineering laboratories of the University of California for the purpose of obtaining experimental data on pressure wave velocities in petroleum oils contained in tubes. The tests will be carried out on a number of oils differing widely in physical and chemical characteristics. It is planned to cover the pressure range from atmospheric to 5000 pounds per square inch and temperatures from 32° to 200°F.

### VIII. Acknowledgment

The writer wishes to express his appreciation to Professor C. J. Vogt of the University of California whose interest, discussion, and criticism have been invaluable in the preparation of this paper. The writer also desires to thank Mr. R. A. Halloran, manager of the research and development department of the Standard Oil Company of California, for permission to release this paper for publication.

---

## Working Stresses for the Rational Design of Concrete Structures

Joseph Marin
*Rutgers University, New Brunswick, N. J.*

This paper presents a new theory of failure for materials subjected to a combined state of stress. The theory is developed for brittle materials, such as concrete, in which the compressive and tensile strengths are of different magnitudes. It is a semi-empirical theory which has some experimental support. Based on it working stresses are defined for various loading conditions. The use of these proposed working stresses in some cases makes considerable difference in design as compared to the present specifications requirements. These working stress values are conveniently represented by a diagram to facilitate the computations in design. The application of this information can be made simply in most cases where there are stresses acting in two right-angled directions—such as slabs in buildings, roads and bridges, retaining walls, dams and other hydraulic structures of concrete and reinforced concrete.

### 1. Introduction

IN most concrete and reinforced concrete structures stresses are produced in two directions at right angles to each other. Considerable effort has been devoted to the determination of these stresses, particularly in the case of slabs.[1] When the stresses have been obtained, however, there arises the question of the mutual influence in producing failure of the stresses acting at right angles to each other at a point. The answer to this requires the formulation of a theory of failure. There have been a number of theories which define the failure of materials subjected to combined stresses.[2, 3] For ductile metals it is satisfactorily established that the maximum shear energy theory is a good approximation. For a brittle material such as concrete, however, none of the theories that have been developed can be correctly used; since, with the exception of a modified internal friction theory developed by the writer,[3] all these theories require that the strength in tension and compression be equal. This is far from the truth particularly in the case of concrete. It seems appropriate therefore to develop a theory which considers the difference between the tensile and compressive strength.

[1] H. M. Westergaard, *Formulas for the Design of Rectangular Floor Slabs and the Supporting Girders* (American Concrete Institute, August, 1926), p. 1.

[2] S. Timoshenko, *Strength of Materials*, Vol. 2 (D. Van Nostrand, 1930).

[3] J. Marin, "Failure Theories of Materials Subjected to Combined Stresses," Proc. A.S.C.E. August, 1935, and Trans. A.S.C.E. 1936.

## 2. Formulation of Theory

The theory will be limited to the two-dimensional case of bi-axial stresses. Consider an element subjected to the principal stresses $S_1$ and $S_2$ as shown in Fig. 1(a). It will be assumed that the material is homogeneous and isotropic. This is not actually the case, but since the theory will be a semi-empirical one this assumption has

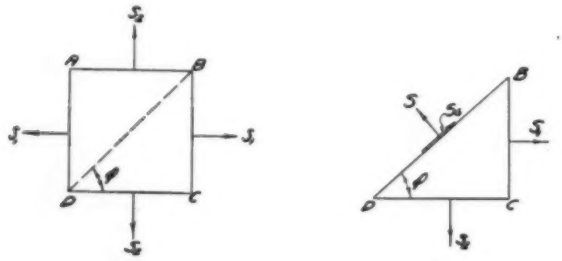

(a) (b)

Fig. 1.

reasonable justification. Brandtzaeg[4] has developed a theory for concrete considering initially that the material is nonisotropic. The Brandtzaeg theory however is not in such a form that it can be of use to the designer. A simplification of this theory does not seem possible.

Considering the stressed element in Fig. 1, it will be assumed that there is a critical plane $BD$ which is a plane of limiting shear or sliding—a plane where failure will first occur. It will be assumed, furthermore, that the direction of this plane varies, depending on the ratio of the principal stresses $S_1$ $S_2$. This is equivalent to assuming that there is a limiting shear stress $S_s$ acting along the plane $BD$ equal to a constant stress plus a frictional stress produced by the normal stress $S$ on the plane of sliding. That is the shear stress is a function of the normal stress or

$$S_s = f(S). \qquad \text{(a)}$$

This is a statement of the general shear theory as stated by Mohr. The purpose of this paper is to extend this hypothesis so that working stresses can be established for the design of concrete structures.

For the equilibrium of the element in Fig. 1(b) and for $S_1 > S_2$

$$S = (S_1+S_2)/2 + (S_1-S_2)/2 \cos 2\varphi, \qquad \text{(b)}$$

$$S_s = (S_1-S_2)/2 \sin 2\varphi. \qquad \text{(c)}$$

The values of the stresses $S$ and $S_s$ which produce failure depend on the values of the stresses $S_1$, $S_2$ and the angle $\varphi$. These values can be represented graphically by the coordinates of points such as $P$ indicated in Fig. 2. It can be easily shown by geometry that Eqs. (b) and (c) are graphically represented in Fig. 2.[2] For the case of simple compression ($S_c$), $S_1 = S_c$, $S_2 = 0$ and the circle becomes $DEO$ where $OD = S_c$. Similarly simple tension is represented by the circle $OFG$, where $OG = S_t$ the tensile strength of the material. For other ratios of the principal stresses circles similar to $ABC$ could be drawn if the values $S_1$ and $S_2$ that produce failure were known. Experimental data on brittle materials including concrete made by von Kármán,[5] Böker[6] and Roš

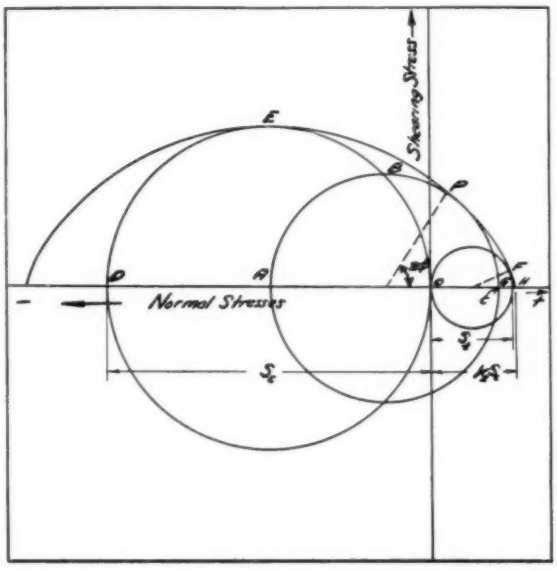


Fig. 2.

and Eichinger[7] show that the envelope $EPF$ to the stress circles is of the general form shown in Fig. 2. There is not conclusive experimental

[4] A. Brandtzaeg, "Failure of Materials Composed of Non-Isotropic Elements," Det Klg. Norske Videnskabers, Selskake Skrifter, No. 2, Trandhjem, Norway (1927).

[5] von Kármán, "Festigkeitsversuche unter allseitigen Druck," Mitteilungen uber Forschungsarbeiten, V. D. I., 118 (1912).

[6] R. Böker, "Die Mechanik der bleibenden Formänderung in Kristallinisch aufgebauten Körpern," Mitteilungen uber Forschungsarbeiten, V. D. I., 175–176 (1915).

[7] M. Roš and A. Eichinger, "Eidgenössische Materialprüfungsanstalt an der E. T. H. in Zürich, Versûche zur Klarung der Frage der Bruchgefahr," Diskussionsbericht, No. 28 (1928) and No. 34 (1929).

evidence to definitely define the equation of this envelope. In view of this uncertainty, it will be assumed that the equation of $EPF$ is an ellipse with a tangent horizontal at $E$ and symmetrical about the axes $EA$ and $DO$. In this way the relation $S_s=f(S)$ expressed in Eq. (a) becomes—

$$(S+S_c/2)^2+(a/b)^2S_s^2=a^2, \qquad \text{(d)}$$

where $a$ and $b$ are the major and minor axes of the ellipse and of values $a=S_c/2+k_2S_c$ and $b=S_c/2$. The relation between the principal stresses at failure is defined by placing values of $S$ and $S_s$ from (b) and (c) in (d). Then

$$\cos^2 2\varphi[x-y]^2[-4(k_2+k_2^2)] \pm 2\cos 2\varphi[x^2-y^2+x-y]+[x+y]^2 +2[x+y]+(1+2k_2)^2[x-y]^2 -4(k_2+k_2^2)=0, \qquad \text{(e)}$$

where $x=S_1/S_c$ and $y=S_2/S_c$. Eq. (e) would completely define the stress $S_1$ at failure for a given stress $S_2$ if a relation between the angle $\varphi$ and the principal stresses were known. To determine such a relation consider the case of simple compression. Then $S_2=0$, $S_1=S_c$ and by reason of the assumed ellipse in Fig. 2, it is necessary that $\varphi=45°$. It is convenient to represent the value of $\varphi$ as a function of the stress ratio $S_2/S_1$ as shown in Fig. 3(a). Then $S_2/S_1=0$ for simple compression and it is represented by the point $B$ in Fig. 3(a). For $S_1=S_2$ the stress circle becomes a point on the $x$ axis, the angle $\varphi$ approaching zero. This case is thus represented by the point $C$. It will be assumed for simplicity that for any other ratio of the principal stresses the value of $\varphi$ is represented by the ordinates to the curve $ABC$. This assumption is obviously incorrect for values of $S_1$ and $S_2$ of opposite signs. It is justified however in that it is a simplifying approximation; the error resulting being small, particularly compared to the assumption involved by neglecting the difference in the tensile and compressive strengths of concrete. From Fig. 3(a) the relation between $\cos 2\phi$ and the stress ratio $S_2/S_1$ is determined as shown in Fig. 3(b). The equation of $BC$ is

$$\cos 2\varphi=y/x. \qquad \text{(f)}$$

In this way a relation is obtained between the angle $\varphi$ and the stress ratio $(y/x)$. Placing the values of $\varphi$ from (f) in (e)

$$(y/x)^2(x-y)^2(-4k_2-4k_2^2) +(2y/x)(x^2-y^2+x-y)+(x+y)^2 +2(x+y)+(1+2k_2)^2(x-y)^2 -4(k_2+k_2^2)=0. \qquad \text{(g)}$$

This gives the value of the stress $S_1$ for a stress $S_2$ in terms of the compressive strength $S_c$ and the constant $k_2$—the intercept $OM/S_c$. To determine $k_2$ consider the case of simple tension represented by the circle $OFG$. Then $x=S_1/S_c=S_t/S_c$ and $y=S_2/S_c=0$, where $S_t$ = the tensile strength. To proceed further it is necessary to know the relative value of the strength in tension to that in compression, that is the ratio $S_t/S_c=k_1$. There is little information on the strength of concrete in tension.[8] A reasonable assumption is that $S_t/S_c=0.1=k_1$. The procedure used in the following can be easily modified for other values of $k_1$. Placing $x=0.1$ and $y=0$ in Eq. (g), the value of $k_2$ is

$$k_2=0.055. \qquad \text{(h)}$$

Placing this value of $k_2$ in Eq. (g) the value of $S_1$ producing failure for a given value of $S_2$ is completely defined in terms of the compressive

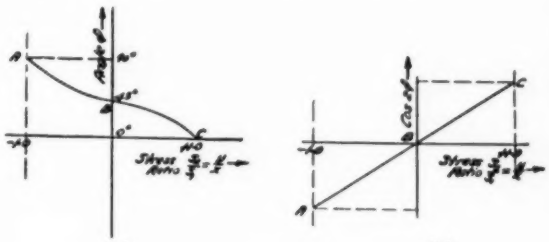

(a) (b)

FIG. 3.

strength $S_c$ namely

$$(y/x)^2(x-y)^2-8.62(y/x)(x^2-y^2+x-y) -9.62(x^2+y^2)-8.61(x+y)+2xy+1=0 \qquad (1)$$

or

$$(S_2/S_1)^2(S_1-S_2)^2 -8.62(S_2/S_1)(S_1^2-S_2^2+S_1S_c-S_2S_c) -9.62(S_1^2+S_2^2)-8.61(S_1S_c+S_2S_c) +2S_1S_2+S_c^2=0. \qquad \text{(1a)}$$

A plot showing the relation between the principal stresses for failure is represented in Fig. 4 by

[8] *Report on Significance of Tests of Concrete and Concrete Aggregates*, A.S.T.M. Publication (1935).

plotting Eq. (1). Similar diagrams can be easily obtained for other ratios of $S_t/S_c=k_1$. Due to the complexity of Eq. (1) it seems desirable to approximate the equation by a simpler one. This is shown by the ellipse shown dotted in Fig. 4, obtained by passing an ellipse through the points *ABCDEF*. The value of the stress $S_1$ at failure for a given stress $S_2$ is then

$$x^2+y^2-0.206xy+0.90x+0.90y-0.10=0 \quad (2)$$

or

$$S_1^2+S_2^2-0.206S_1S_2+0.90S_1S_c +0.90S_2S_c=0.10S_c^2. \quad (2a)$$

That is for a given value of the stress component $S_2$ the value of $S_1$ which produces failure is defined by Eq. (2a) for a concrete with a compressive strength of $S_c$. It is now convenient to formulate working stresses for various possible combinations of stress.

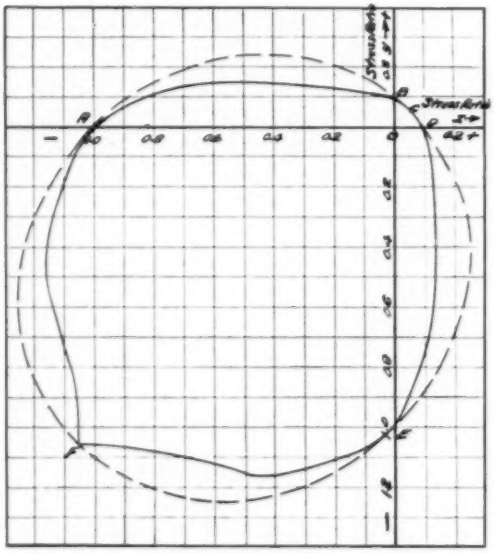

FIG. 4.

### 3. WORKING STRESSES

Considering that the stress $S_1$ is always greater than $S_2$, the value of $S_1$ to produce failure for a given value of $S_2$ is defined by solving for $S_1$ in Eq. (2a). Then

$$S_1=(2S_c/9(1+R)\pm(121+162R+121R^2)^{\frac{1}{2}}), \quad \text{(i)}$$

where $R=$ the stress ratio $(S_2/S_1)$. The working stress value for $S_1=[S_1]_w$ is now obtained from (i) by dividing the right side of Eq. (i) by an appropriate factor of safety $n$. That is

$$[S_1]_w=[S_c/n] \times(2/9(1+R)\pm(121+162R+121R^2)^{\frac{1}{2}}). \quad (3)$$

A plot is shown in Fig. 5 giving the relation between the working stress and stress ratio $R=S_2/S_1$. In a particular design it is necessary to first select the point having the critical stress ratio,—that is the stress ratio which gives the minimum working stress value $[S_1]_w$. In the design of some concrete and reinforced concrete structures this can be determined by inspection and the working stress $[S_1]_w$ is then directly selected from Fig. 5. In the case where the critical stress ratio $R$ is not known directly the value of the stress ratio $R$ for the governing working stress can be evaluated from Eq. (3) using the condition for a minimum; namely, $d(S_1)_w/dR=0$. The approximation in Eq. (3) produces a relatively small error in the working stress values.

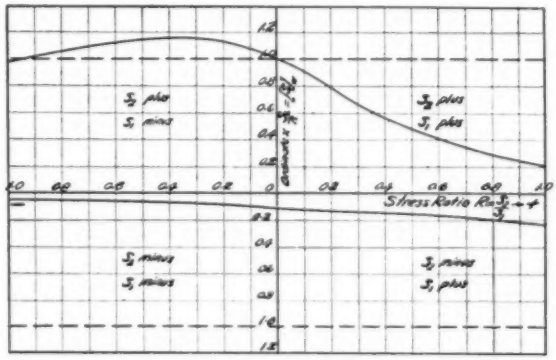

FIG. 5. Working stress values $[S_1]_w$. Note:—$S_1>S_2$

With the working stresses as formulated above, it is comparatively a simple matter to plot design charts defining required sizes of parts for various concrete structures.

### 4. CONCLUSION

A semi-empirical theory is formulated by the above analysis defining failure in the case of combined stress, based on the physical concept that failure is due to a sliding on a plane of weakness—the direction of this plane depending upon the ratio of the principal stresses. It is

significant that this theory considers the difference in the tensile and compressive strength of concrete. This leads to a rational theory based on certain simplifying assumptions, with a resulting theory in general agreement with test results. A simplification of this theory is approximated in order to define working stresses which can be easily used by the designer. Relations similar to Eq. (3) for various values of $k_1$ could be easily incorporated in present specifications relating to working stresses in such cases as slabs subjected to bending moments in two directions at right angles to each other. It may also be convenient to compute design charts for the various types of structures in which a combined state of stress occurs. It should be noted that the experimental verification of the above theory is meagre and there is hence a need for experimental results on the problem of the failure in concrete subjected to combined stresses.

## On Convection Currents in High Pressure Mercury Arcs

CARL KENTY
*General Electric Vapor Lamp Company, Hoboken, New Jersey*
(Received November 29, 1937)

Convection speeds in commercial high pressure Hg vapor lamps are measured by photographing on a moving film, the tracks of incandescent particles of CaO and MgO. A deep red filter and panchromatic film are used. The convection system is found to consist of a laminar flow of hot gas upward in the center and of cold gas downward near the walls. For the 400 watt lamp ($p \leqq 1$ atmosphere, $m$ = mass of Hg per cm of tube length = 11.5 mg cm$^{-1}$) an upward speed of about 40 cm sec.$^{-1}$ is found at the axis in the mid-section of the lamp. The speed is somewhat greater near the bottom, this effect increasing with $m$. Speeds are found to increase somewhat less rapidly than in proportion to $m$ as predicted. An approximate theory of these currents is presented, based largely on the work of Elenbaas, which accounts sufficiently well for the order of magnitude of the observed speeds. For *similar* discharges, speeds do not depend on the tube diameter but simply on $m$; for such discharges the watts lost by convection are proportional to $m^2$ and independent of diameter and length. Convection losses for the 400-w, 250-w and 85-watt lamps are calculated to be 12-w and roughly 0.9-w and 0.8-w, respectively. When a lamp is operated on half-wave a dark space develops at the bottom of the arc in the off half-cycle, due to uprush of cold gas from below. Convection speeds estimated from the length of this dark space and the period of zero current are about twice too high; probable reasons for this are given. When the lamp is operated in the horizontal position, the arc bows up against the wall of the tube and softens it. The magnetic force necessary to keep the arc in the axial position is measured and found to be proportional to $m$ ($F = 0.126m$ dyne cm$^{-1}$). This force will be independent of tube diameter for *similar* discharges. An approximate theory is developed which accounts sufficiently well for the order of magnitude of this force. Rotation is also used to center the arc in the horizontal position; for the 400-watt lamp a speed of at least 7 r.p.s. is necessary for this purpose. No appreciable changes in arc voltage or efficiency are found for horizontal operation with magnetic or rotational control as compared with vertical operation. Photographs of particle tracks show in a striking manner the migration of ions in the electric field; Ca and Mg vapors from the evaporating particles are strongly ionized and excited at the high temperatures and progress rapidly in the field.

### INTRODUCTION

A COMPLETE theory of an electric discharge at high pressure must take into account the effect of convection currents on the heat losses and on the form of the arc. In a splendid series[1] of studies of these discharges Elenbaas[2] has shown that the convection speed should increase in proportion to $m$, the mass of Hg per unit length of the tube, and the convection loss in proportion to $m^2$. It is well known that as $m$ is increased beyond a certain limit the arc begins to "snake" around the tube. Elenbaas has given evidence based on measurements of critical $m$

[1] W. Elenbaas, Physica **1**, 211, 673 (1934); **2**, 45, 155, 169, 757, 763, 787 (1935); **3**, 12, 219, 484, 859, 947 (1936); **4**, 279, 413, 747 (1937); De Ingenieur **50**, E83 (1935); Zeits. f. Tech. Physik **17**, 61 (1936).

[2] W. Elenbaas, **3**, 484 (1936).

values and theoretical calculations that this is the point at which a laminar flow begins to change into a turbulent flow.

In order to test further the quantitative aspects of Elenbaas' theory it was thought worth while to attempt to measure the actual vapor velocities existing in these tubes.

The principal method adopted was to photograph on a moving film the motions of incandescent particles of oxide such as CaO or MgO introduced into the tube for the purpose. The movements of such particles accidently appearing in lamps were noted by Elenbaas[3] and have been frequently observed in this laboratory. They are plainly visible through a red glass and yield by visual study a certain amount of information about the convection currents. But it remained for the photographs to show up the relatively high vapor velocities existing upward in the center of the arc.

## Apparatus and Method

Figure 1 shows some common commercial types of high pressure Hg lamps, and Table I some of their characteristics. Of these the 400-w lamp was made the principal object of this study.

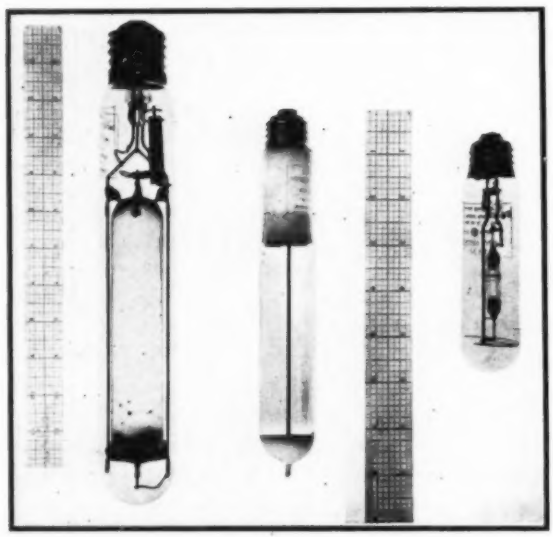

Fig. 1. Some typical commercial high pressure Hg vapor lamps. Left, 400-watt type; center, 250-watt type; right, 85-watt type. Left scale for 400-w lamp, right scale for 250 and 85-w lamps.

[3] W. Elenbaas, Physica **1**, 211 (1934).

Fig. 2 shows the experimental arrangement for introducing the oxide particles. A small amount of carefully dried and baked out oxide powder O is introduced into the side arm *A*. Several $\frac{1}{8}$-inch ball bearings are also put in this tube, and one of them at a time is held as shown by the electromagnet *M*. When released, this ball bearing carries a minute amount of the powder along with it into the tube. A number of incandescent

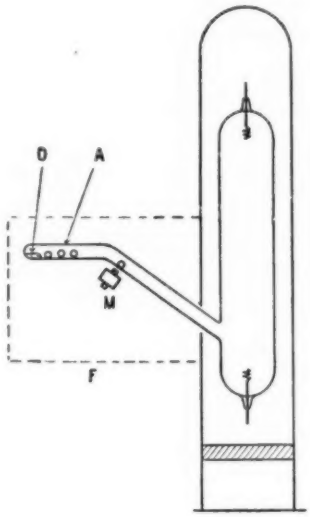


Fig. 2. Arrangement for introducing oxide particles at proper times to be photographed.

particles can then usually be seen rising up rapidly in the arc stream. By a suitable arrangement, the ball bearing is released and the camera shutter opened at the proper times so that the particles are photographed on the moving film. Very distinct tracks are obtained by using a deep red filter and panchromatic film.

In order to keep the Hg from condensing in the side arm a furnace *F* is provided. The glass envelope around the tube likewise prevents condensation of Hg in the tube. In these lamps an excess of Hg was provided and the *m* value

Table I. *Characteristics of some typical commercial high pressure Hg vapor lamps.*

| Wattage Type | Current (amp.) | Voltage | Internal Diameter (cm) | Distance between Electrodes (cm) | *m* mg per cm | Approximate Pressure (Atmospheres) |
|---|---|---|---|---|---|---|
| 400 | 2.9 | 147 | 3.33 | 15.5 | 11.5 | 1 |
| 250 | 3.9 | 70 | 2.67 | 10.5 | 3.2 | 0.5 |
| 85 | .43 | 250 | .42 | 1.8 | 3 | 25 |

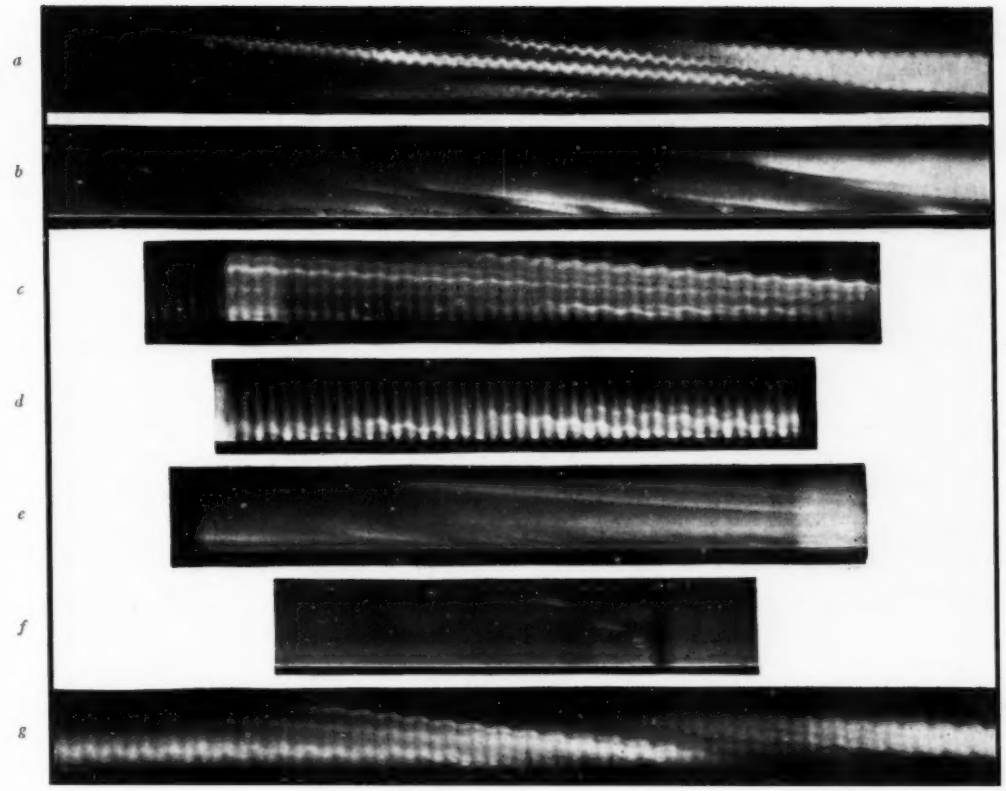


FIG. 3. Tracks of incandescent oxide particles in 400-w type lamp photographed on moving film. *a*, Particles of CaO, arc operated on a.c. at 100 volts; *b*, CaO, d.c. 100 v; *c*, CaO, d.c. 145 v; *d*, same as *c* but blue filter; *e*, CaO, d.c. 145 v; *f*, MgO, a.c. 145 v; *g*, CaO, a.c. 200 v. Time increases from right to left.

determined from the voltage by a method given below.

## DISCUSSION OF PHOTOGRAPHS

Some typical examples of the tracks obtained are shown in Fig. 3. With the exception of film *d*, see below, these were all taken with a deep red filter (Corning No. 241 and No. 242). The arc current was 2.9 amp. in all cases. At *a* is a film obtained in the case of a.c. operation of the lamp at 100 volts ($m = 6.1$ mg per cm). The flicker of the lamp is brought out strongly. From this the time scale is easily obtained. The image of part of an 85 w lamp, operating on a.c. is seen at the top. This is provided for timing in cases of d.c. operation. The paths of a number of incandescent particles can be seen passing diagonally across the film. Knowing the arc length (15.5 cm between electrodes) the upward speed of a particle at any point can be calculated from the slope of the track at this point.

Very striking is the 60-cycle wave superposed on the otherwise straight paths of the particles. This is caused by the luminous highly ionized vapor given off by the evaporating particle which is drawn by the electric field first one way and then the other. This interesting and unexpected phenomenon is being studied further and will be discussed in a later paper. The fact that the particles themselves make straight tracks shows that they bear relatively small electric charges.

*b* is a photograph taken with d.c. operation, also at 100 volts. The bright line at the bottom is the image of the anode which in all these lamps runs hotter than the cathode. (In the a.c. cases the traces of the electrode are seen to be of equal brightness.) The particle tracks are seen to be shaded away from the anode; this represents the cloud of ionized vapor being swept away toward the cathode by the field.

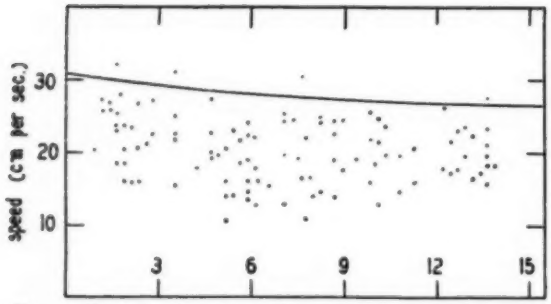


FIG. 4. Distribution of particle speeds as calculated from track slopes at various heights in the lamp. (100 volt arc, $m = 6.1$ mg per cm.) [Ordinate should read "cm from bottom of arc."]

*c* was taken with 145 volt operation and thus is representative of the standard 400-w lamp.

*d* was also taken at 145 volts but with a combination of blue filters (Corning 385 and 986) which transmitted only the *H* and *K* lines of $Ca^+$ (at 3934, 3968A) together with 4047 of Hg.

Films *e* and *f* show d.c. tracks at 145 v the first with CaO powder, the second with MgO powder. It is seen that the MgO particles rarely vaporize. Considering that CaO melts at 2570°K and MgO at 2800°K it appears that the temperatures attained by these particles are probably less than 2800°K, far below the gas temperature (around 6000°K) in which they are. Undoubtedly the particles cool themselves by radiating as black bodies and in the case of CaO also by evaporation.

Film *g* is taken at 200 volts with CaO.

As Fig. 3 shows, the tracks are quite linear and the gas flow is therefore essentially laminar as Elenbaas concluded.

The films do not of course, disclose the position of the particles in the lamp in regard to their distance from the axis. But since vapor speeds will be highest in the center, particles located in the center should give tracks of the greatest slope. Since the temperature is highest in the center, these tracks should also be the brightest, and since the lives of most particles are terminated by evaporation these tracks should also be the shortest. That the shortest and the brightest tracks also have the greatest slope was confirmed by the analysis of a large number of tracks. Some examples of this can be seen in Fig. 3.

In general, the slopes of the tracks will not give the true velocity of the gas in which the particles are, but this velocity minus the rate of free fall of the particles. But tracks near their ends, where the particles have almost wholly evaporated should represent quite closely by their slopes the true vapor velocities. Frequently such tracks do indeed show an increase of slope near their ends but the increase is not very great and suggests that the rate of free fall of the particles here used is small compared with the velocities of gas flow.

The slopes of the tracks were found with the help of a mechanical device which enabled

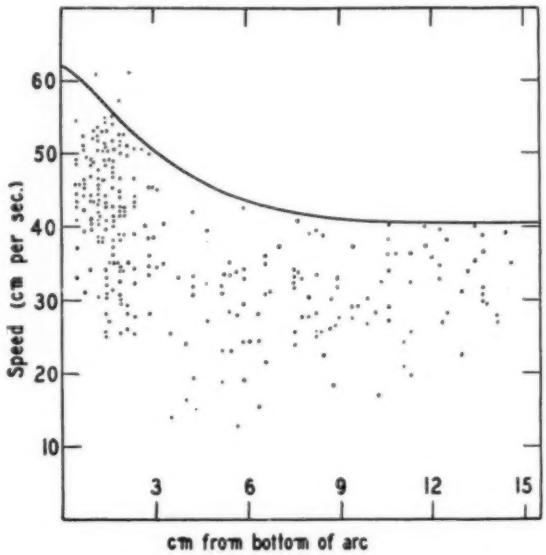


FIG. 5. Distribution of particle speeds for 145 volt arc ($m = 11.5$ mg per cm).

measurements to be repeated within about 2 percent for tracks 2.5 cm or more in length. The distances from the bottom electrode at which the slopes were measured were recorded. In the case of long tracks the slope was measured at several points. In all about 400 tracks were measured which appeared on some 70 photographs, taken at one or other of the three voltages shown in Fig. 3.

For each operating voltage speeds were plotted against distances from the bottom of the lamp. The results are shown in Figs. 4, 5 and 6 where each point represents a measured slope. The curves are drawn to represent maximum velocities and are taken to represent the true upward speed of the gas at the axis.

Velocities are clearly higher toward the bottom

of the lamp particularly at the higher voltages. This behavior will be discussed further below.

Velocities are seen to increase with the voltage so that at 200 volts they are about double their value at 100 volts. A quantitative explanation of this fact will appear in the following approximate theory of the convection currents which is in large measure due to Elenbaas.[2]

## Theoretical

Figure 7 curve $v$ shows the main features of the convection currents in these lamps. Hot gas flows upward in the center and cold gas downward on the outside. At some point $A$ the velocity is zero. Experimentally it has been possible to locate this point approximately by observation of the movements of oxide particles.[4] At the wall $v$ must be zero. Finally as much gas must flow upward as flows downward, this condition can be expressed by

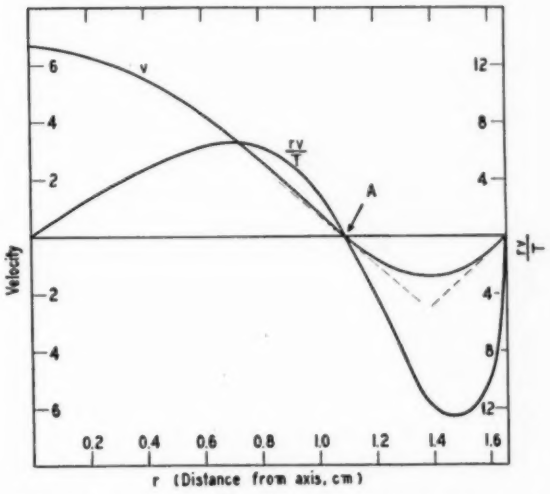


Fig. 7. Velocity distribution of gas flow. For the $v$ curve each unit of the ordinate scale represents a speed of $a$ cm per sec. For the $rv/T$ curve each unit of the ordinate scale represents $10^{-4}a$ cm$^2$ sec.$^{-1}$ deg.$^{-1}$.

$$2\pi\int_{r=0}^{r_A}\frac{rvdr}{T}=-2\pi\int_{r=r_A}^{r_0}\frac{rvdr}{T}, \qquad (1)$$

where $T$ is the absolute temperature at a distance $r$ from the axis. Since the pressure is the same everywhere in the tube the density is inversely proportional to $T$. It will be seen that a smooth curve drawn to fulfill all these conditions has its form fairly well determined. The curve $v$ of Fig. 7 is such a curve drawn to an arbitrary velocity scale $a$. The $rv/T$ curve of Fig. 7 is drawn to correspond with the $v$ curve shown and is such that the area above the $v$ axis is equal to that below this axis (Eq. (1)). In practice these areas were measured with a planimeter and a number of $v$ curves had to be tried before one was found whose $rv/T$ curve would satisfy this condition.

In order to fix the magnitude of the velocity unit $a$, consider an imaginary cylinder to exist in the tube of radius $r_A$ and of length $H$ substantially equal to the length of the tube but leaving sufficient openings at top and bottom for the free flow of gas. Suppose the motion is completely laminar so that no gas flows through this cylinder.

Then an average hydrostatic pressure $P$ may be supposed to exist at the bottom of the tube, which is expressed by

$$\pi r_0^2 P=(m/1000)gH-2\pi H\eta_0(dv/dr)_{r=r_0}, \qquad (2)$$

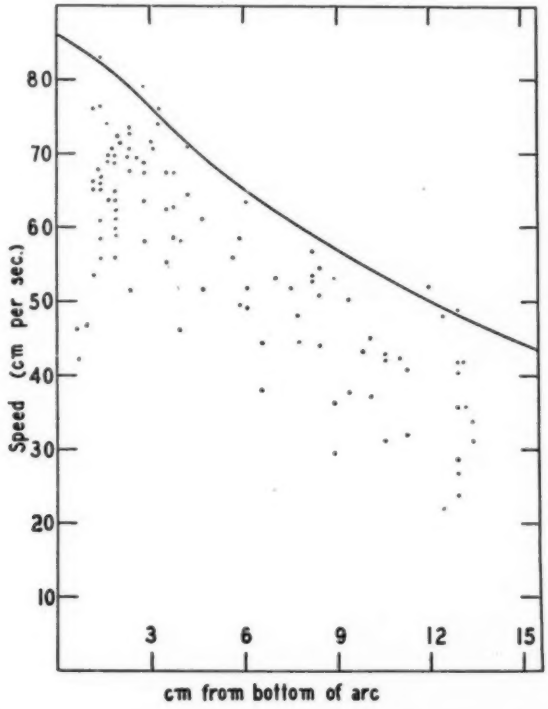


Fig. 6. Distribution of particle speeds for 200 volt arc ($m=19.1$ mg per cm).

[4] The present treatment differs from that of Elenbaas in that the point $A$ is here experimentally determined. However, both methods give substantially the same numerical results in the present case.

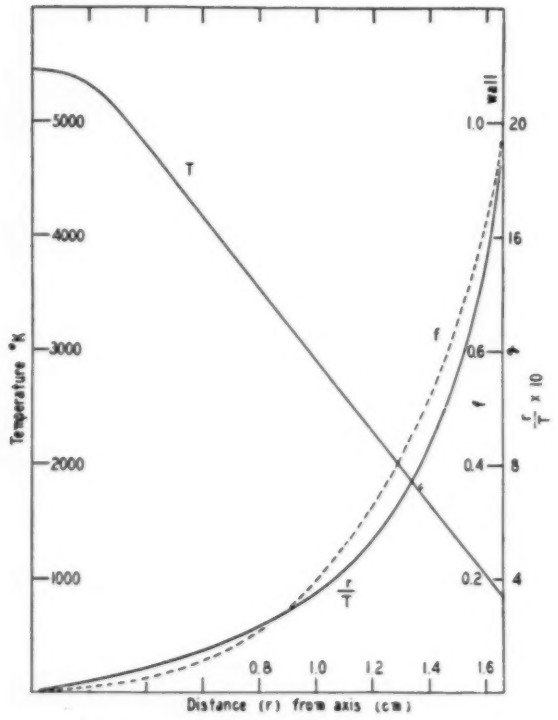


FIG. 8. Temperature distribution $T$ in 400-w lamp, and the fraction $f$ of the gas within a radius $r$. Tube radius 1.66 cm. [$r/T\times 10$ should be $r/T\times 10^4$].

where $H$ is the height of the cylinder (supposed large compared with $r_0$), $\eta_0$ is the coefficient of viscosity of Hg at the wall temperature and $m$ is in mg per cm. This equation expresses that the area of cross section at the bottom times $P$ is equal to the total mass of Hg in the tube minus the frictional drag at the wall.

It follows then, neglecting end effects, that

$$\pi r_A^2 P - f_A(m/1000)gH = -2\pi r_A H \eta_A (dv/dr)_{r=r_A}, \quad (3)$$

where $f_A$ is the fraction of gas inside the cylinder $r=r_A$ and $\eta_A$ is the coefficient of viscosity of Hg at the temperature $T_A$. This equation expresses that the force due to $P$ on the bottom of the cylinder $A$ is balanced by the weight of Hg within this cylinder and the frictional drag at the surface of the cylinder.

From the $v$ curve already set up $dv/dr$ is obtained graphically at $r_A$ and $r_0$ in terms of the arbitrary velocity unit $a$. Thus $(dv/dr)_{r=r_A} = -8.8\cdot a$ sec.$^{-1}$ and $(dv/dr)_{r=0}=9.0$ sec.$^{-1}$. $f_A$ is found with the help of Fig. 8. Here $T$ is the temperature distribution for the 400-w lamp as given by the work of Elenbaas.[5] The fraction of gas $f$ inside a radius $r$ is found by graphical integration under the corresponding $r/T$ curve as

$$f = 2\pi\int_0^{r_A}(rdr/T) \div 2\pi\int_0^{r_0}(rdr/T). \quad (4)$$

$r_A$ was determined visually as above noted to be about 1.1 cm for the 400 w lamp and thus from curve $f$, $f_A=0.252$.

Braune, Basch and Wentzel[6] have measured $\eta$ for Hg between 491 and 883°K. They found that their data could be represented by a Sutherland formula with a Sutherland constant of 942. Fig. 9 curve (1) shows their data extrapolated by

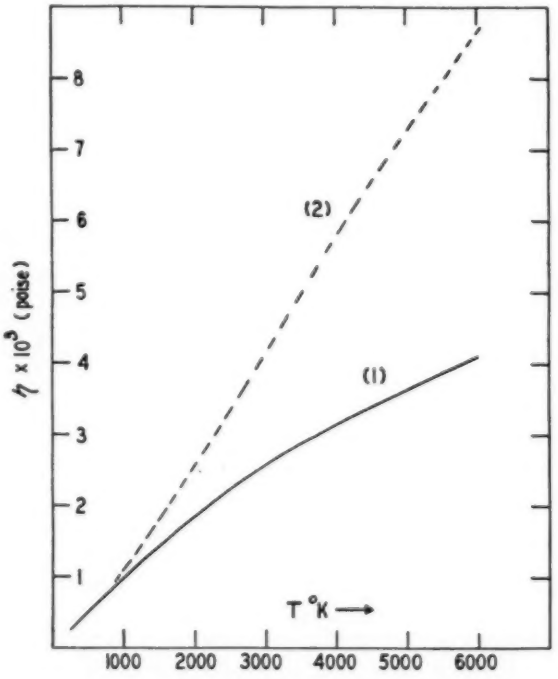


FIG. 9. Viscosity of Hg from Braune, Basch and Wentzel's data, extrapolated to high temperatures (1) by a Sutherland formula and (2) by the method of Hasse and Cook.

[5] W. Elenbaas, De Ingenieur **50**, E83 (1935). The temperature curve given in Elenbaas' paper for $m=3$ mg per cm and $L=40$ watts per cm is adjusted by means of the formula $T_{eff}=6025[L/(8.5+5.75m)]^{0.1}$ (W. Elenbaas, Physica **2**, 757 (1935)) to suit the present case where $L=23.4$ and $m=11.5$. The maximum temperature in Fig. 8 is chosen 100° higher than $T_{eff}$ given by this formula, following Elenbaas. The wall temperature was found experimentally by the use of small thermocouples cemented to the glass.

[6] H. Braune, R. Basch and W. Wentzel, Zeits. f. physik. Chemie **A137**, 447 (1928).

this formula to the higher temperatures existing in the 400-w lamp. Hasse and Cook,[7] however, have analyzed Braune, Basch and Wentzel's data assuming a molecular repulsive force varying as $r^{-9}$ and an attractive force varying as $r^{-5}$ and have arrived at a formula which is plotted as curve (2), Fig. 9. Taking $T_0$ as 850° and $T_A$ as 2540° from Fig. 8, $\eta_0$ and $\eta_A$ are found from curve (2) to be $0.83\times10^{-3}$ and $3.4\times10^{-3}$ poise, respectively.

Eliminating $P$ between (2) and (3) and rearranging the results in

$$\frac{\eta_0}{r_0}\left(\frac{dv}{dr}\right)_{r=r_0} - \frac{\eta_A}{r_A}\left(\frac{dv}{dr}\right)_{r=r_A} = \frac{mg}{2000\pi}\left(\frac{1}{r_0^2} - \frac{f_A}{r_A^2}\right). \quad (5)$$

This equation is independent of $H$ signifying that the convection speeds are independent of the tube length as would be expected. Substituting in (5) the values of the various quantities already given and g, there results

$$a = 0.77m. \quad (6)$$

For the 400-w lamp, $m = 11.5$ mg per cm[8] so that $a = 8.9$ cm sec.$^{-1}$. This gives the axial velocity in Fig. 7 to be 58 cm sec.$^{-1}$. From Fig. 5 the measured value of this velocity throughout the greater (middle and upper) part of the tube, which is the region where this theory ought to apply best, is about 41 cm sec.$^{-1}$. The agreement is as close as could be expected in view of the very approximate nature of the treatment, and uncertainties in the location of the point $A$ and in $\eta$ for Hg at these high temperatures.

Provided the temperature distribution is the same for the three discharges[9] of Figs. 4, 5 and 6

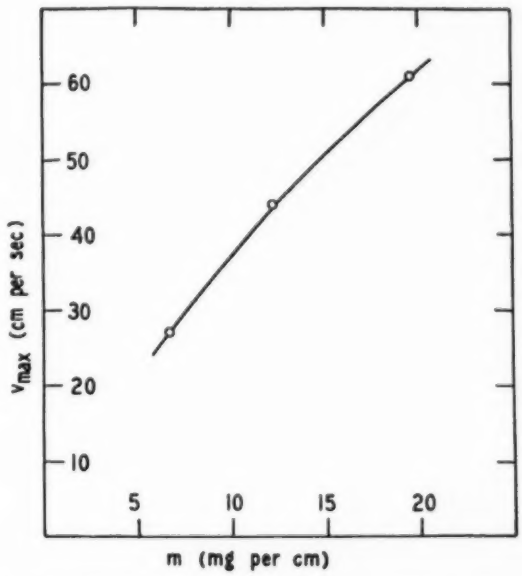


FIG. 10. Measured axial velocity of convection current in mid portion of tube (400-w lamp except variable $m$).

it is reasonable that the point $A$ of zero velocity will be the same for all cases. Since the viscosity of a gas at a given temperature is independent of the pressure the frictional drag restraining the flow will be the same in all cases. But the driving force will be proportional to $m$. Hence the velocities of flow including $v_{max}$ should increase in proportion to $m$.

By means of the gradient formula of Elenbaas[9] namely

$$G = \frac{m^{\frac{1}{2}}(8.5+5.75m)^{\frac{1}{2}}\cdot 10^2}{d^{1\frac{1}{2}}}, \quad (7)$$

where $d$ is the tube diameter in mm, it is found that $m$ for the 100, 145 and 200 volt cases is 6.1, 11.5 and 19.1 mg per cm, respectively.[10] In Fig. 10 the values of $v_{max}$ (for the central portion of the tube) from Figs. 4, 5 and 6 are plotted against these $m$ values and a rough proportionality is seen to exist.

For similar discharges in tubes of different diameter, but with the same $m$ values it may be

[7] H. R. Hasse and W. R. Cook, Proc. Roy. Soc. **A125**, 196 (1929).

[8] As found by dividing the weight (in mg) of Hg added by the total volume of the bulb and multiplying by the cross-sectional area of the bulb; end corrections are then applied following essentially the method of Elenbaas, Physica **1**, 211 (1934).

[9] Elenbaas, Physica **2**, 169 (1935) defines *similar* discharges as those in which $T$ is the same for corresponding points.

*Note added in proof, December 23, 1937.*—In regard to reference 9, discharges are here defined, substantially following Heller (Physics **6**, 389 (1935), Eq. (13)), to be approximately similar if $L = A + Bm$ where $A$ and $B$ are constants for a particular family of similar discharges, $A$ being the heat loss per cm by conduction and $Bm$ the similar loss by radiation. Elenbaas has shown that $A$ is nearly the same for different discharges and is about 9 or 10 w cm$^{-1}$. With $L = 23.4$, $m = 11.5$, for the 145 v case (400-w lamp), and with $A = 9$, $B$ for this case comes out to be 1.25. With these values of $A$ and $B$, the formula then gives for $L$, for the 100 v and 200 v cases ($m = 6.1$ and 19.1, respectively) values which are within 3 percent of the observed values. The three discharges may therefore be regarded as substantially similar.

[10] In applying this formula a combined electrode drop of 15 volts was assumed.

inferred that the convection velocity distributions will be similar. For the relative distributions of mass will be the same by definition and it is to

FIG. 11. Some types of orbit frequently made by oxide particles in 400-w lamp.

be expected that $r_A/r_0$ will be the same. Further by doubling the diameter we halve the velocity gradients everywhere but double the surfaces over which the frictional drags act. Therefore these will remain constant.

While in the above no gas was assumed to flow through the cylindrical surface $A$, actually some flow exists as shown by the visual observation of oxide particles. Thus particles have been observed to make orbits as shown in Fig. 11. These orbits are characterized by rapid upward movement in or near the arc and a much slower downward movement on the outside. Some of these orbits, particularly the smaller ones, are so stable as to suggest the presence of stabilizing action. In one very outstanding case a particle was observed in an orbit like that on the right in Fig. 11 to make about 46 revolutions per minute over a period of 30 min. These motions show that the flow while not strictly laminar is nevertheless far from being turbulent. The extent of the influx of gas into the arc stream all along its length, i.e., across the surface of the imaginary cylinder $A$ mentioned above, is believed to be small enough in relation to the main currents not to effect the order of magnitude of the calculated results.

As already noted, Figs. 4, 5 and 6 indicate that convection velocities are higher toward the bottom of the arc, particularly at the higher pressures. This is believed to be associated with a higher degree of constriction which is observed to exist toward the bottom of the arc. The effect, shown schematically in Fig. 11, is not noticeable at 100 volts but at 200 volts the arc begins at a height of several cm to narrow down till at the bottom it has less than half its diameter in the rest of the tube. But the intrinsic brilliancy of the arc increases so that the light output per cm of length is somewhat greater. These facts were found by scanning the image of the arc crosswise and lengthwise with a slit and photocell. Evidently a higher temperature exists at the bottom. This is also shown by a higher ratio of the yellow to green lines[11] there. Smaller density in arc at the bottom due to higher temperature would make for higher convection speeds but probably the main factor is a relatively low viscosity at the margin of the arc toward the bottom due to the low temperature of the gas rushing into the arc in this region. The same inrush would help to account for the increased constriction.

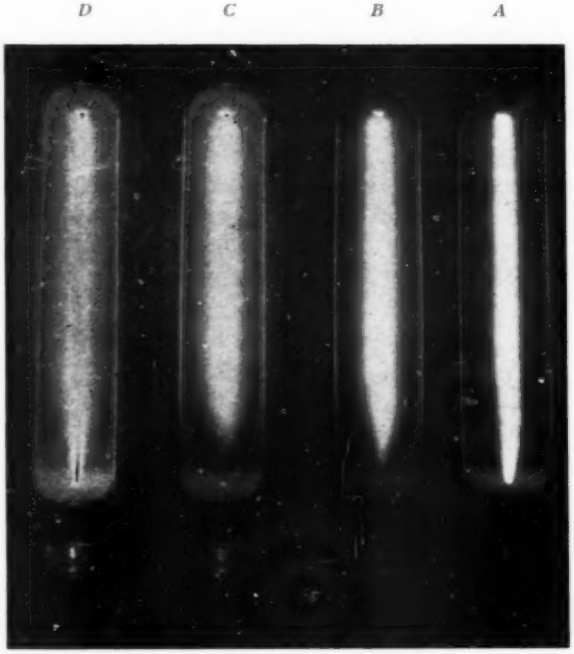


FIG. 12. Photographs at 400-w lamp operating on half-wave, taken at the times indicated in Fig. 13. Exposure times were 0.25 sec., 10 sec. 11 min. and 10 min. for $A$, $B$, $C$ and $D$, respectively.

[11] W. Elenbaas, Physica **1**, 673 (1934).

### Evidence from Half-Wave Operation

If a 400-w lamp is operated on half-wave and observed through a stroboscopic disk, a dark space of about 2 cm length is seen to develop at the bottom of the tube, regardless of polarity, during the 0.01 sec. approx. that the arc is out. In the rest of the tube there is a considerable afterglow right up to the end of the zero current period. Interpreting this dark space as due to uprush of cold gas to supplant the rising column of hot luminescent gas, it should be possible to estimate the convection speed in this way.

Figure 12 shows photographs of a 400-w lamp taken at different times in the cycle by means of a camera just in front of whose lens of small aperture revolved a stroboscopic disk with narrow slits. The disk was mounted on a synchronous motor operated from a Selsyn generator. The phase of the disk could thus be varied by changing the angular position of the armature of the Selsyn, the latter being read off from an angular scale and pointer. In Fig. 12 the lamp was operated from a 550-volt transformer with a rectifier and pure resistance ballast of about 50 ohms. The lamp could not operate on a lower voltage than this. The average current was 2.9 amp. The phase of the pictures is indicated in Fig. 13. Fig. 13 shows the luminosity of the lamp as a function of phase angle as found by replacing the camera film with a G.E. barrier layer photo-cell, found to be linear in the present set up by tests with calibrated wire screens.

In Fig. 12, at *B*, *C* and *D* the afterglow, which was bluish in color, can be seen broadening out and shortening from the bottom with the time. Notable in picture *D* is the very narrow and bright streak, reversed in the photograph, which appears at the bottom. The first appearance of this streak, at *S* in Fig. 13, was taken to represent the starting of the current in the new cycle. Probably nearly the whole applied voltage of 550 is concentrated in this region (the remainder of the tube being sufficiently conductive) at this time, which voltage is necessary to break down the cold and unionized gap. Very good evidence for this lies in the fact that the same lamp operated in the horizontal position with magnetic control (see below), where the convection currents are weaker, required only 300 volts for

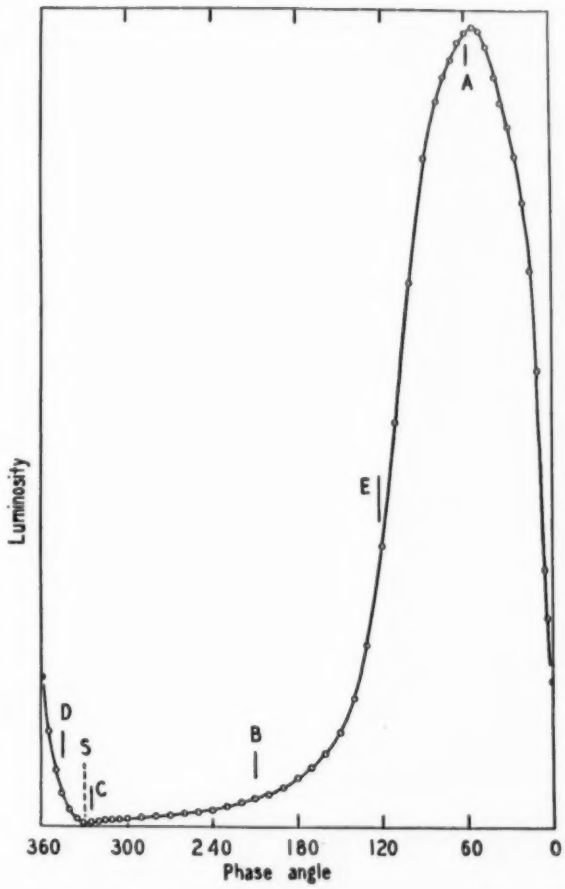


Fig. 13. Light output as a function of phase angle in electrical degrees (reckoned from an arbitrary zero point) for 400-w lamp operating on half-wave. Ordinate scale arbitrary. *A*, *B*, *C*, *D* are respectively points at which photographs in Fig. 12 were taken. *S* indicates starting point of new arc.

similar operation with pure resistance ballast. After its onset, the luminous streak rapidly grows longer and wider as may be inferred from Fig. 13, until soon the new arc is fully established.

Assuming that the current ceases at *E*, approximately, in Fig. 13, there is a period of about 215 electrical degrees or about 0.01 second of zero current before picture *C* of Fig. 12 was taken. Estimating the height of the dark space in picture *B* as roughly 1.5 cm a convection speed of 150 cm per sec. is obtained while Fig. 5 indicates a maximum speed at the bottom of about 60 cm per sec.

Before interpreting this as a discrepancy however it is necessary to consider the effect of the

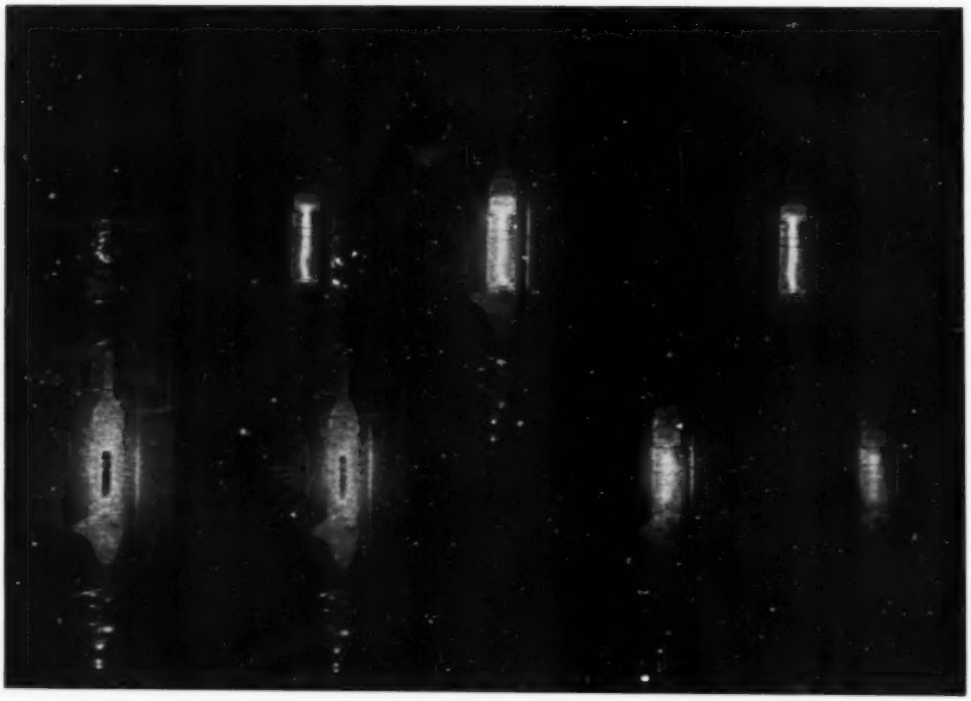

FIG. 14. Photographs of 85-w lamp operating on half-wave. Upper (direct) series taken at time *A*, Fig. 15, lower (afterglow) series at time *B*.

cold gas currents entering the arc from the sides near the bottom; these will tend to collapse the arc space and provide a high temperature gradient for the abnormally rapid cooling of the axial gas. The net effect will be to cause the region of luminosity to recede upward faster than the actual motion of the gas. The conical shape of the bottom of the luminous column as compared with the full appearance at the top (see picture *B* particularly) is well explained by such currents.

Figure 14 shows photographs, similar to Fig. 12, of the 85-w lamp on half-wave operation. Here the lamp was run at $\frac{1}{2}$ amp. average current in a circuit containing an F.G. 17 thyratron as rectifier, a resistance ballast of about 800 ohms and an inductance of 0.7 henry on a 1600 volt transformer. Without any inductance, the lamp would not run on 2000 volts, indicating a great rapidity of recovery of dielectric strength at these high pressures (25 atmospheres). Fig. 15, shows the luminosity as a function of phase angle measured as in Fig. 13. The upper (direct) series of pictures (Fig. 14) were taken at the time *A* Fig. 15 and the lower (afterglow) series at *B*. Different exposure times and apertures were used but in general the afterglow exposures were several hundred times as great as the direct exposures. The first two afterglow pictures are seen to be reversed.

Here as in the 400-w lamp a dark space is seen at the bottom of the afterglow. Estimating the length of this dark space as 0.25 cm and the time between the cessation of current and *A* in Fig. 15 as 110 degrees or 0.005 sec. a convection speed of 50 cm per sec. is obtained. If as in the 400-w lamp this figure is too high by a factor of 2.5 the convection speed in the 85-w lamp at the bottom would be 20 cm per sec. This may be compared with 15 cm per sec. calculated by multiplying the observed speed at the bottom of the 400 w lamp (60 cm per sec.) by the ratio of the $m$'s ($3/11.5 \leqq 1/4$). A few visual observations of the motions of incidental oxide particles in these lamps indicate that the motions here are of the same type as in the 400-w lamp.

### HEAT LOSS BY CONVECTION

Referring to Fig. 7 the heat energy of the gas flowing upward in the cylinder *A* per sec. can be

shown to be, in watts

$$Q_1 = 0.506\pi p \int_0^{r_A} rv dr, \qquad (8)$$

where $p$ is the pressure in atmospheres. In obtaining this expression the energy per atom (corresponding to $C_p$) was taken as $(5/2)kT$. Since the density of atoms is $1.01\times10^6 p/kT$, $T$ does not appear in the expression. Similarly the rate at which heat is flowing downward outside $A$ is

$$Q_2 = 0.506\pi p \int_{r_A}^{r_0} rv dr. \qquad (9)$$

Assuming that the gas flowing down between $A$ and the wall maintains its same temperature as it enters $A$ at the bottom, it follows that $Q_2$ is also the heat energy flowing into $A$ per sec. and thus the net heat loss is $Q_1 - Q_2$. The integrals are evaluated with a planimeter using an $rv$ curve corresponding to the $v$ curve of Fig. 7 taking $a$ as $0.55m$ (instead of $0.77m$ as in Eq. (6)) to give an axial velocity equal to the measured axial velocity (41 cm sec.$^{-1}$). It is thus found that[12]

$$Q_1 - Q_2 = 19.5 - 7.5 = 12 \text{ watts.}$$

This is only 3 percent of the total watts consumed in the 400-w lamp and therefore convection as an agency for heat dissipation is as Elenbaas assumed[1] of very minor importance compared with conduction and radiation.

Since in expressions (8) and (9) both $p$ and $v$ are proportional to $m$ for similar discharges in tubes of the same diameter the convection loss will be proportional to $m^2$. If the diameters are different but the discharges still similar $p$ will be proportional to $m/r_0^2$ and the integrals of (8) and (9) to $mr_0^2$ (since as has been noted above $v$ at *corresponding* points will simply be proportional to $m$). Thus as long as the discharges are similar, the convection loss will be independent of tube diameter as well as length and only depend on $m^2$. It is assumed that the discharge in the 85-w lamp is sufficiently similar to that in the 400-w lamp to establish the order of magnitude of the convection loss in the former as $12\times(3/11.5)^2$ or 0.8 watt. In the 250-w lamp the loss would on the same basis be $12\times(3.2/11.5)^2 = 0.9$ watt.

Calculations using Saha's and Boltzmann's equations indicate that the fractions of atoms in the ionized and excited states are so small as to render their energy negligible compared with the heat content of the neutral atoms.

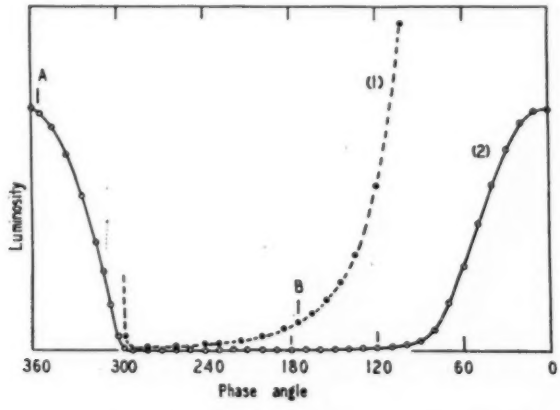


FIG. 15. Similar to Fig. 13. Light output of 85 w lamp operating on half-wave. Ordinate scales arbitrary, that for (1) being 60-fold greater than that for (2). The upper series of photographs in Fig. 14 were taken at $A$, the lower afterglow series at $B$.

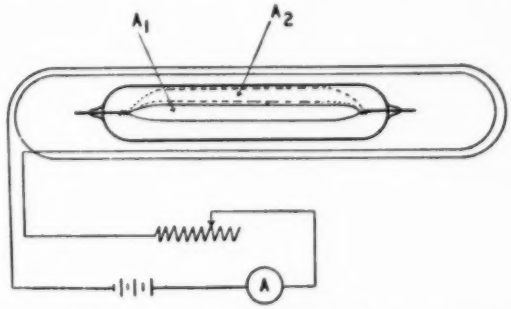


FIG. 16. Apparatus for measuring force necessary to keep horizontal arc in axial position ($A_1$). Without magnetic field arc rests against top wall (position $A_2$).

## HORIZONTAL OPERATION

In the horizontal position, the arc bows up against the tube wall as indicated in Fig. 16 and quickly softens the glass. A suitable magnetic field will, however, keep the arc in the axial position and magnets have been devised which will accomplish this purpose satisfactorily in practice.[13, 14]

[12] $p$ is here taken as 1.08 atmospheres for the 400-w lamp in order to be consistent with the temperature curve of Fig. 18 and $m = 11.5$ mg cm$^{-1}$.

[13] R. Maxted, U. S. Pat. 2037387, Electrical Rev. Feb. 28, p. 309 (1936).

[14] C. Kenty, U. S. Pat. 2027383.

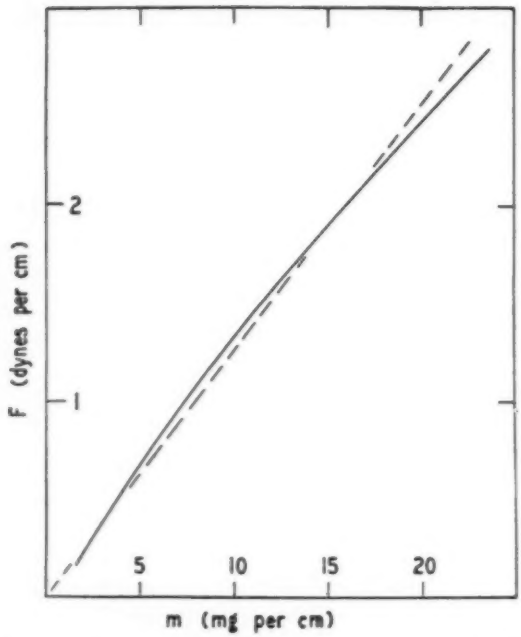


FIG. 17. Force on 2.9 amp. arc necessary to keep it in the axial position when lamp is operated horizontally with magnetic control (400-w lamp except with variable $m$).

Figure 16 shows an experimental arrangement which was used to measure the force necessary to keep the arc in the axial position. Here the magnetic field is supplied by a coil of wires as shown. The current is adjusted until the arc assumes the axial position. The force on the arc will then be

$$F = 4nII'/100r_m, \tag{10}$$

where $F$ is dynes per cm, $r_m$ is the mean distance of the wires from the axis in cm, $n$ is the number of turns and $I$ and $I'$ are the currents (d.c.) in the lamp and in the control circuit respectively. $F$ was thus found for the 400-w lamp to be 1.5 dynes per cm.

In order to study further this force as a function of $m$, lamps were run at a constant (d.c.) current of 2.9 amp. and while they were heating up $I'$ was continually adjusted to keep the arc in the center. At various arc voltages $V_1$, $I'$ was recorded. A number of such runs were made with two different tubes, one a standard 400-w lamp and one a similar lamp but with twice the normal amount of Hg and all values were plotted on coordinate paper. A smooth curve was then drawn to represent the points as nearly as possible. Voltages were then converted to $m$ values by means of the gradient formula already given.[15] Calculating $F$ from $I'$ by (10) and plotting $F$ against $m$ the curve of Fig. 17 was obtained. This curve is seen to depart only slightly from a straight line, so that approximately

$$F = Km, \tag{11}$$

where $K$ for the dotted line shown is 0.126 dyne mg$^{-1}$.

In the following rough attempt to account for this force on the arc, the arc core is treated simply as a light body buoyed up in a denser fluid. If $\rho_c$ is the mean density of the core and $\rho_m$ that of the surrounding mantle the buoyant force will be

$$F = \pi r_c^2(\rho_m - \rho_c)g \tag{12}$$

by Archimedes' principle where $F$ is in dynes per cm and $r_c$ is the radius of the luminous core, measured roughly as 0.63 cm. If $f_c$ is the fraction of the gas which is in the core Eq. (12) can be put in the form

$$F = \frac{mg}{1000}\left(\frac{r_c^2 - f_c r_0^2}{r_0^2 - r_c^2}\right). \tag{13}$$

It was observed that $r_c$ changed very little over most of the range of $m$; only at the very lowest values was it appreciably greater. Assuming that $f_c$ remained also constant[16] (13) reduces to (11). From Fig. 8 the value of $f_c$ at $r = 0.63$ is read from the $f$ curve as 0.060. With $r_c$ as above and $r_0 = 1.66$ cm, $K$ is then calculated to be 0.095. The agreement in order of magnitude with the observed value of 0.126 is considered sufficient in view of the approximate nature of the treatment.

[15] Careful tests in which 400-w lamps were operated normally (2.9 amp. Hg all vaporized) first vertically and then horizontally with magnetic control of the arc in the axial position indicated a 1 percent lower voltage in the later case. For a similar lamp but with $m = 23$ no difference was found. The gradient formula was therefore considered as applying to horizontal as well as vertical operation. At the lowest voltages $m$ values were obtained directly with the help of the curves of $Gd^{\frac{1}{4}}$ against $L$ given by Elenbaas, reference 9.

[16] As Elenbaas has pointed out (Physica **4**, 474 (1937)), with increasing $L$ (in this case also with increasing $m$) the wall temperature will rise in greater proportion than the core temperature. This will have the effect of displacing gas toward the center and of increasing $f_c$ in (13) and hence of decreasing $F$. Some of the decrease of slope of the curve of Fig. 18 with increasing $m$ may thus be accounted for. The same effect could partly explain why the upward convection speeds did not increase in proportion to $m$ (Fig. 10).

Insofar as $f_c$ and the ratio $r_c/r_0$ remain constant in (13) as will be the case for similar discharges, the force $F$ will depend only on $m$ and not on the tube diameter. In the case of the 85-w lamp $F$ was found to be about 0.4 dyne $cm^{-1}$ as compared with 0.38 dyne $cm^{-1}$ calculated from (11) with $K=0.126$ and $m=3$.

When the arc is displaced from the axial position there is a restoring force which has its origin in the fact that the heat lost by conduction to the walls is least for this position. Since the heat conduction loss is independent of $m$ and also (for similar discharges) on tube diameter, this restoring force will be relatively constant for a given fractional displacement for tubes of different $m$ and diameter. Hence in horizontal operation the natural displacement upward from the axial position (expressed as a fraction of the tube radius), will decrease as $m$ decreases. In the 250-w and 85-w lamps ($m=3.2$ and 3, respectively), the arc bows up relatively little in the horizontal position.

Closer study by observations of incandescent particles of MgO introduced for the purpose indicates that the gas is in a state of considerable motion and that the above calculations are too simplified. Fig. 18 shows the general scheme of the stream lines as indicated by the particle motions and the vertical components of speed at the different levels shown. The scale is such as to make the maximum speed shown about 20 or 30 cm per sec. The measured magnetic forces in the four positions from left to right in Fig. 18 were 2.5, 1.5, 0.5 and substantially 0 dynes $cm^{-1}$, respectively. Particles were frequently observed to make many revolutions in orbits shown and the estimation of the circumferences of orbits and periods of revolution helped in gaining ideas of the actual speeds.

Notable in Fig. 18 are the *downward* currents through the middle of the arc; they show the strong reaction of the magnetic field, initially on the electrons, but ultimately on the gas itself.[17] Since force will be necessary to maintain these currents against the frictional drags, the observed $F$ will be greater than $F$ as calculated above as is found to be the case.

[17] J. Slepian, *Conduction of Electricity in Gases*, pp. 185, 186.

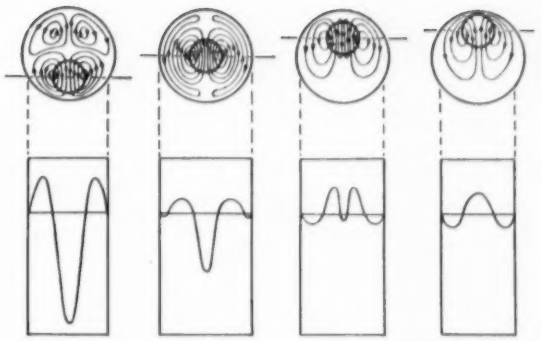

FIG. 18. Schematic view of convection currents in 400-w lamp operating horizontally under magnetic control. Four different arc positions are shown corresponding to four different field strengths. Below, also schematically are the vertical components of convection speed at the levels indicated.

A careful comparison of the luminous efficiencies of the arc in the horizontal axial position and in the vertical position revealed no detectable difference (within $\frac{1}{2}$ percent). This might be expected since convection is present in both cases and is of small importance in heat dissipation in any case.

### The Effect of Rotation

Another method that suggests itself for centering the arc is to rotate the tube. By means of a suitable lathe chuck and slip rings, the lamp could be rotated about its axis at any desired speed. Starting at very low speed, with the arc resting against the top of the tube, the first effect of rotation was to carry the arc sidewise. With increasing speed the arc then worked downward and inward to the axial position; first in the central portion at 6 r.p.s. and finally also in the end portions[18] at 7.2 r.p.s. Thereafter the arc remained centered up to 30 r.p.s., the highest speed tried.

Careful tests in which a 400-w lamp was operated first vertically at 3 r.p.s. and then horizontally at 12 r.p.s. revealed a 1 percent increase in efficiency and no change in voltage in the latter case; a 3 percent increase in efficiency was expected on the view that the rotation in the horizontal position would prevent all convection and corresponding loss (see above). A

[18] The cause of this stronger tendency to bow up near the ends is under investigation. To counteract the effect in practice a magnet has been developed whose field is stronger near the ends than at the middle (reference 14).

similar experiment with the 400-w type lamp with $m=23$ also yielded a 1 percent increase in efficiency and no change in voltage in the horizontal case. Here a gain of about 5 percent was expected (arc wattage: 230 volts$\times$2.9 amp. $=668$; convection loss in the vertical position, estimated from the above 400 w lamp loss: $12\times2\times60/41=35$ watts, where the factor 2 is for the ratio of the $m$'s and the factor 60 41 is for the approximate ratio of the measured axial velocities).

The reason for this failure to find the expected gains in efficiency is under further investigation, but is probably associated with the difficulty of perfectly centering the arc. Even if the tube and electrodes are perfectly centered the arc may not be at its ends depending on the location of the cathode spot.

In conclusion I wish to thank Dr. R. D. Mailey of this company for his continued interest and encouragement throughout the course of this work; Dr. C. G. Suits of the General Electric Company Research Laboratory at Schenectady for suggesting the photographic method of measuring particle speeds and for acquainting me with the work of Hasse and Cook; and my colleagues Messrs. J. A. St. Louis, L. B. Johnson, W. F. Hodge, J. D. Forney and R. J. Kennedy for data and helpful discussion on the commercial lamps here studied.